Pillar 3 – Topological superconductivity

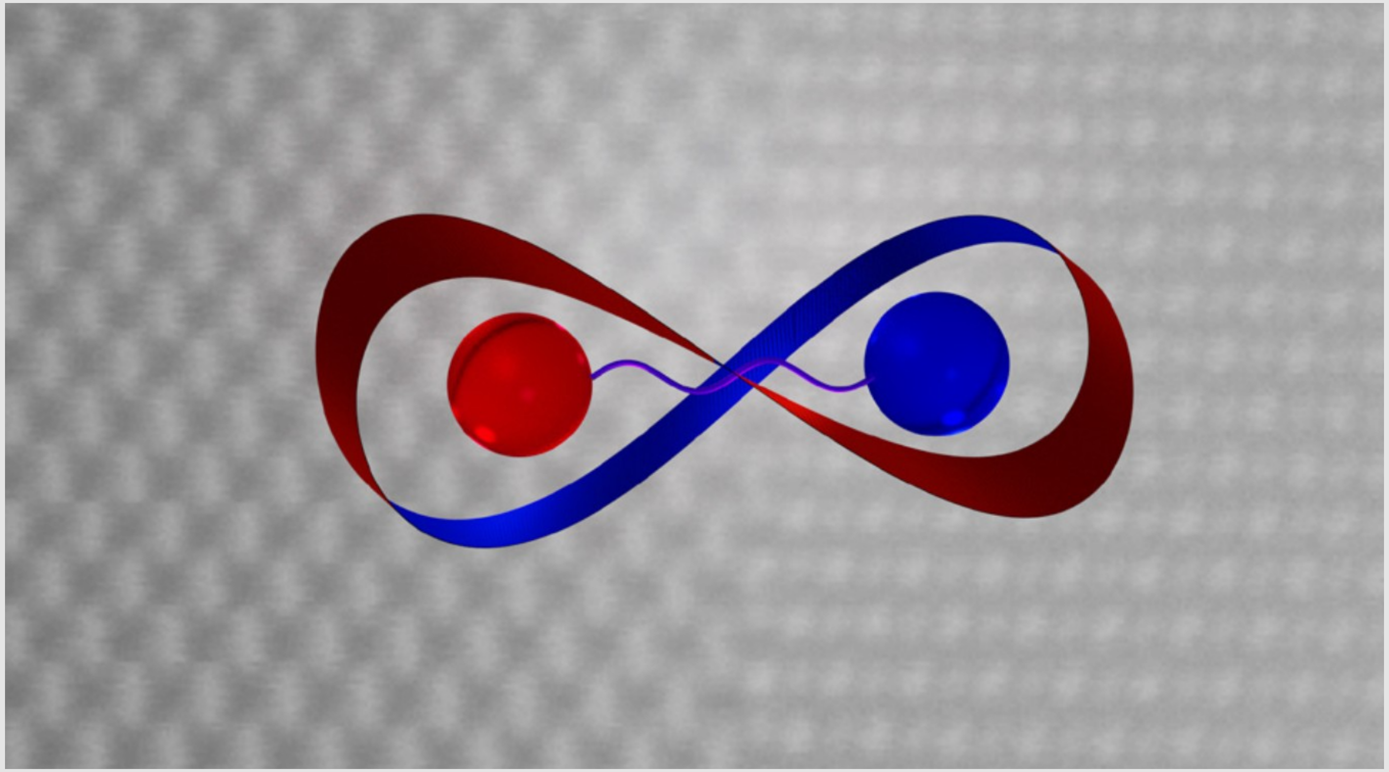

Introduction to pillar 3

Erik Bakkers(TU/e) & Alexander Brinkman (UT)

3.1 Topological superconductor-semiconductor heterostructures with extreme properties

Riccardo Reho (UU Theory), and Jason Jung (TU/e Experiment)

3.2 Topological superconductivity based on transition metal dichalcogenides

Justin Ye (RUG)

3.3 Topological superconductivity in Kitaev chains

Srijit Goswami (TUD)

Majorana Zero Modes in a Nanowire

Majorana Zero Modes should emerge in engineered solid state systems:

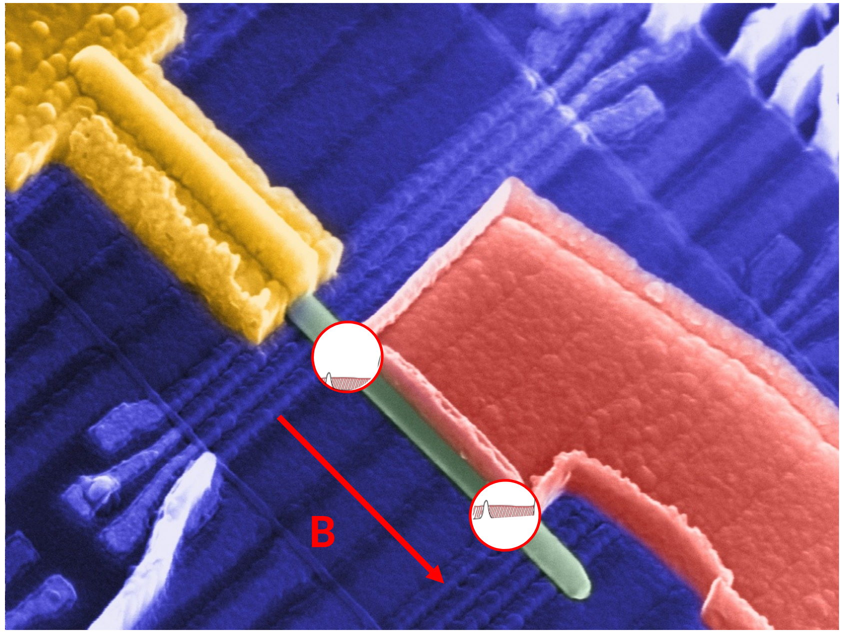

V. Mourik *et al*., *Science* **2012**, 336, 1003

Ingredients:

- 1D semiconductor
- Strong Spin-orbit interactions
- Proximity-induced Superconductivity
- Magnetic field

Based on 2010 proposals:

- Roman M. Lutchyn, Jay D. Sau, S. Das Sarma
- Yuval Oreg, Gil Refael, Felix von Oppen

Disorder in a Device

Superconductor:
- Grain boundaries/defects
- Thickness variations

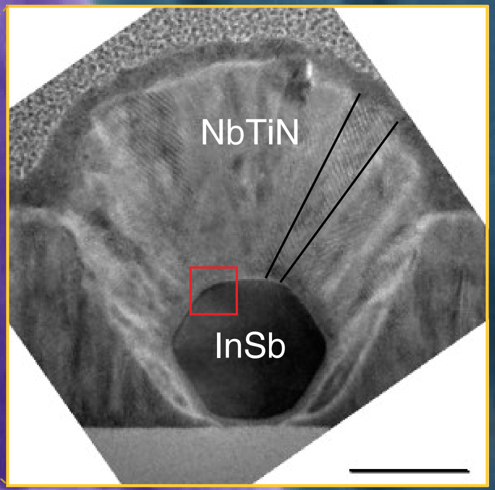

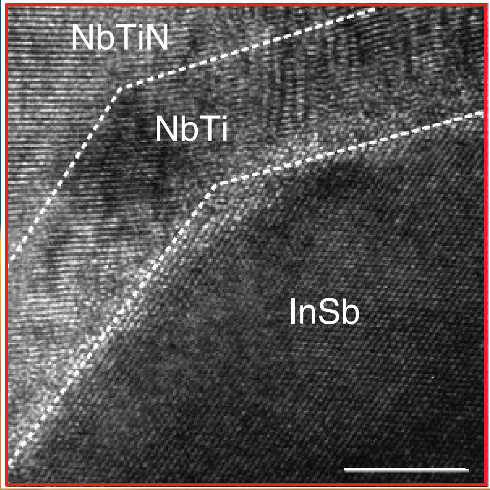

Super/Semi interface:
- Roughness
- Metallization

Semiconductor wire
- Defects/impurities
- Surface
- Quantization

Strain and thermal expansion

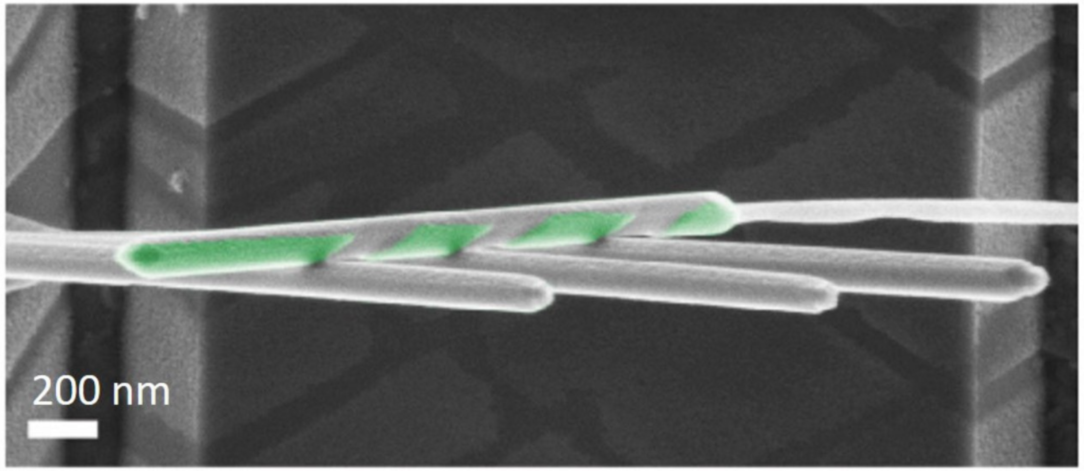

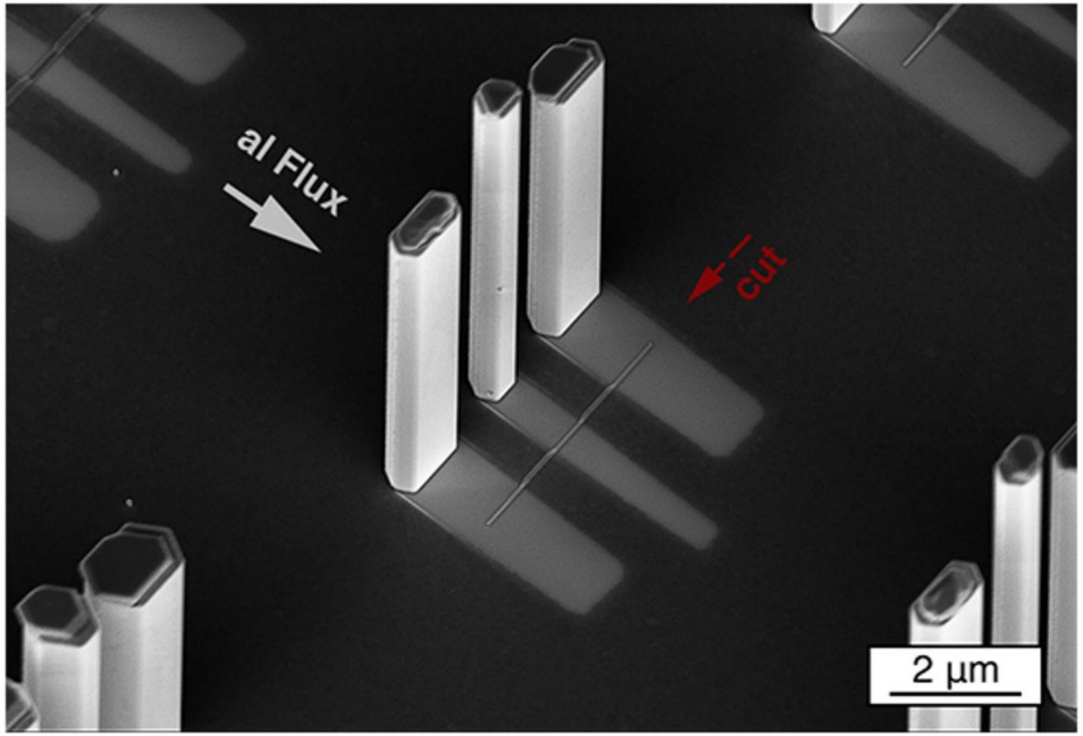

How to overcome these challenges ?

Need

- More advanced device fabrication
- More extreme materials
- Better understanding of interfaces

Pillar 3

Open research questions

- *Can we realize Majorana- and parafermions in topological materials and unambiguously prove their existence by demonstration of their unique features?*

- *Can we probe and control the non-local nature of Majoranas and parafermions? Length scales?*

- *Which material-related factors determine the robustness of the Majorana and parafermion quantum states? Can we increase (1) the gap of the topological insulator, (2) the gap of the superconductors?*

Central goal is to demonstrate and manipulate Majorana (MZM) and parafermion modes

Expected breakthroughs in Pillar 3

New Materials

- New hybrid semiconductor/superconductor nanowire architectures with atomically sharp interfaces.
- Use of robust quantum spin Hall insulators proximitized by novel broad-gap 2D superconductors.

New measurement techniques

- Improve the local characterization of MZM by combining wavefunction amplitude measurements with noise measurements, phase measurements and detection of non-local correlations.
- Study fusion of Majorana and parafermion states by using interferometric devices.
- New types of scanning probe experiments that come very close to braiding.

Getting Ge devices "topo-ready"

Semiconductor	Superconductor	μ ($\times 10^3$ cm^2/Vs)	$\hbar/2\tau$ (μeV)	Δ^* (μeV)	l_{SO} (nm)	g^*	T_1 (ms)	T_2^* (ns)	1Q gate fidelity (%)
Ge/SiGe, 2D	PtSiGe	615	10	70	76	0.76-15	32	830	99.99
InSb, nw	Al	44	940	250	100	26-51	na	8	na
InAs, nw	Al	25	890	270	60	8	0.001	8	na
	Pb			1250					
InAs, 2D	Al	60	370	190	45	10	na	na	na
InSbAs, 2D	Al	28	1200	220	60	55	na	na	na

NB: Material platforms with a hard-gap measured in SN spectroscopy only

Increase the superconducting gap by:

- Stacks of superconductors
- New superconducing ge-silicides with higher T_c

⇓

Applications:

- Topological superconductivity in planar JJ
- Kitaev chains
- Coupling of spin-qubits via topo-protected links

InAs-Al Hybrid Devices Passing the Topological Gap Protocol

Microsoft Quantum†
(Dated: July 11, 2022)

In the limit in which the clean topological gap Δ_T is small, the stability condition for the topological phase is $\ell_c > \xi_T$ [90], where ℓ_c is the localization length in the normal state (which in one dimension is equal to twice the mean free path for short-range disorder [98]) and ξ_T is the coherence length in the clean topological superconductor. Equivalently, this can be rephrased in terms of energy scales as $\Delta_T\tau > \hbar/2$, where τ is the elastic scattering

arXiv:2207.02472v2

Planar Josephson junctions

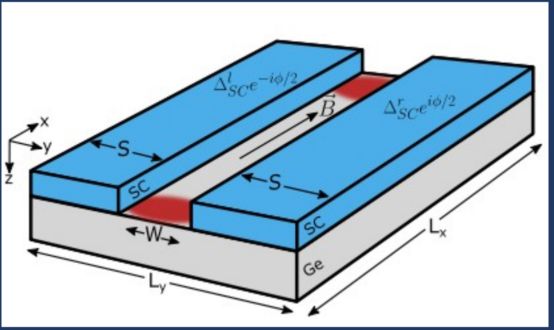

Luethi et al arxiv2022

Artificial Kitaev chain

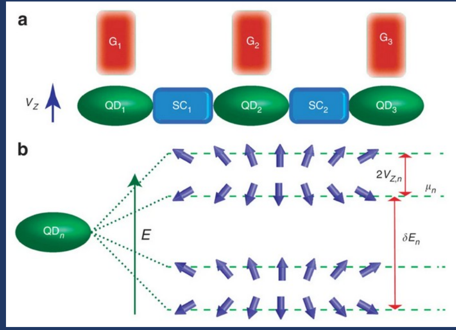

Saul & Das Sarma NatComm 2012)

Spin-qubit coupling *via* cross Andreev reflection

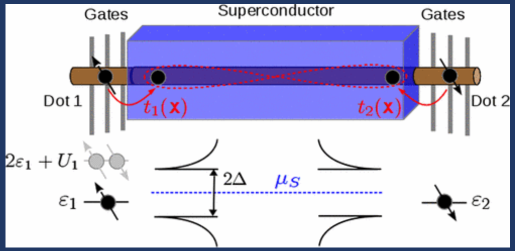

Leijnse et al. PRL (2013)

Low-disorder holes in strained germanium quantum wells

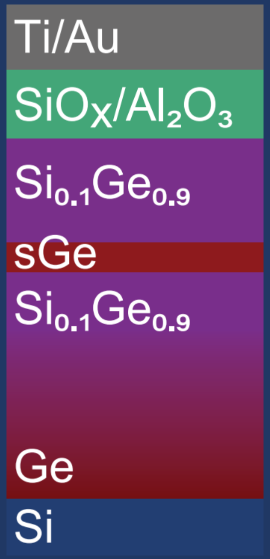

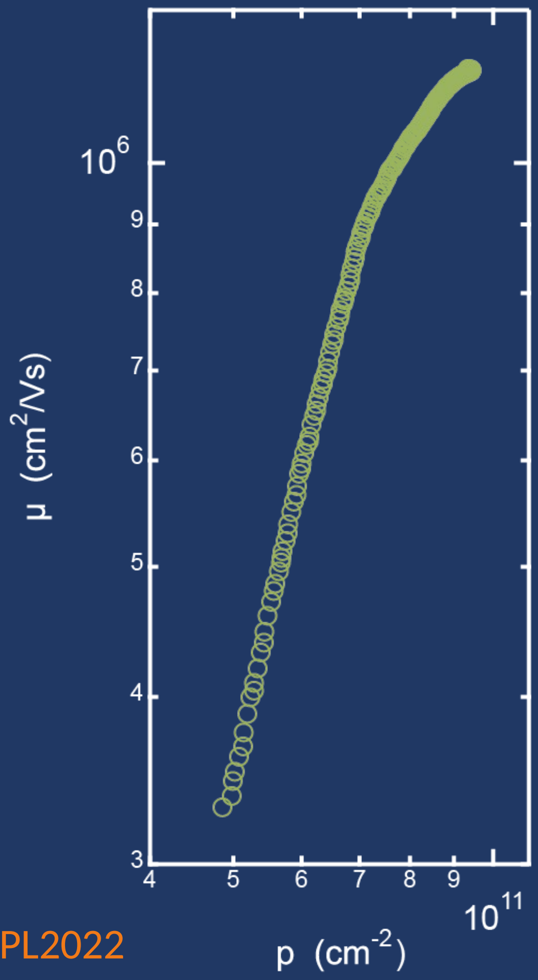

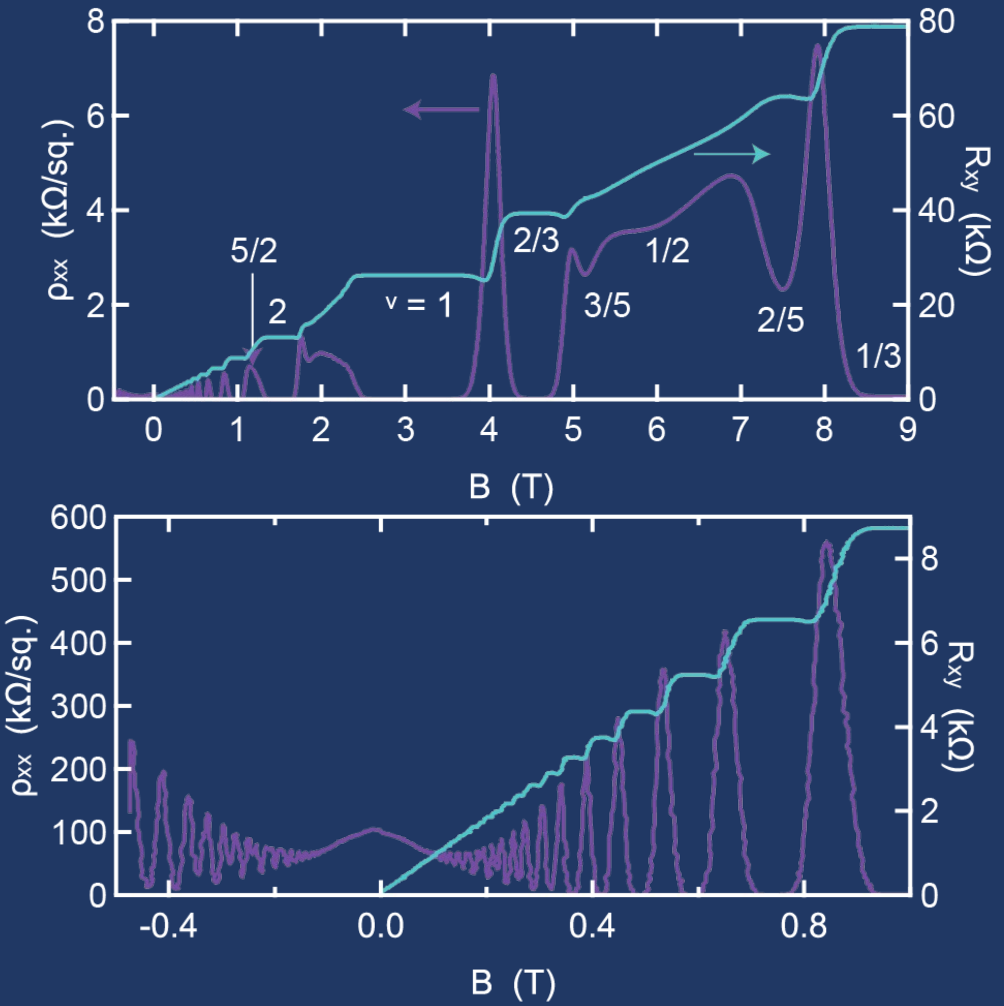

Lodari et al. APL2022

By tuning strain in the quantum well, high mobility and spin orbit engineering.

Superconductivity in low-disorder Ge/SiGe

Tosato et al arXiv 2022

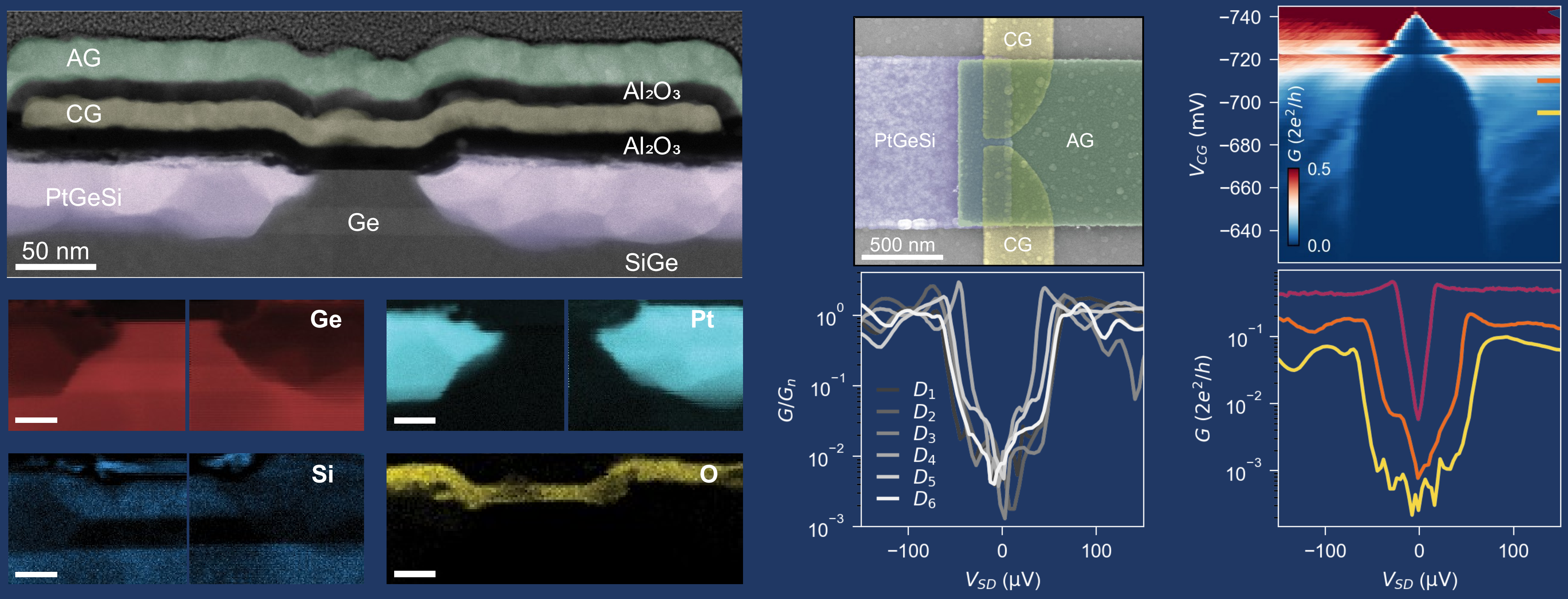

- Ge-silicidation for superconducting PtGeSi: additive nanofab
- Quantum well is buried -> High mobility Ge (6x10^{5}cm^2/Vs)
- Semi-super oxygen free interface
- SN QPC spectroscopy: reproducible superconducting gap free of subgap states (hard gap across devices)

Superconductivity and intrinsic topology

Read-Green (2000): chiral p-wave superconductor has special edge states

Fu-Kane (2008): chiral Majorana at the STI-MTI interface, or at a vortex

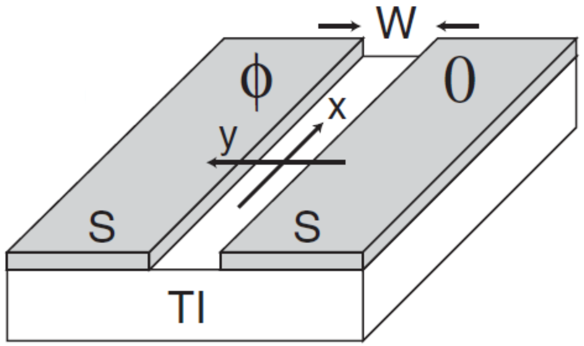

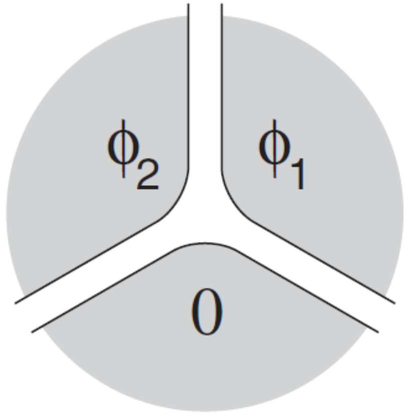

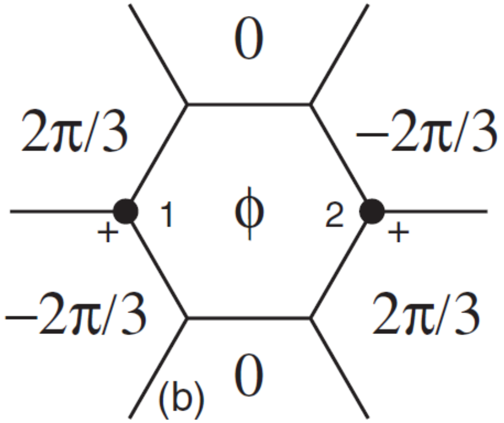

Superconductors with strong SOI

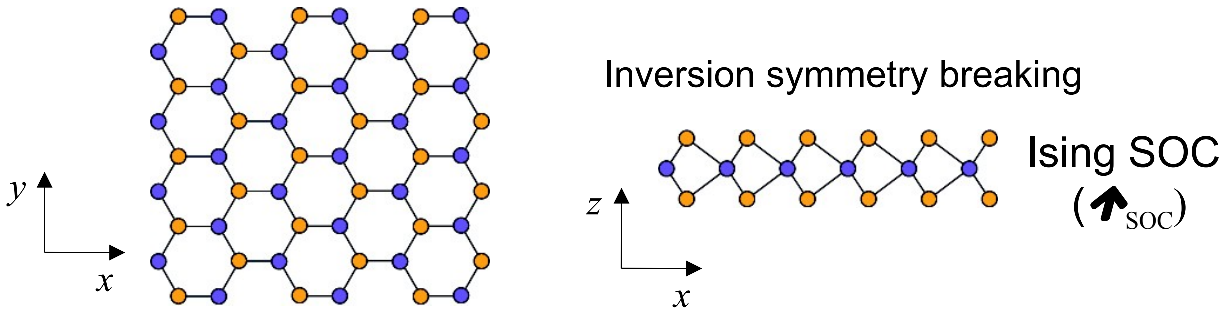

Crystal structure of transition metal dichalcogenides
(MoS_2, WS_2, $NbSe_2$…)

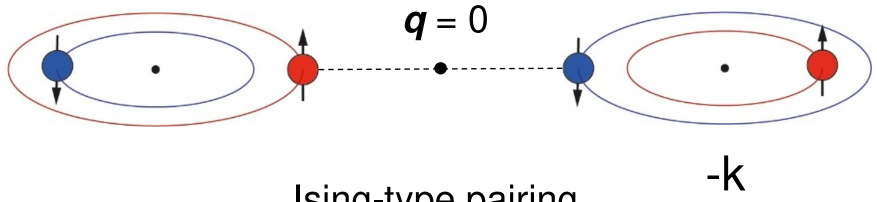

Ising-type pairing

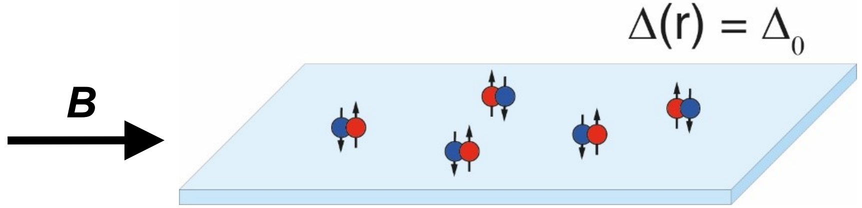

Uniform Ising superconductivity

k

Lu, J. M., et al. "Evidence for two-dimensional Ising superconductivity in gated MoS2." *Science* 350.6266 (2015): 1353-1357.

Topological superconductivity & dimensionality

Read-Green (2000): chiral p-wave superconductor has special edge states

Fu-Kane (2008): chiral Majorana at the STI-MTI interface, or at a vortex

Tanaka-Yokoyama-Nagaosa (2009): chiral Majorana as an Andreev bound state

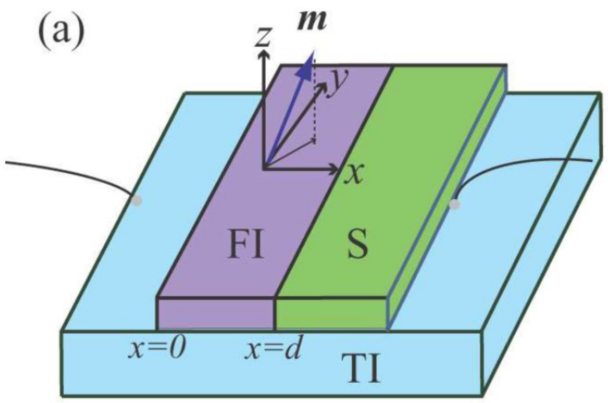

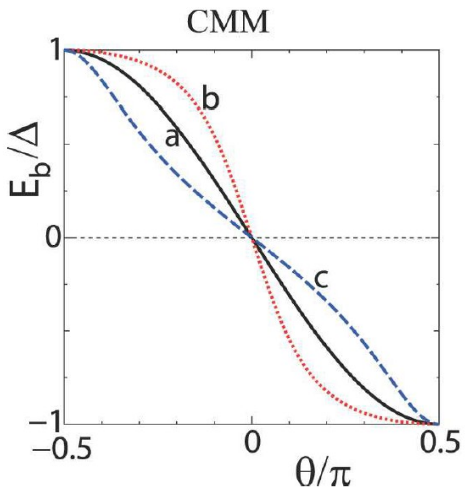

From 2D to 1D

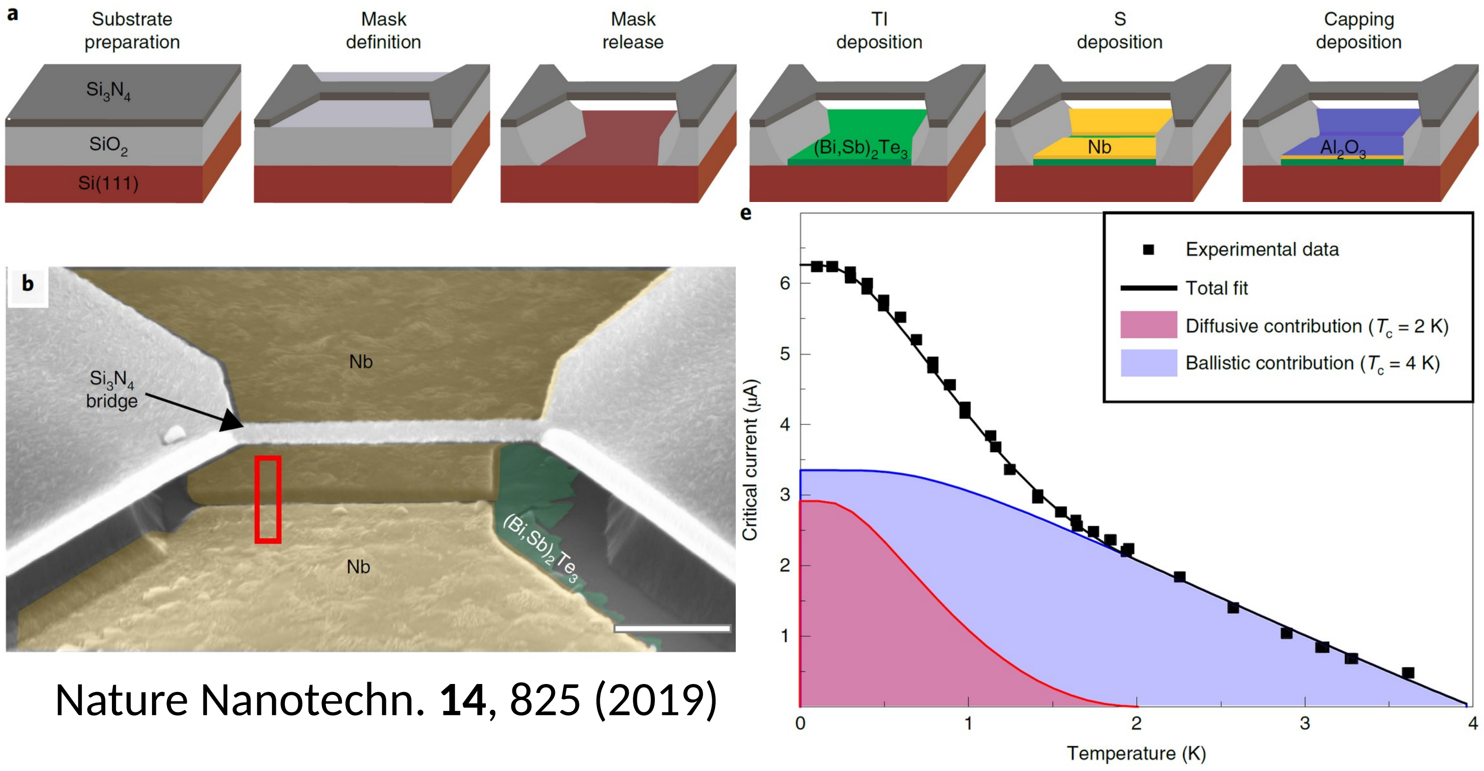

Nature Nanotechn. **14**, 825 (2019)

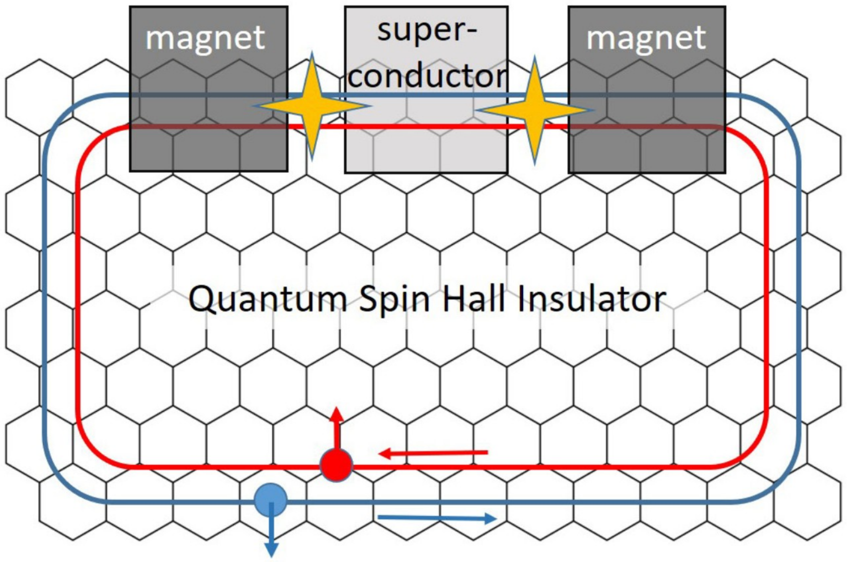

Superconductivity as a probe for edge contribution

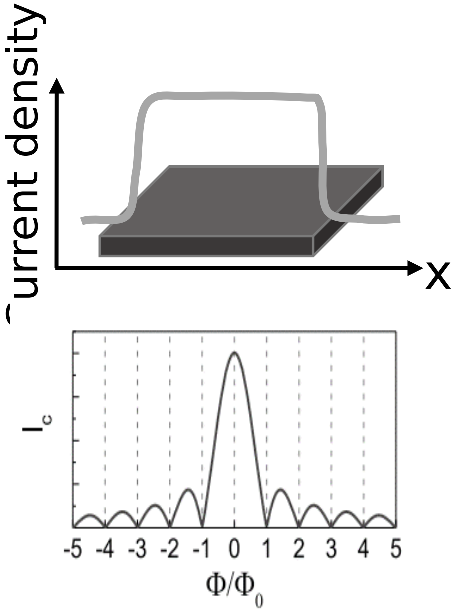

Fraunhofer pattern

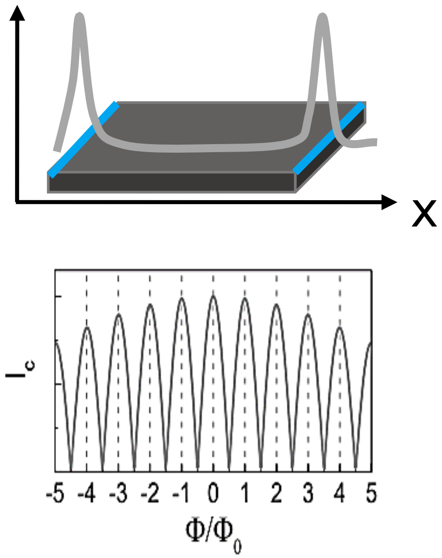

SQUID-like pattern

1D higher order topological hinge states in Cd_3As_2 Dirac semimetal:

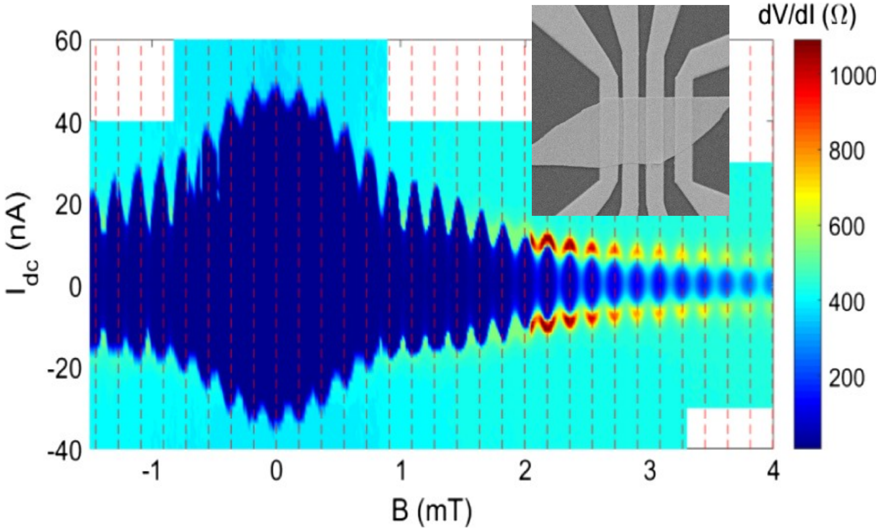

Reducing Electronic Transport Dimension to Topological Hinge States by Increasing Geometry Size of Dirac Semimetal Josephson Junctions
Cai-Zhen Li, An-Qi Wang, Chuan Li, Wen-Zhuang Zheng, Alexander Brinkman, Da-Peng Yu, Zhi-Min Liao
Phys. Rev. Lett. **124**, 156601 (2020).

First-Principles Topological Superconductivity

R. Reho, A. Kole, N. Wittemeier, Z. Zanolli

Debye Institute for Nanomaterials Science, Utrecht University

z.zanolli@uu.nl

October 26, 2022

First-principles quantum simulations

Density Functional Theory

- Fully capture the quantum nature of atomistic interactions
- Parameter-free
- Realistic materials
- Predicts:
    - Structure
    - Electronic bands
    - Magnetism
    - Topology
    - Quantum electron transport

Superconductivity (SC)

- Conventional BCS superconductors
- Unconventional cuprate and iron families of superconductors (high T_c)

First-principles (Topological) superconductivity

- Nature of unconventional SC
- Dimensionality effects
- Interplay between SC and magnetic phases
- Proximity induced SC
- Visualization of zero energy states

First-principles theory and simulation to study exotic forms of superconductivity (SC) in realistic materials

r.reho@uu.nl

BdG + DFT Hamiltonian

$$\psi_i^\sigma \Rightarrow \begin{pmatrix} u_i^\sigma \\ v_i^\sigma \end{pmatrix}$$

electrons

holes

$$H_{\mathrm{DFT}} \Rightarrow \left(\begin{array}{c|c} H_{\mathrm{elec-elec}} & \Delta \\ \hline -(\Delta)^* & -(H_{\mathrm{elec-elec}})^* \end{array}\right)$$

Superconducting (Cooper pairing) potential

- Localized atomic orbitals φ_μ with μ ≡ R, n, l, m (R atom index, n, l, m quantum numbers)

$$\Delta_{\mu\upsilon} = \int \varphi_\mu \Delta \varphi_\upsilon$$

- $\Delta_{\mu\upsilon}$: Coupling between one electron in orbital φ_μ and one hole in orbital φ_υ

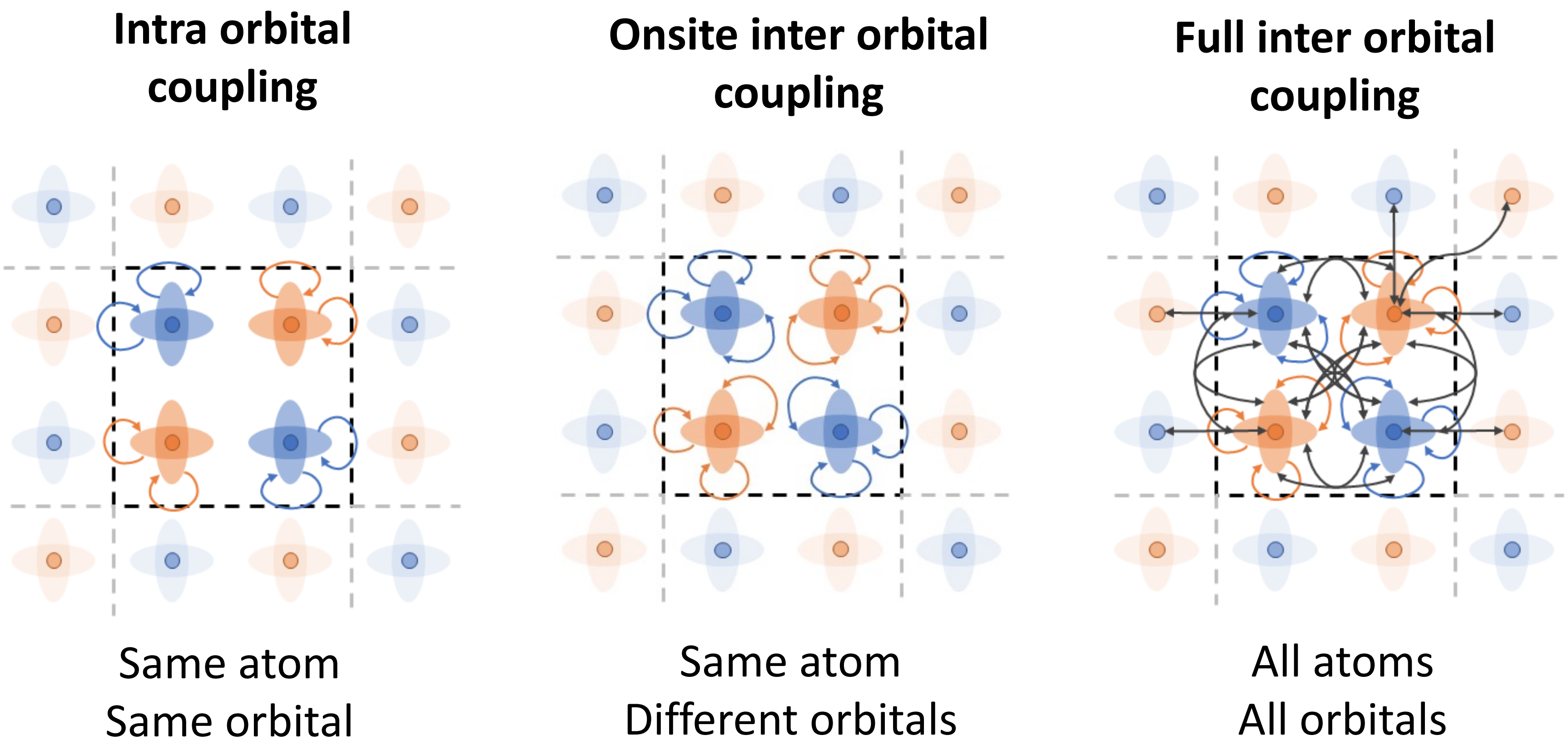

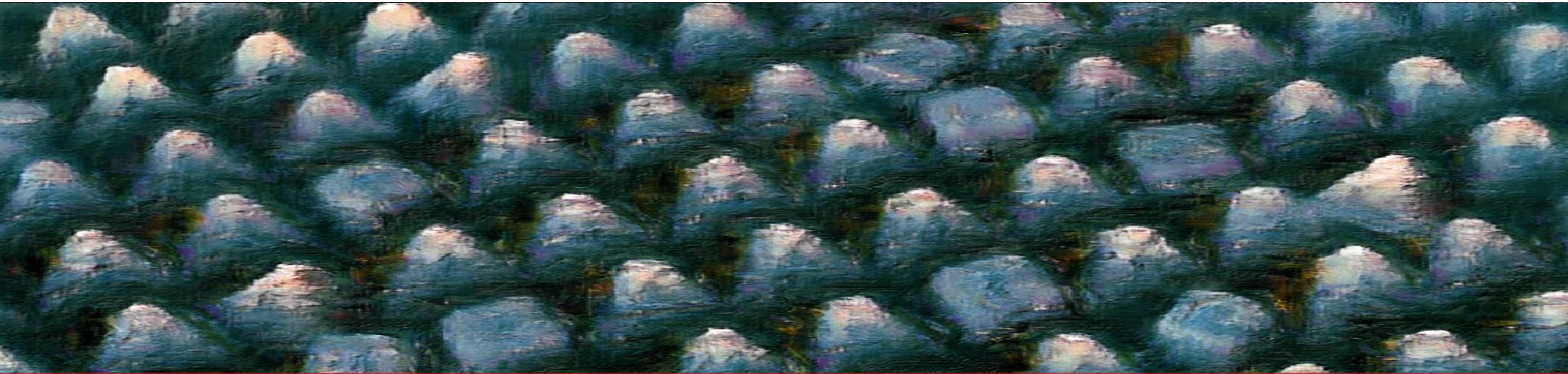

Selective Area Growth of PbTe Nanowire Networks

QuMat Kick-Off

Jason Jung, Sander G. Schellingerhout, Orson A.H. van der Molen, Markus F. Ritter, Sofieke C. ten Kate, Wouter H.J. Peeters, Sem de Loijer, Marcel A. Verheijen, Heike Riel, Fabrizio Nichele, Erik P.A.M. Bakkers

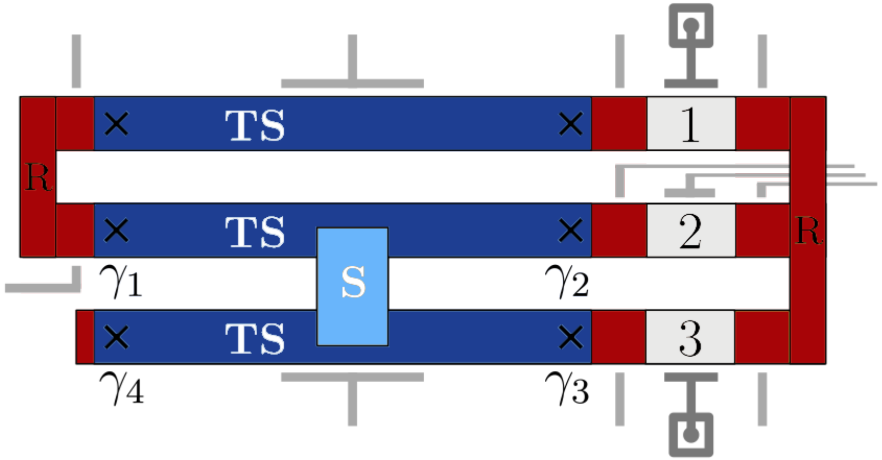

Plugge, S. *et al.* *New Journal of Physics* **19,** 012001 (2017)

Spin-orbit coupling [eV Å]
Landé g-Factor

Lutchyn, R. M. *et al.* *Nature Reviews Materials* **3,** 52–68 (2018)
Yuan, S. *et al.* *Physical Review B* **55,** 4607–4619 (1997)
Cao, Z. *et al.* *Physical Review B* **105,** 085424 (2022)

Goal: Scalable growth of single-crystalline PbTe networks

Layer growth on bare InP (111)A

- 10.1% lattice mismatch
- changing crystal structure (zincblende/rock salt)
- diverging thermal expansion coefficient

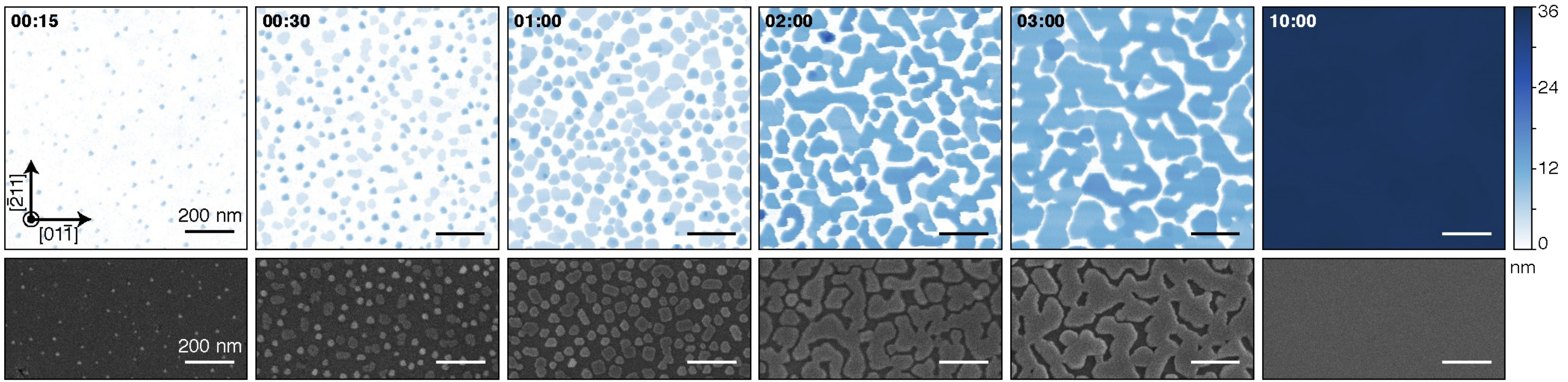

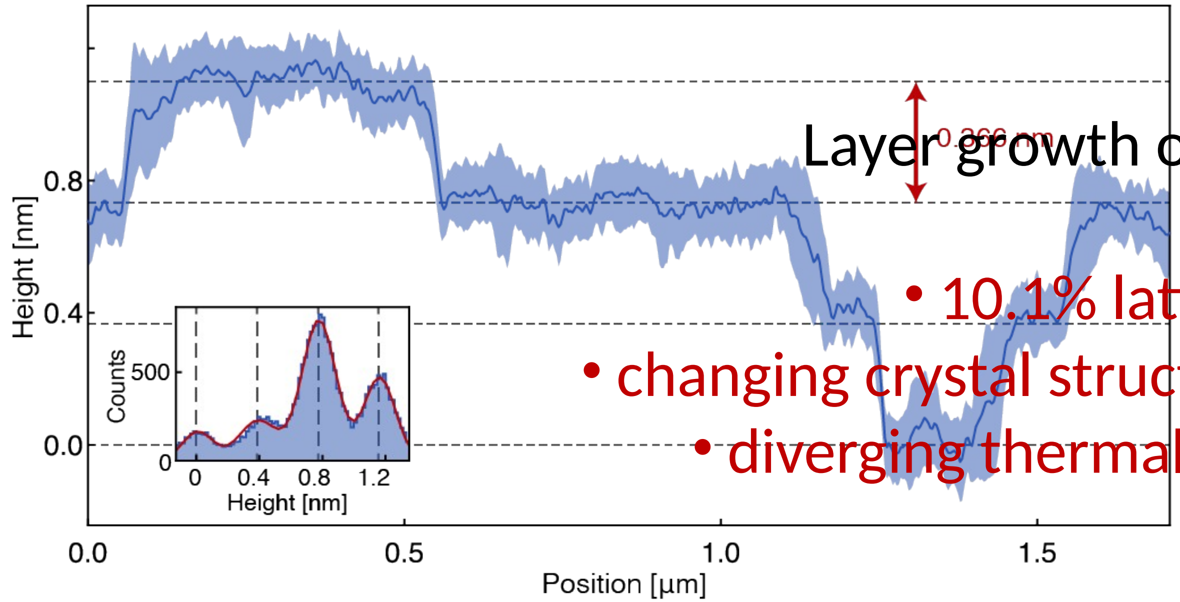

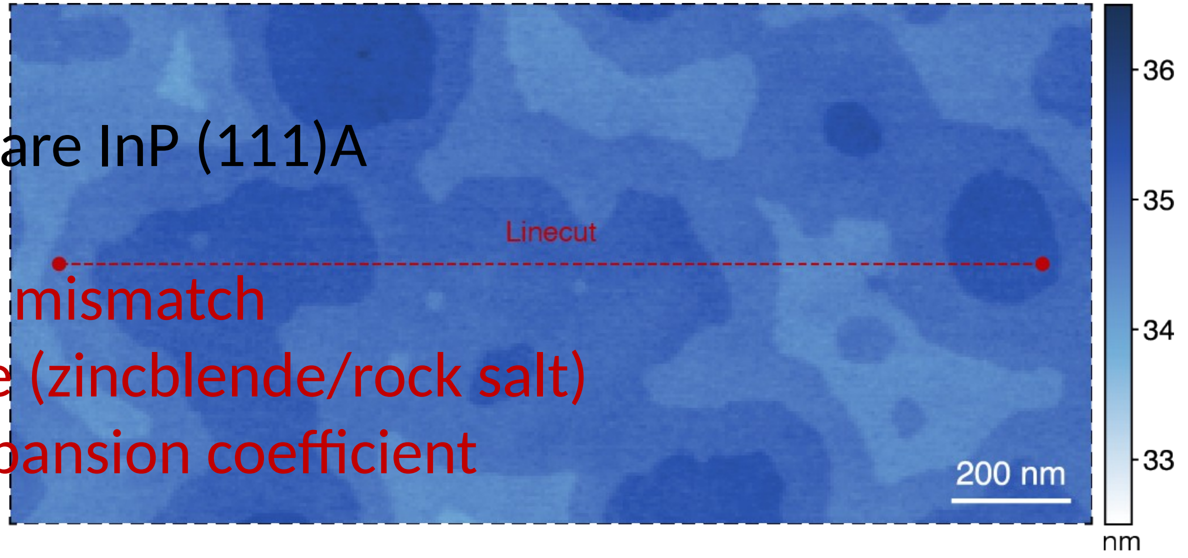

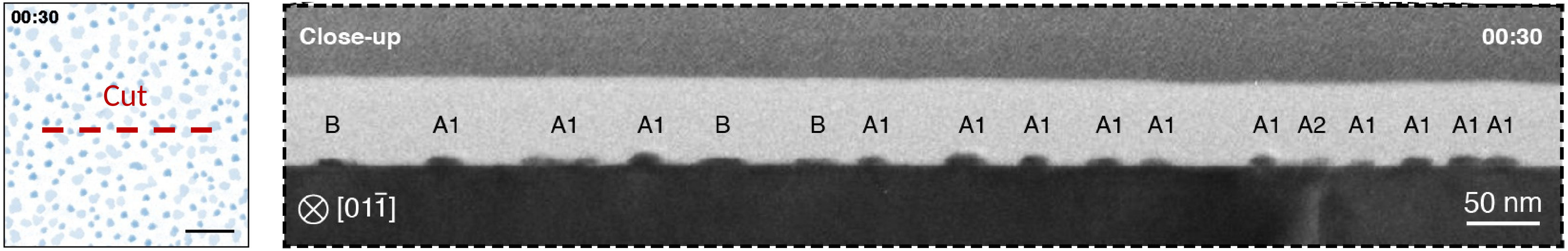

Type A_1 - 73%

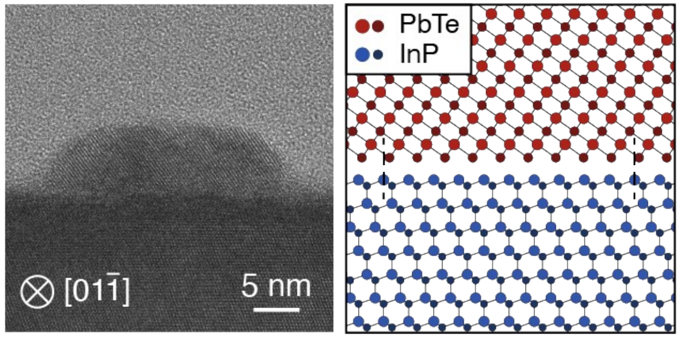

Type A_2 - 7%

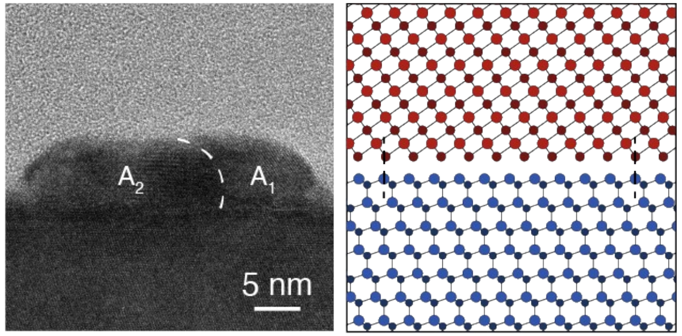

Type B - 20%

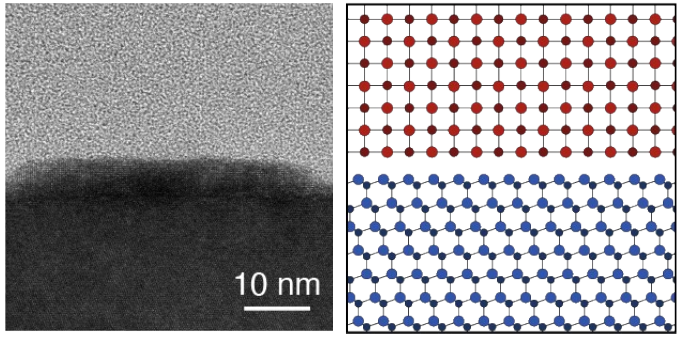

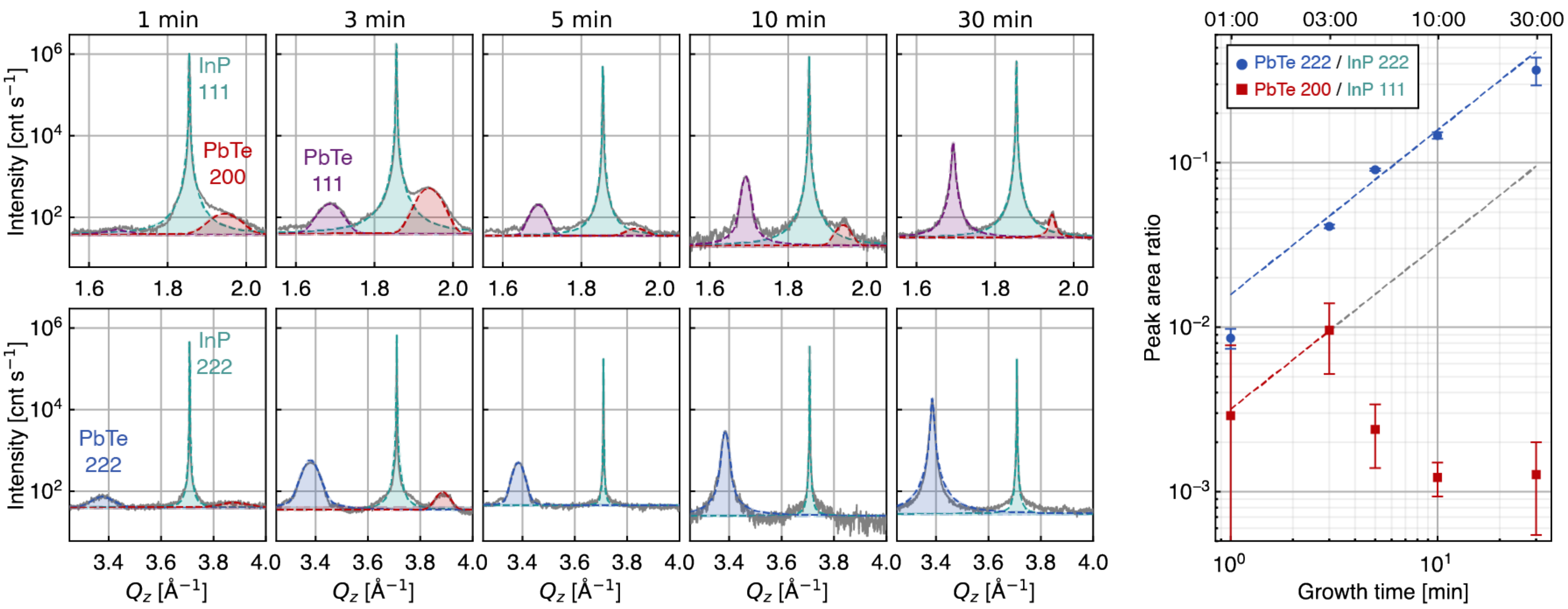

After 30 min 99.84 ± 0.06% of the film volume exhibits the twinned (111)-orientation

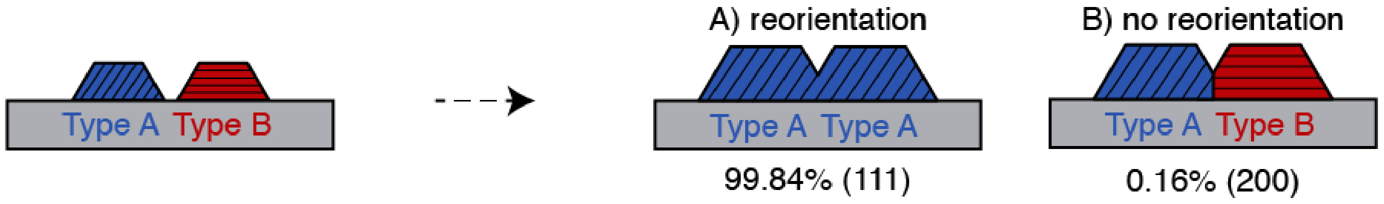

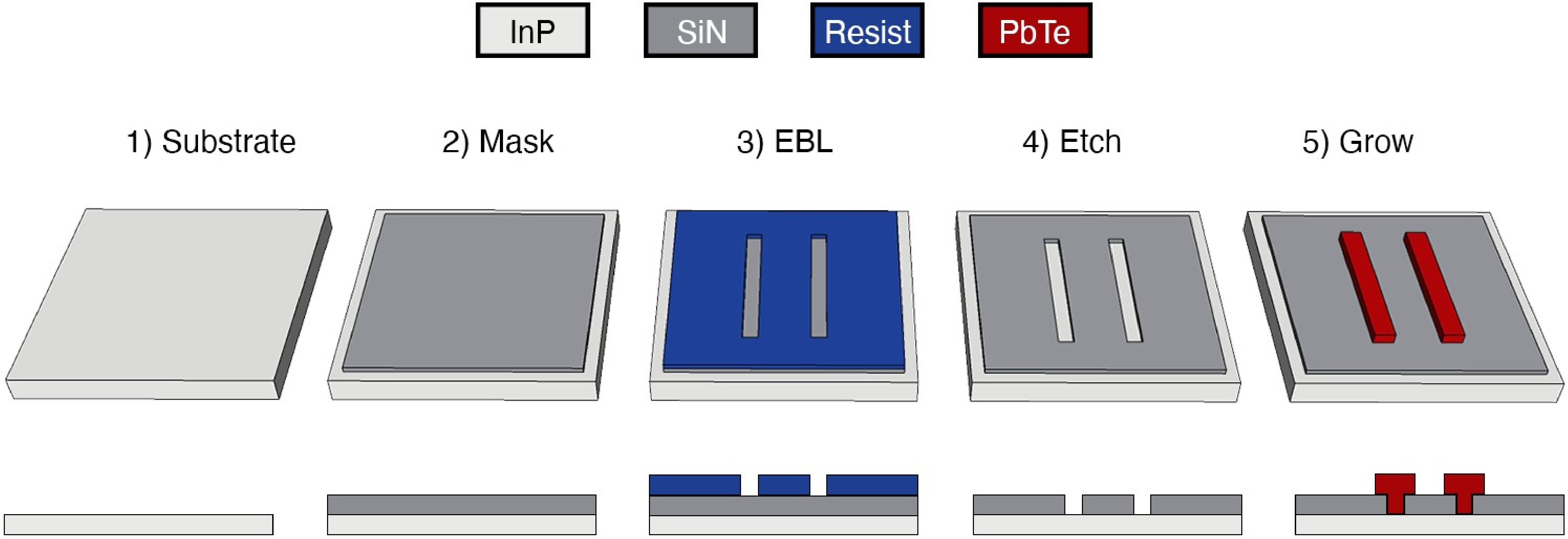
InP
SiN
Resist
PbTe
1) Substrate
2) Mask
3) EBL
4) Etch
5) Grow

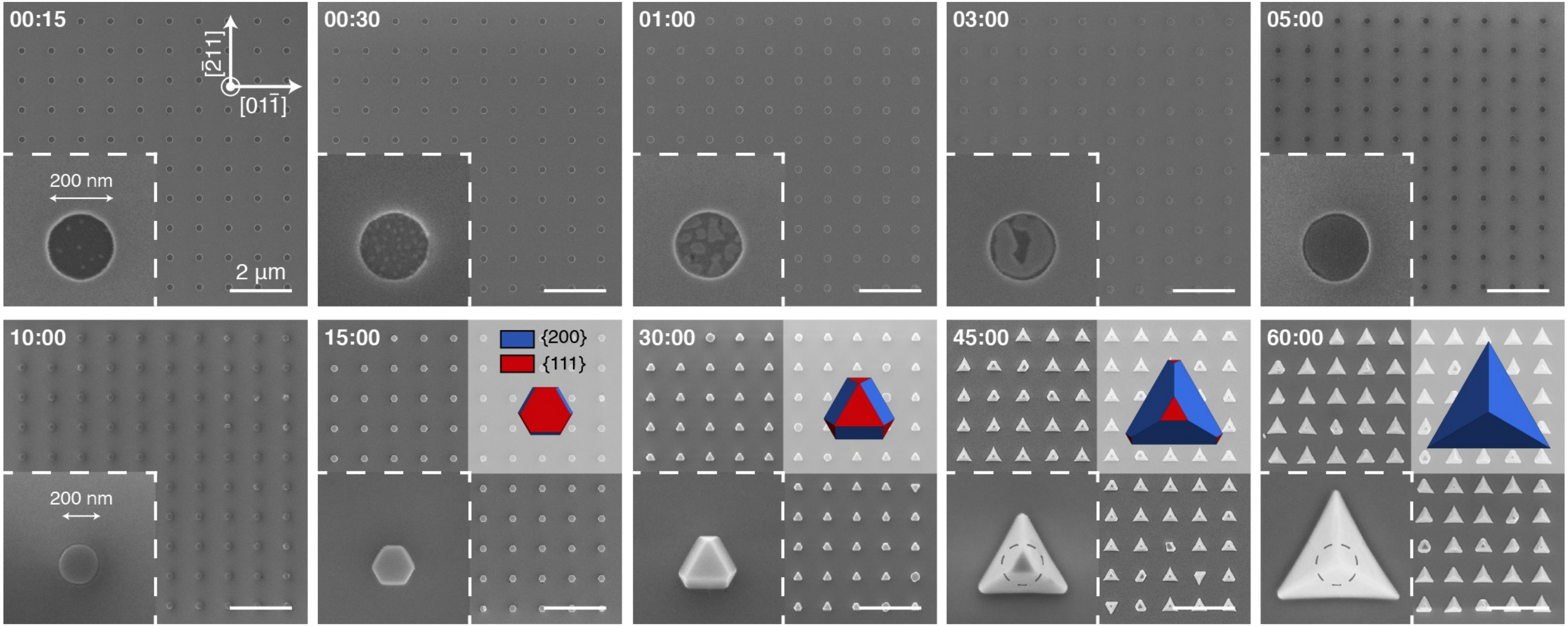

00:15
[2̄11]
[011̄]
200 nm
2 µm
00:30
01:00
03:00
05:00
10:00
200 nm
15:00
{200}
{111}
30:00
45:00
60:00

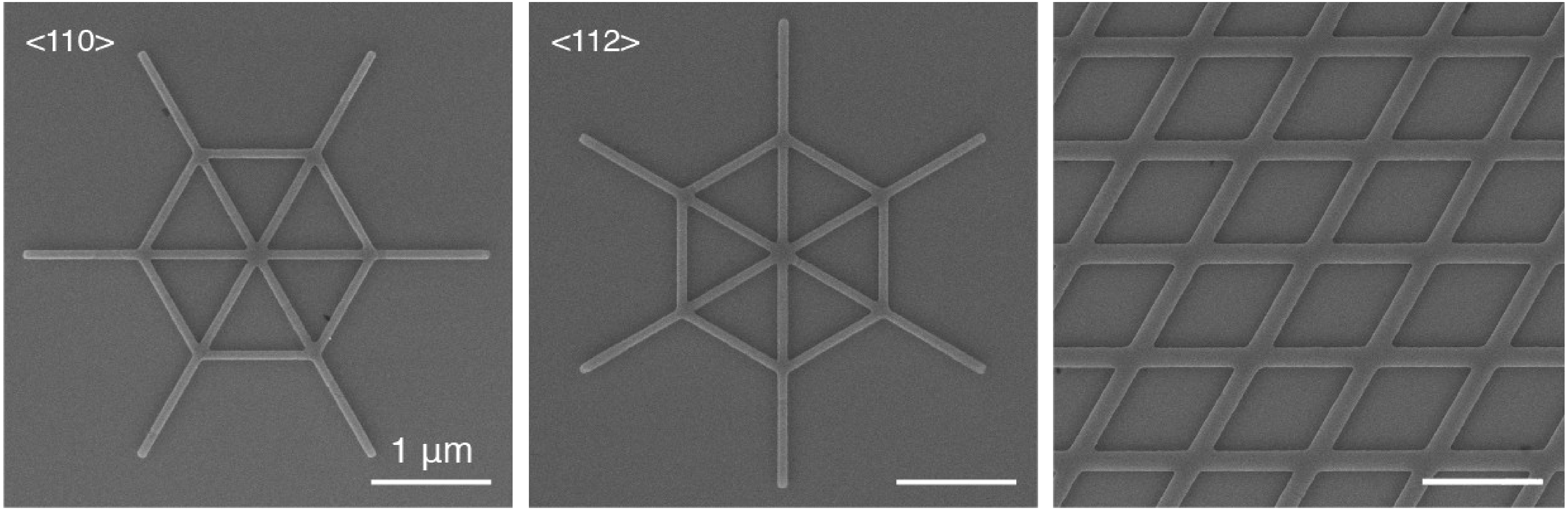
<110>
1 µm
<112>

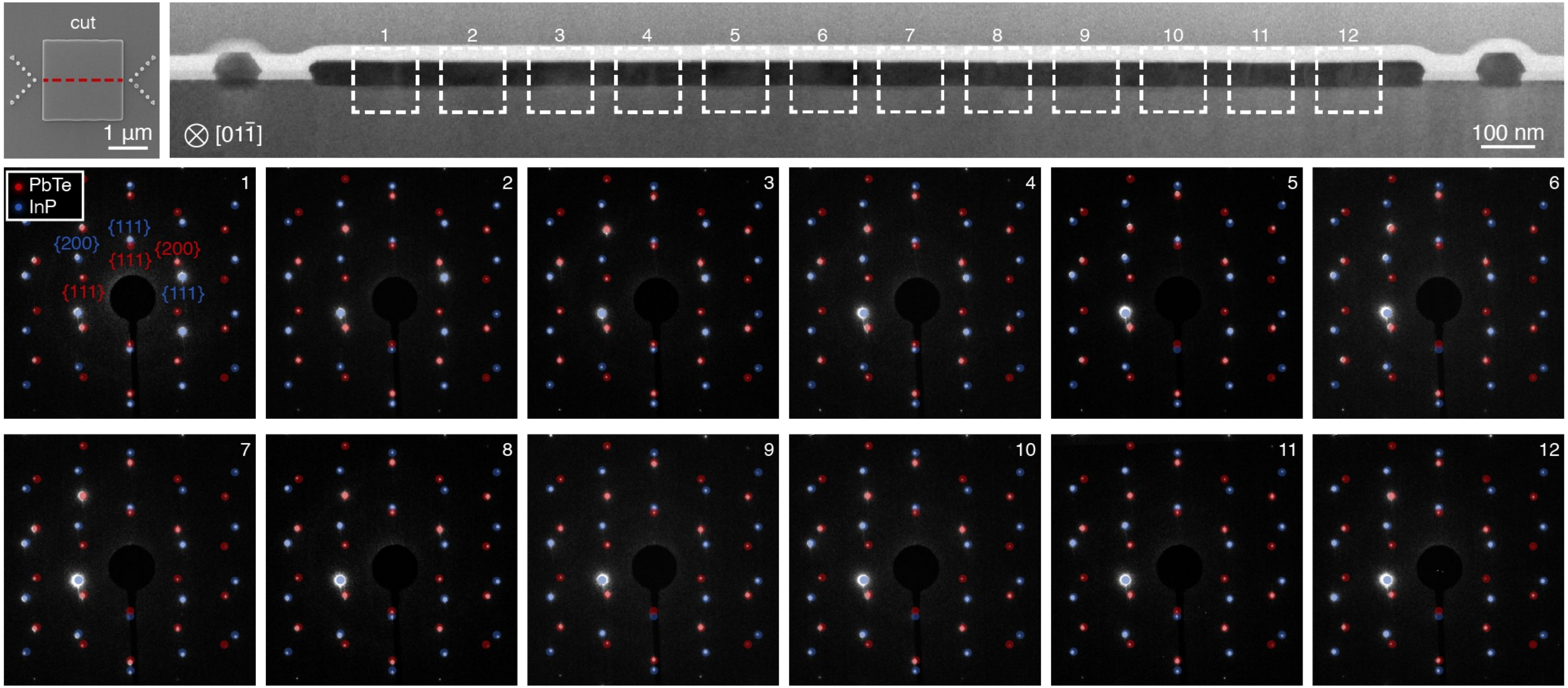
cut
1 µm
1
2
3
4
5
6
7
8
9
10
11
12
⊗ [01$\bar{1}$]
100 nm
PbTe
InP
{111}
{200}
{111}
{200}
{111}
{111}

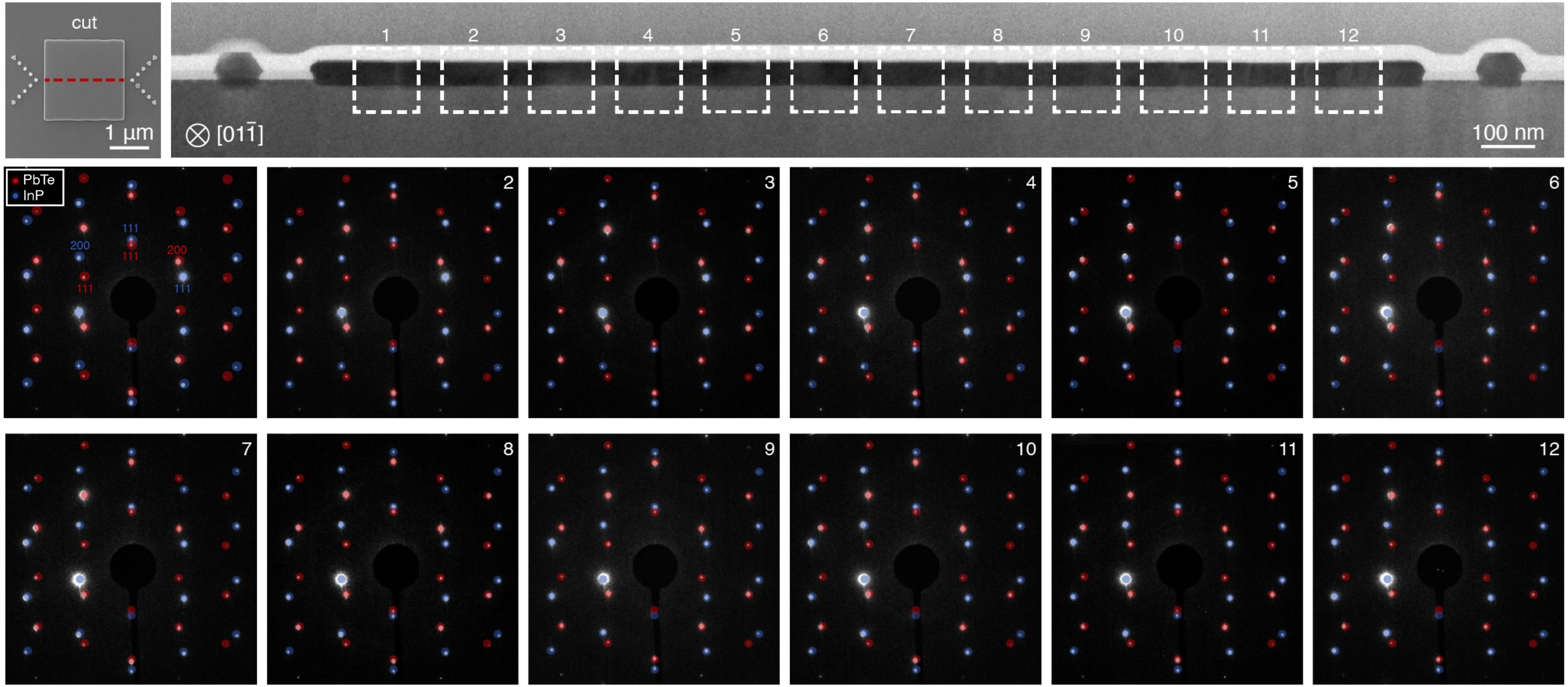

cut
1 µm
1
2
3
4
5
6
7
8
9
10
11
12
[01$\bar{1}$]
100 nm
PbTe
InP
111
200
111
200
111
111
2
3
4
5
6
7
8
9
10
11
12

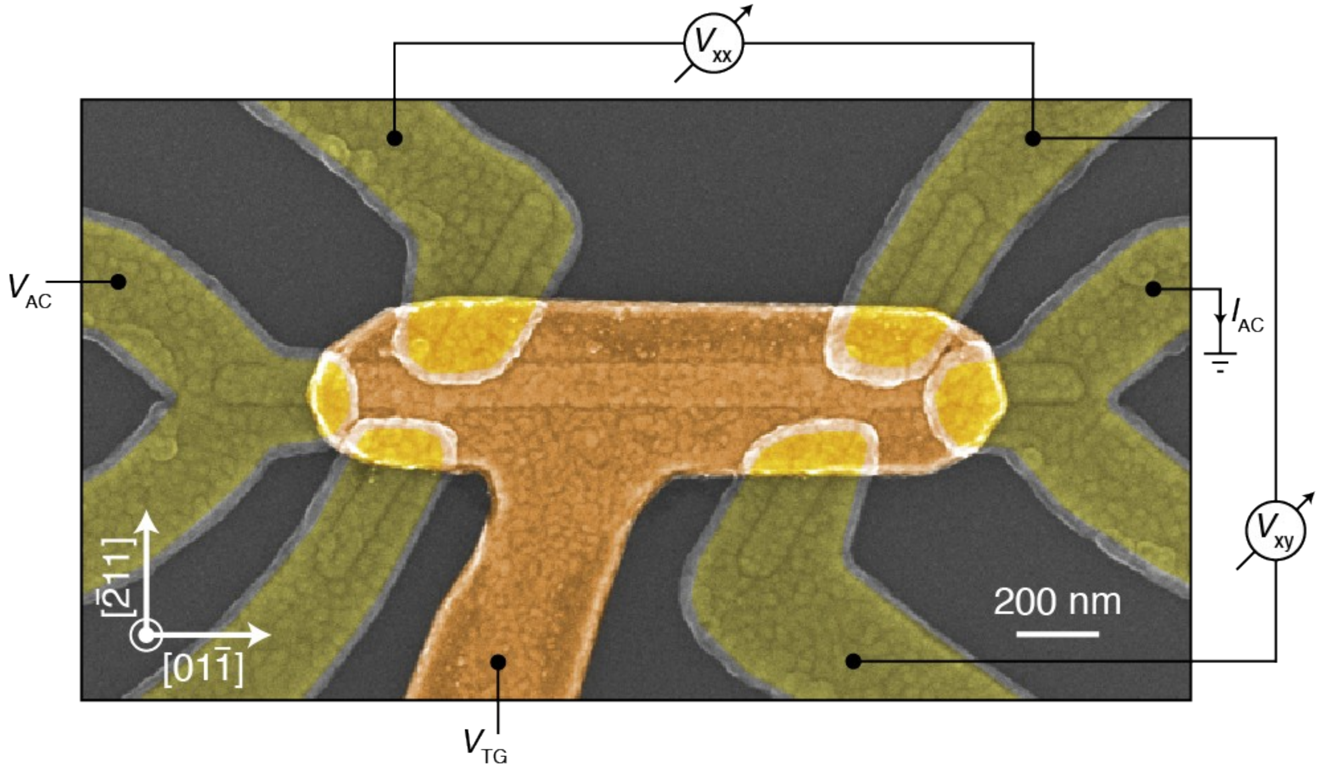

$$\mu_{\mathrm{H}} = 5600\ \mathrm{cm}^2/(\mathrm{Vs})$$

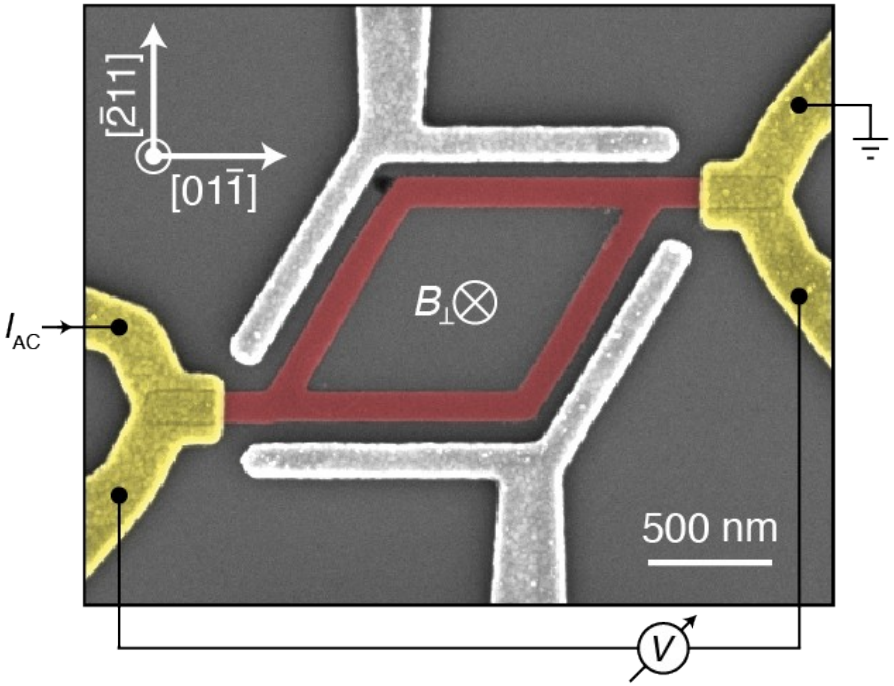

$$l_\phi > 21\ \mu\mathrm{m}$$

Conclusions

- Reorientation process facilitates single crystalline layer
  - large lattice mismatch
  - varying crystal structure
  - diverging thermal expansion coefficient
- SAG of PbTe on InP (111)A
- Flexible in its design, scalable, and reproducible
- Hall mobility up to 5600 $cm^2/(Vs)$ and a phase-coherence length exceeding 21 µm

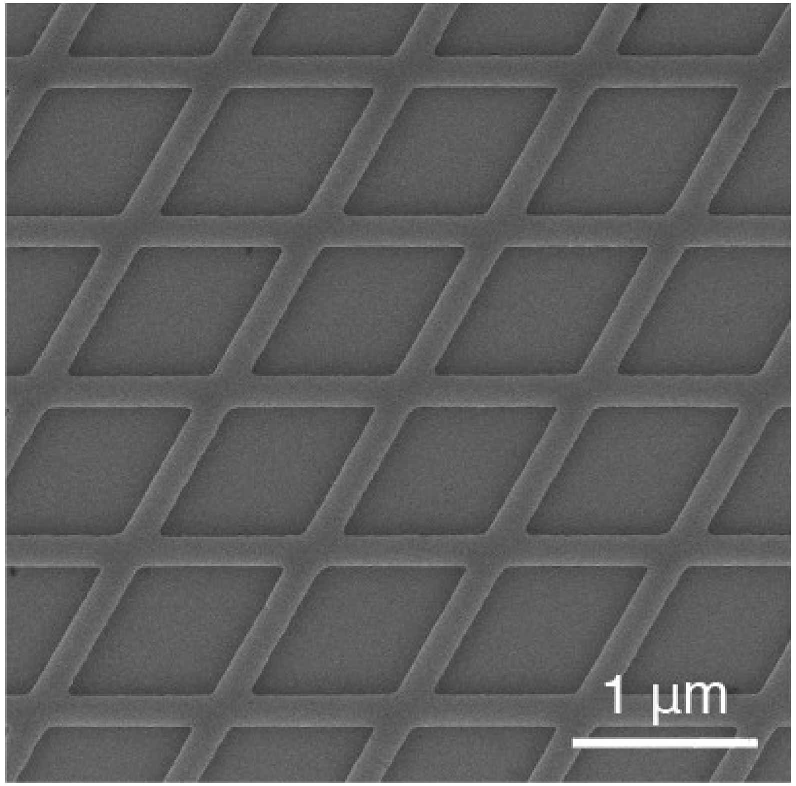

Email: j.jung@tue.nl

Outlook

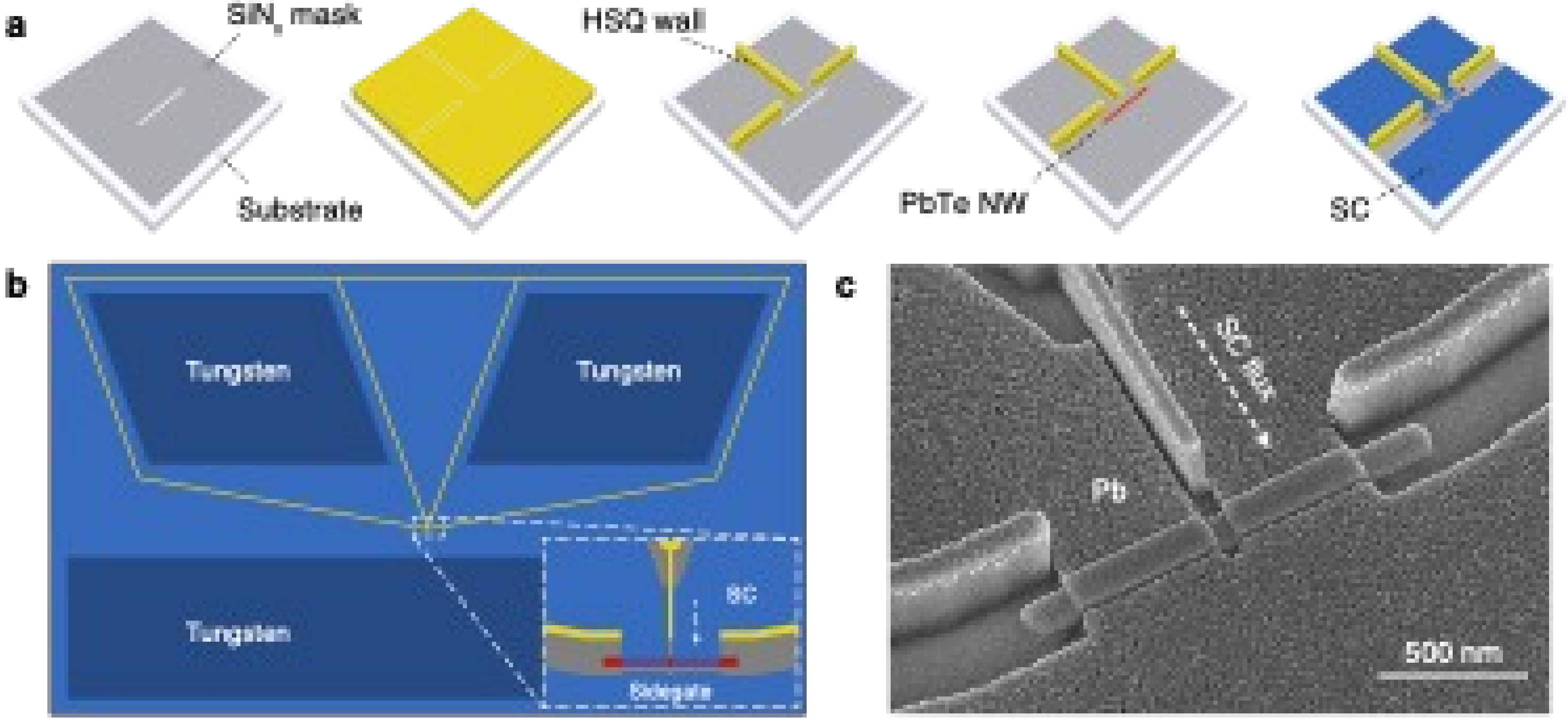
a
SiN mask
Substrate
HSQ wall
PbTe NW
SC
b
Tungsten
Tungsten
Tungsten
SC
Sidegate
c
SC flux
Pb
500 nm

Outlook

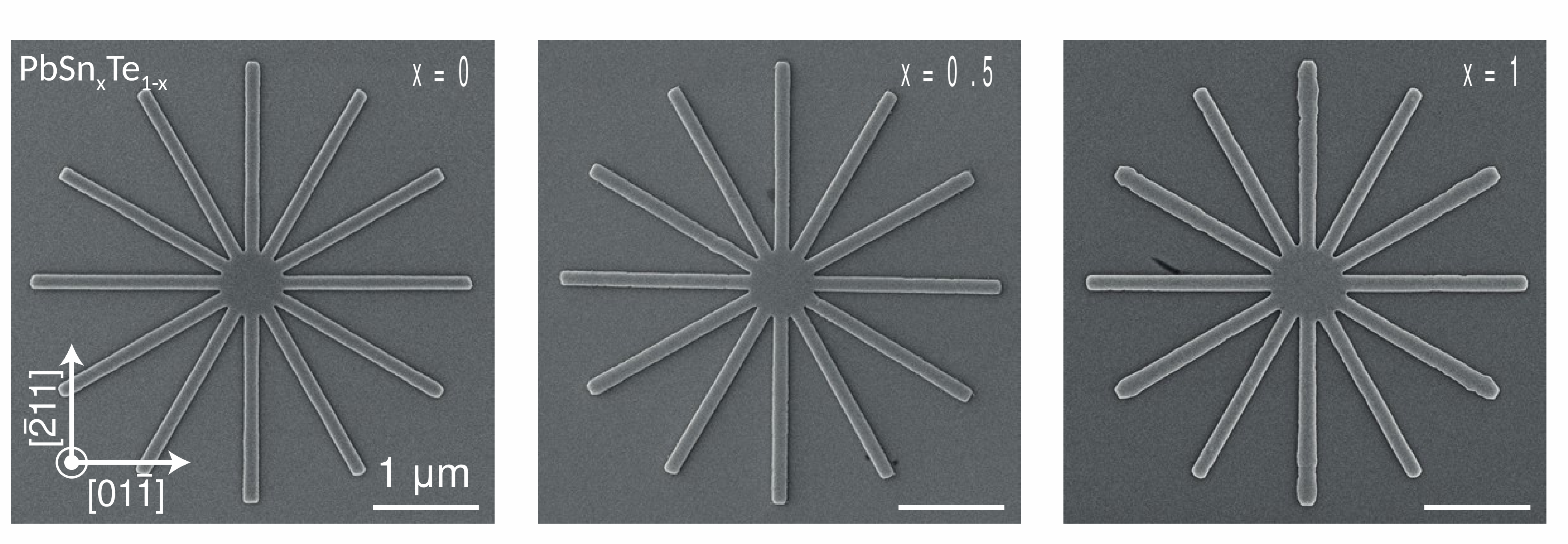

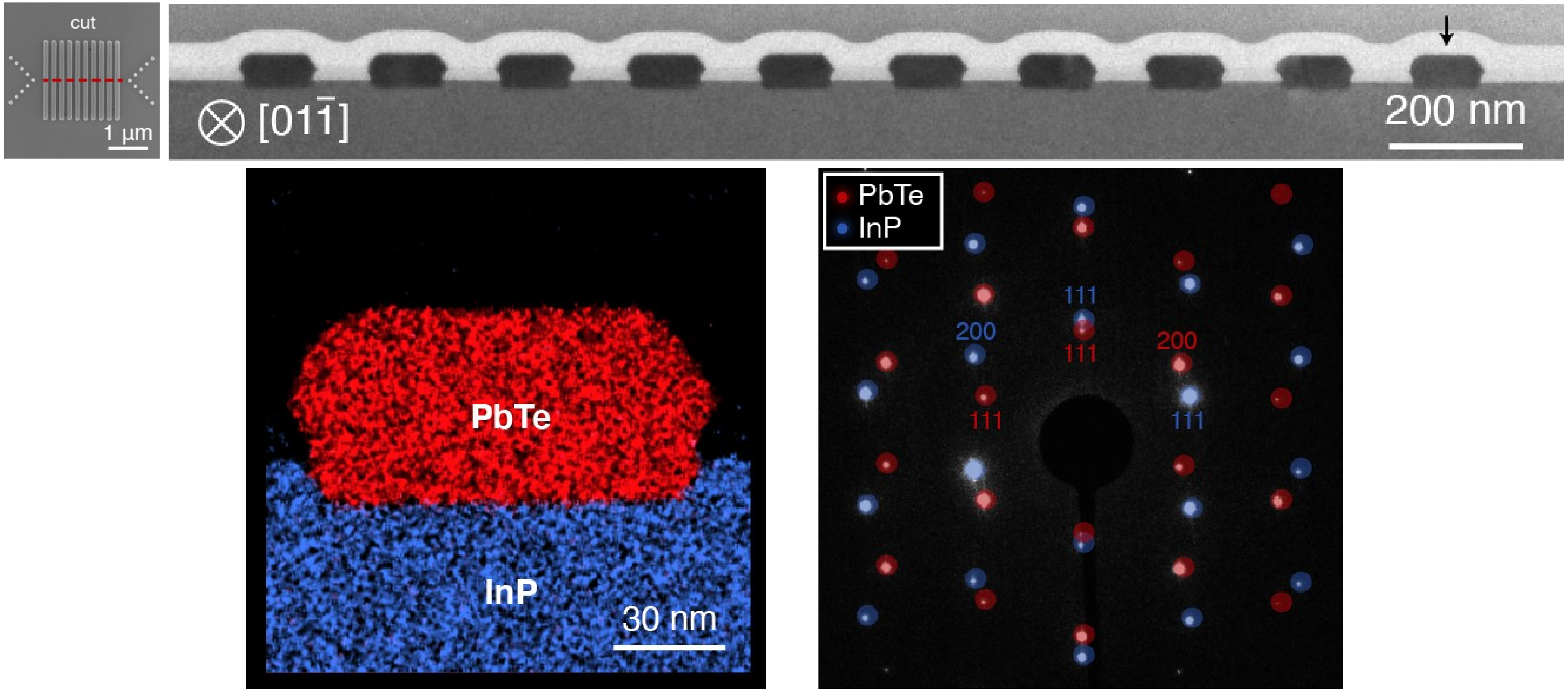
cut
1 µm
[01̄1]
200 nm
PbTe
InP
30 nm
PbTe
InP
111
200
111
200
111
111

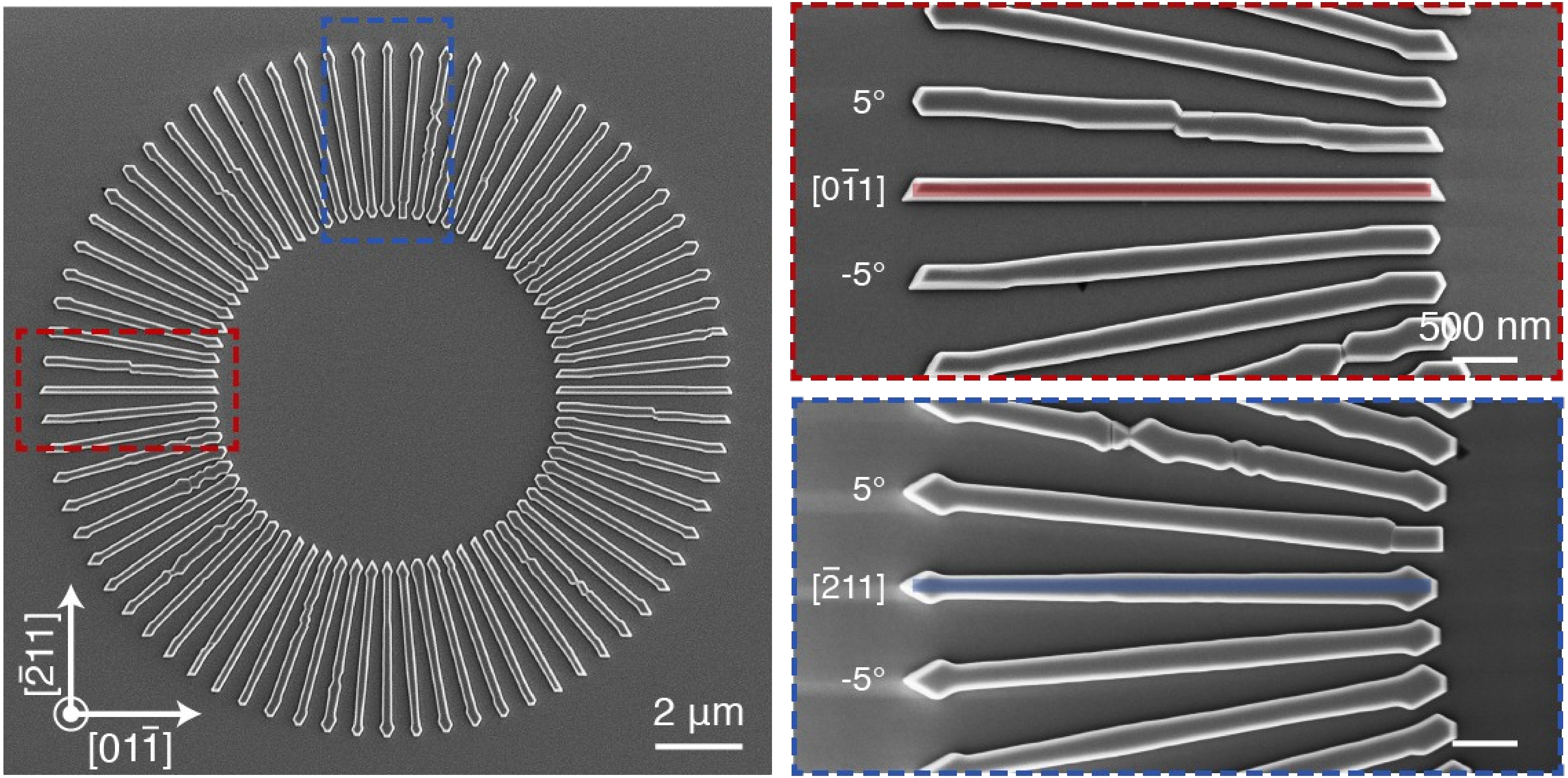

[2̄11]
[011̄]
2 µm
5°
[01̄1]
-5°
500 nm
5°
[2̄11]
-5°

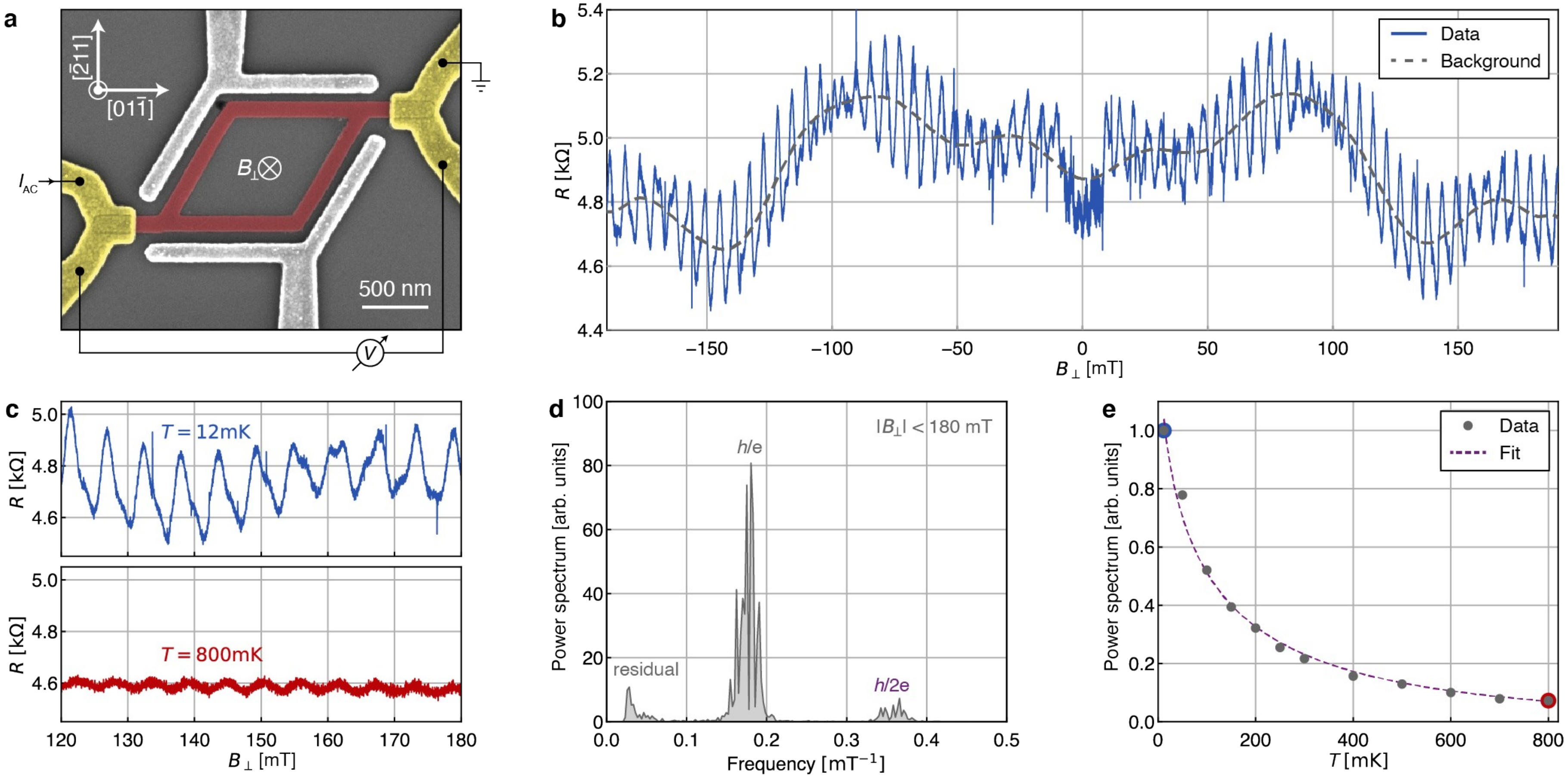
a
[$\bar{2}$11]
[01$\bar{1}$]
$B_\perp$
I_{AC}
500 nm
V
b
Data
Background
R [kΩ]
$B_\perp$ [mT]
c
T = 12mK
T = 800mK
R [kΩ]
$B_\perp$ [mT]
d
|$B_\perp$| < 180 mT
h/e
residual
h/2e
Power spectrum [arb. units]
Frequency [mT^{-1}]
e
Data
Fit
Power spectrum [arb. units]
T [mK]

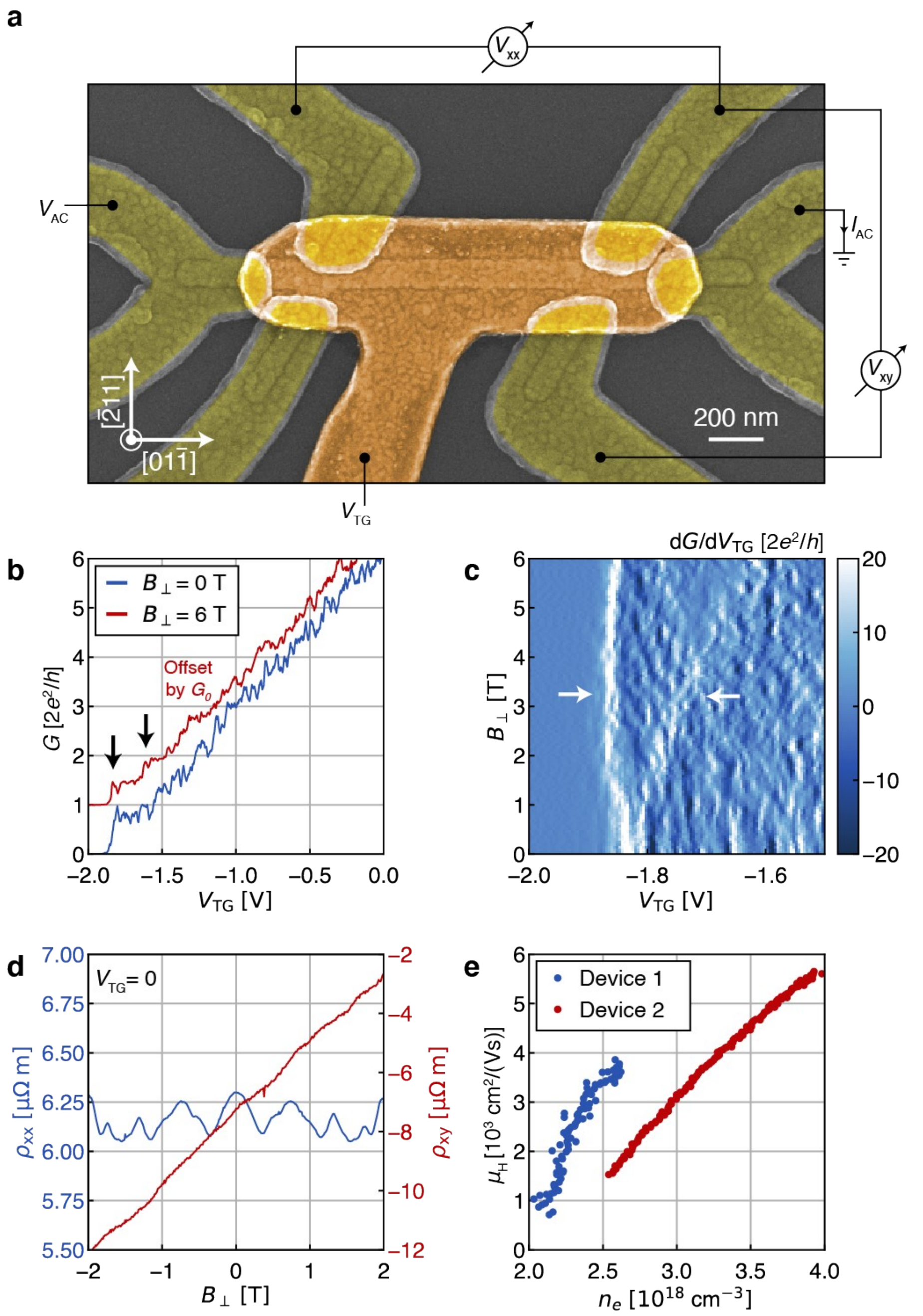

a
V_{xx}
V_{AC}
I_{AC}
V_{xy}
[$\bar{2}$11]
[01$\bar{1}$]
200 nm
V_{TG}
b
$B_\perp = 0$ T
$B_\perp = 6$ T
Offset by G_0
G [$2e^2/h$]
V_{TG} [V]
c
dG/dV_{TG} [$2e^2/h$]
$B_\perp$ [T]
V_{TG} [V]
d
$V_{TG} = 0$
ρ_{xx} [µΩ m]
ρ_{xy} [µΩ m]
$B_\perp$ [T]
e
Device 1
Device 2
μ_H [10^3 cm^2/(Vs)]
n_e [10^{18} cm^{-3}]

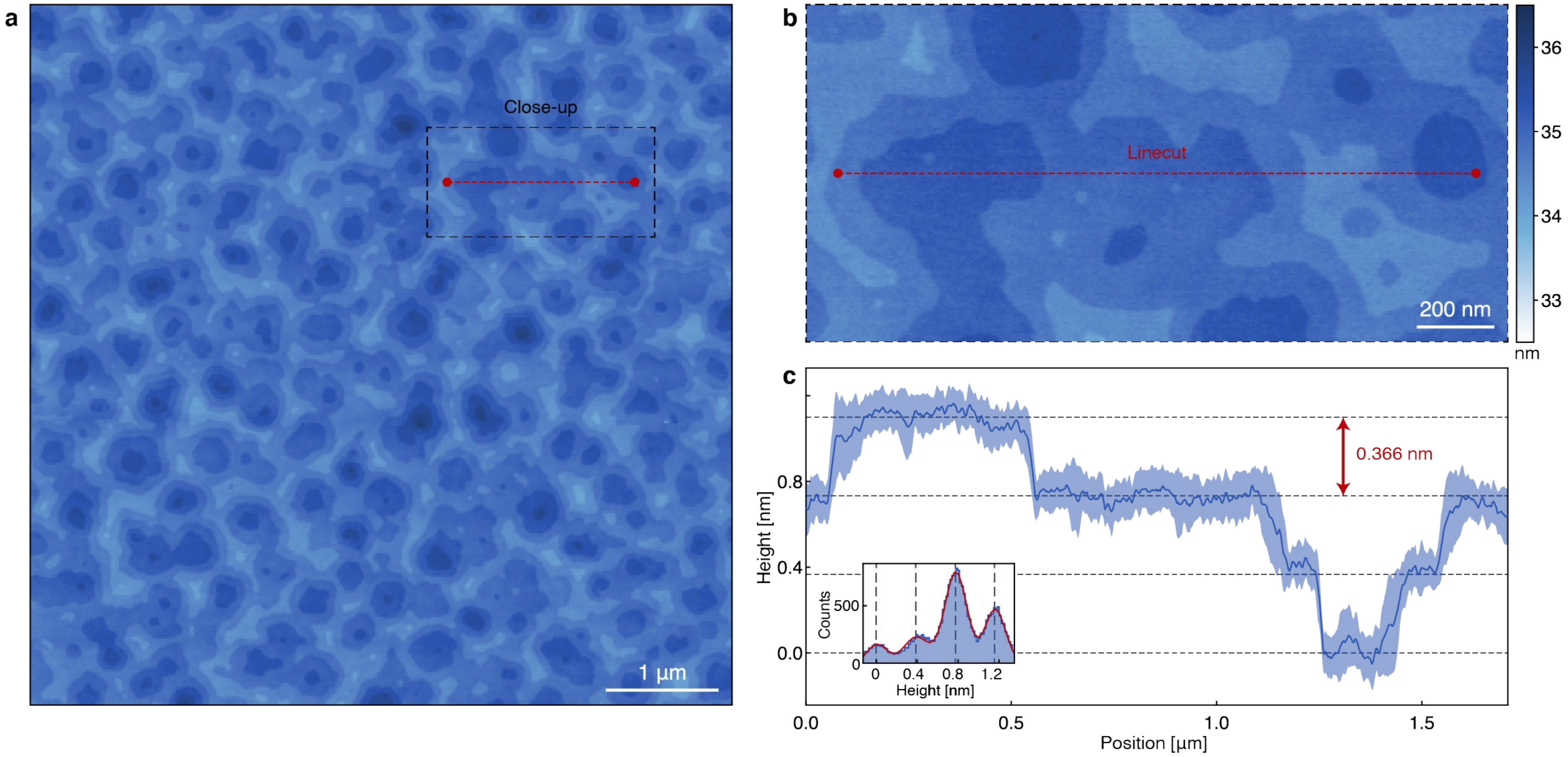
a
Close-up
1 µm
b
Linecut
200 nm
36
35
34
33
nm
c
0.366 nm
0.8
0.4
0.0
Height [nm]
Counts
500
0
0
0.4
0.8
1.2
Height [nm]
0.0
0.5
1.0
1.5
Position [µm]

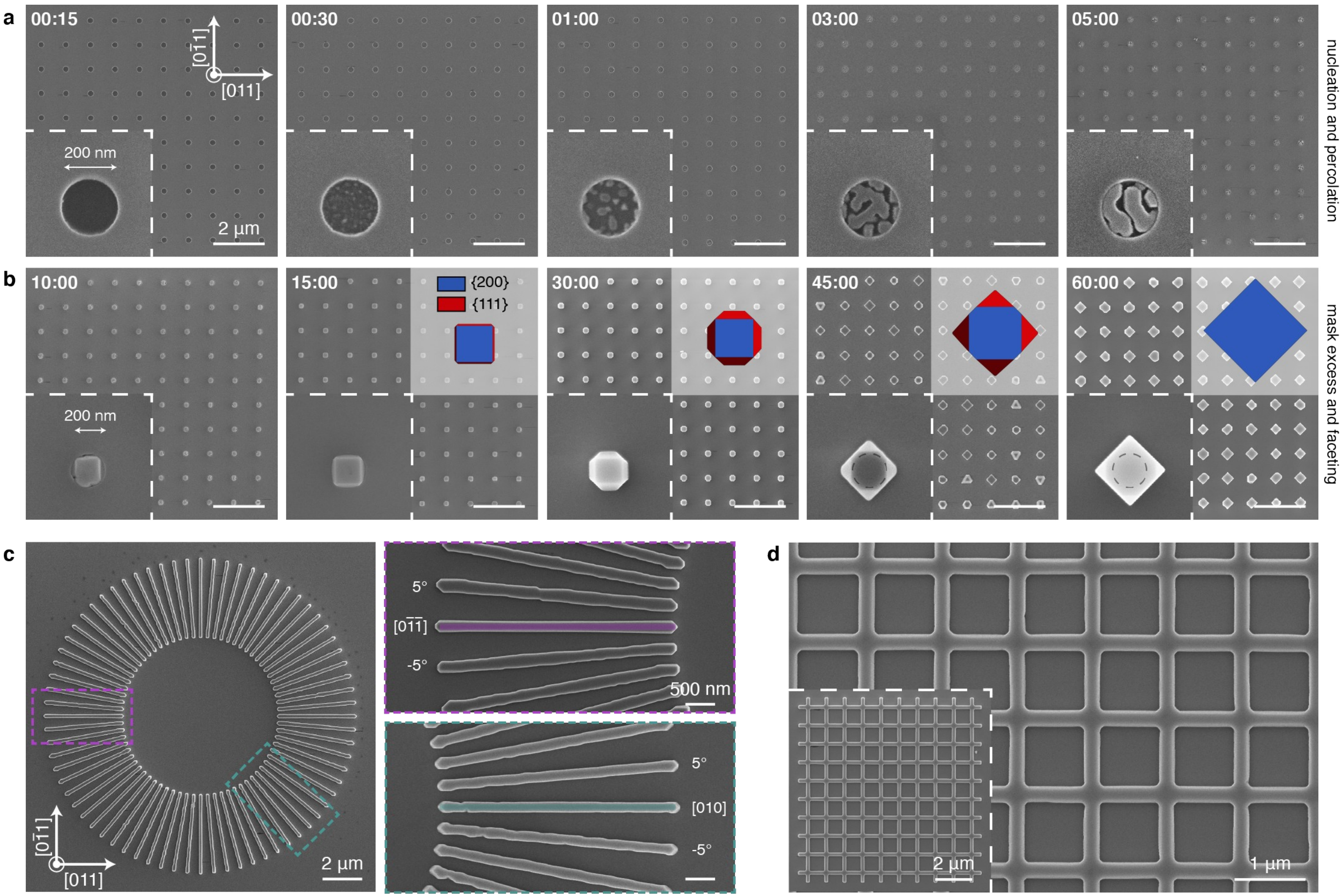

a
00:15
00:30
01:00
03:00
05:00
[011]
200 nm
2 µm
nucleation and percolation
b
10:00
15:00
30:00
45:00
60:00
{200}
{111}
200 nm
mask excess and faceting
c
5°
-5°
500 nm
[010]
[011]
2 µm
d
2 µm
1 µm

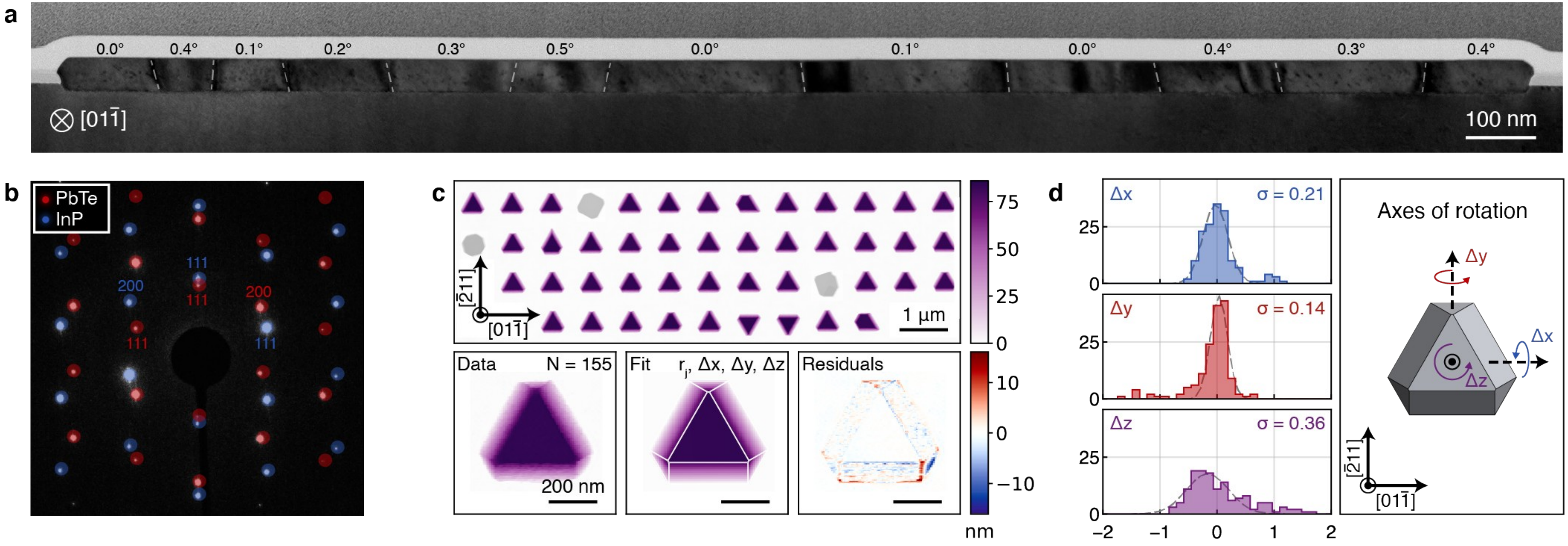
a
0.0°
0.4°
0.1°
0.2°
0.3°
0.5°
0.0°
0.1°
0.0°
0.4°
0.3°
0.4°
[01$\bar{1}$]
100 nm
b
PbTe
InP
111
200
111
200
111
111
111
c
[$\bar{2}$11]
[01$\bar{1}$]
1 μm
75
50
25
0
Data
N = 155
200 nm
Fit
r_j, Δx, Δy, Δz
Residuals
10
0
−10
nm
d
Δx
σ = 0.21
Δy
σ = 0.14
Δz
σ = 0.36
25
0
−2
−1
0
1
2
Axes of rotation
Δy
Δx
Δz
[$\bar{2}$11]
[01$\bar{1}$]

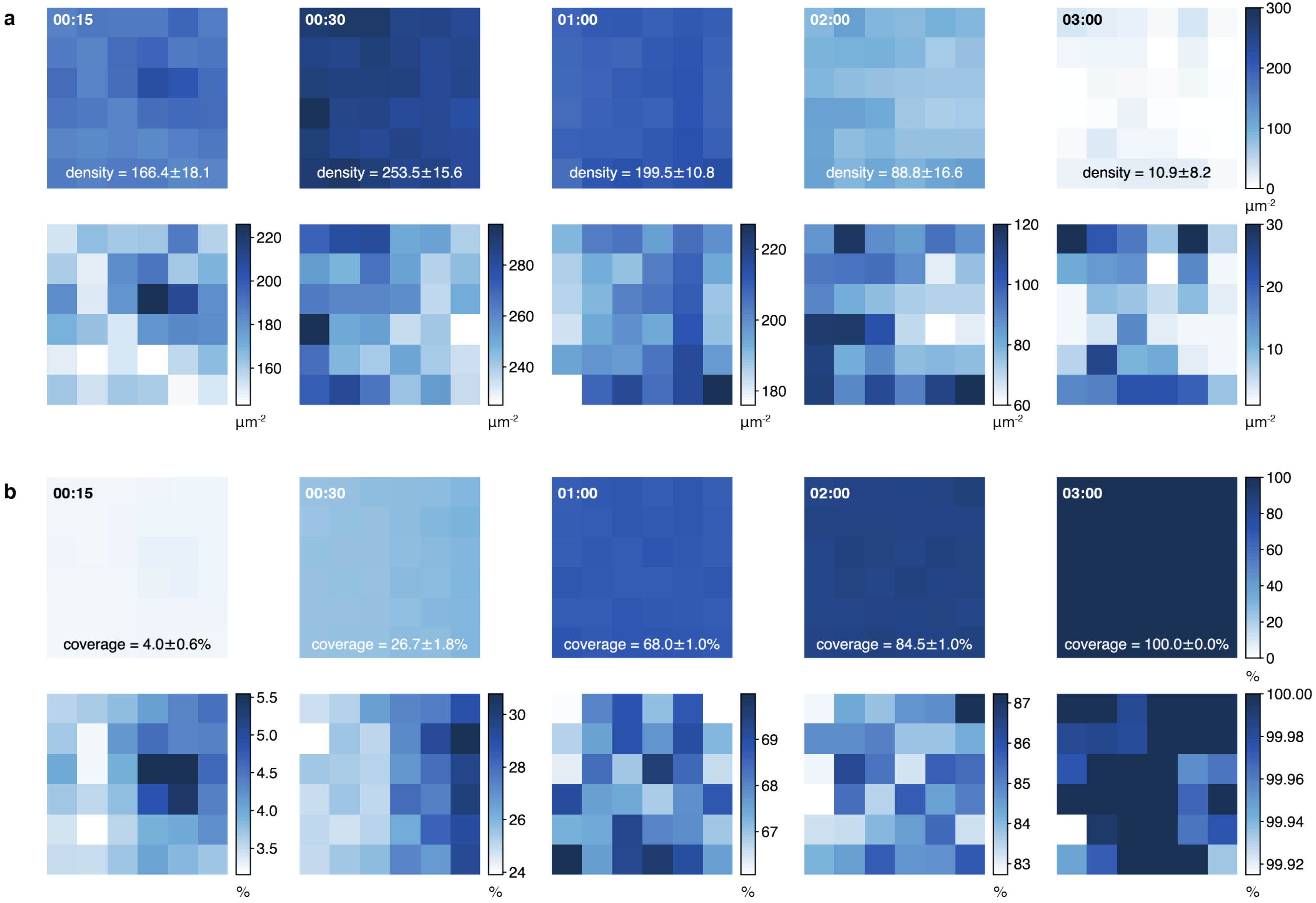
a
00:15
density = 166.4±18.1
00:30
density = 253.5±15.6
01:00
density = 199.5±10.8
02:00
density = 88.8±16.6
03:00
density = 10.9±8.2
300
200
100
0
µm-2
220
200
180
160
µm-2
280
260
240
µm-2
220
200
180
µm-2
120
100
80
60
µm-2
30
20
10
µm-2
b
00:15
coverage = 4.0±0.6%
00:30
coverage = 26.7±1.8%
01:00
coverage = 68.0±1.0%
02:00
coverage = 84.5±1.0%
03:00
coverage = 100.0±0.0%
100
80
60
40
20
0
%
5.5
5.0
4.5
4.0
3.5
%
30
28
26
24
%
69
68
67
%
87
86
85
84
83
%
100.00
99.98
99.96
99.94
99.92
%

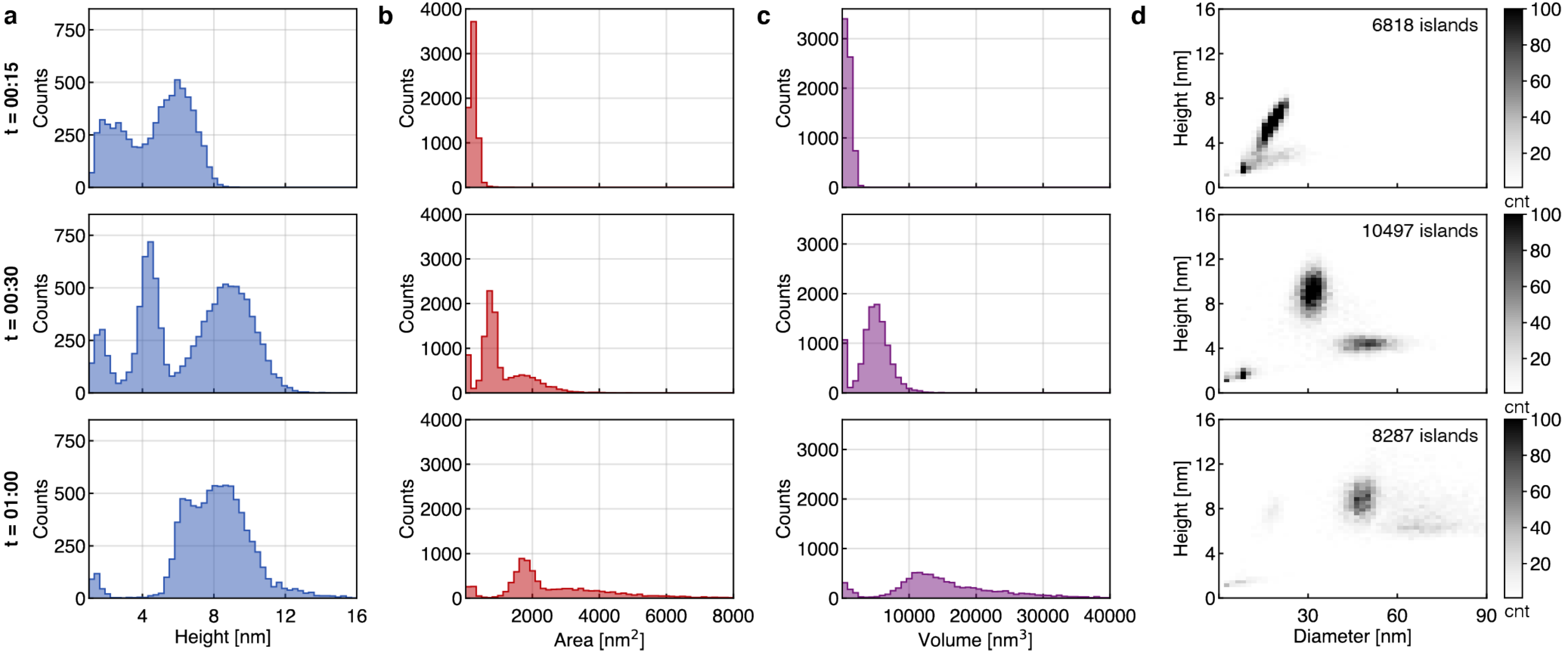

a
b
c
d
t = 00:15
t = 00:30
t = 01:00
Counts
Height [nm]
Area [nm^2]
Volume [nm^3]
Diameter [nm]
6818 islands
10497 islands
8287 islands
cnt

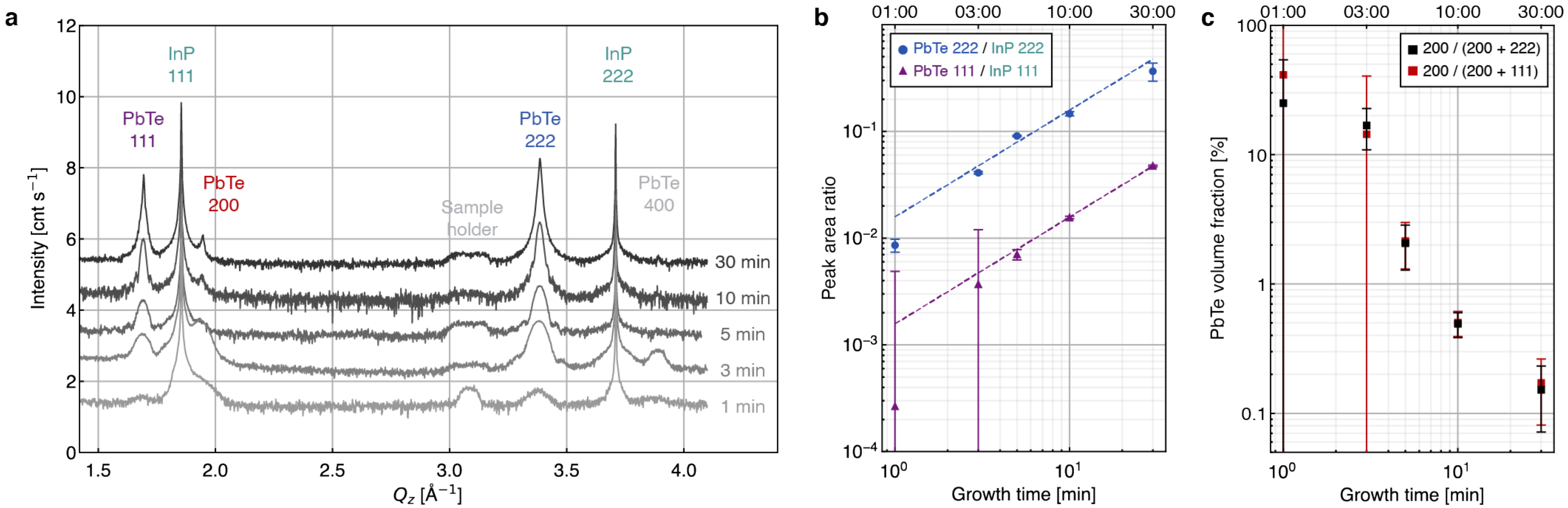
a
b
c
InP 111
InP 222
PbTe 111
PbTe 222
PbTe 200
PbTe 400
Sample holder
30 min
10 min
5 min
3 min
1 min
Intensity [cnt s^{-1}]
Q_z [Å^{-1}]
Peak area ratio
PbTe 222 / InP 222
PbTe 111 / InP 111
Growth time [min]
01:00
03:00
10:00
30:00
PbTe volume fraction [%]
200 / (200 + 222)
200 / (200 + 111)

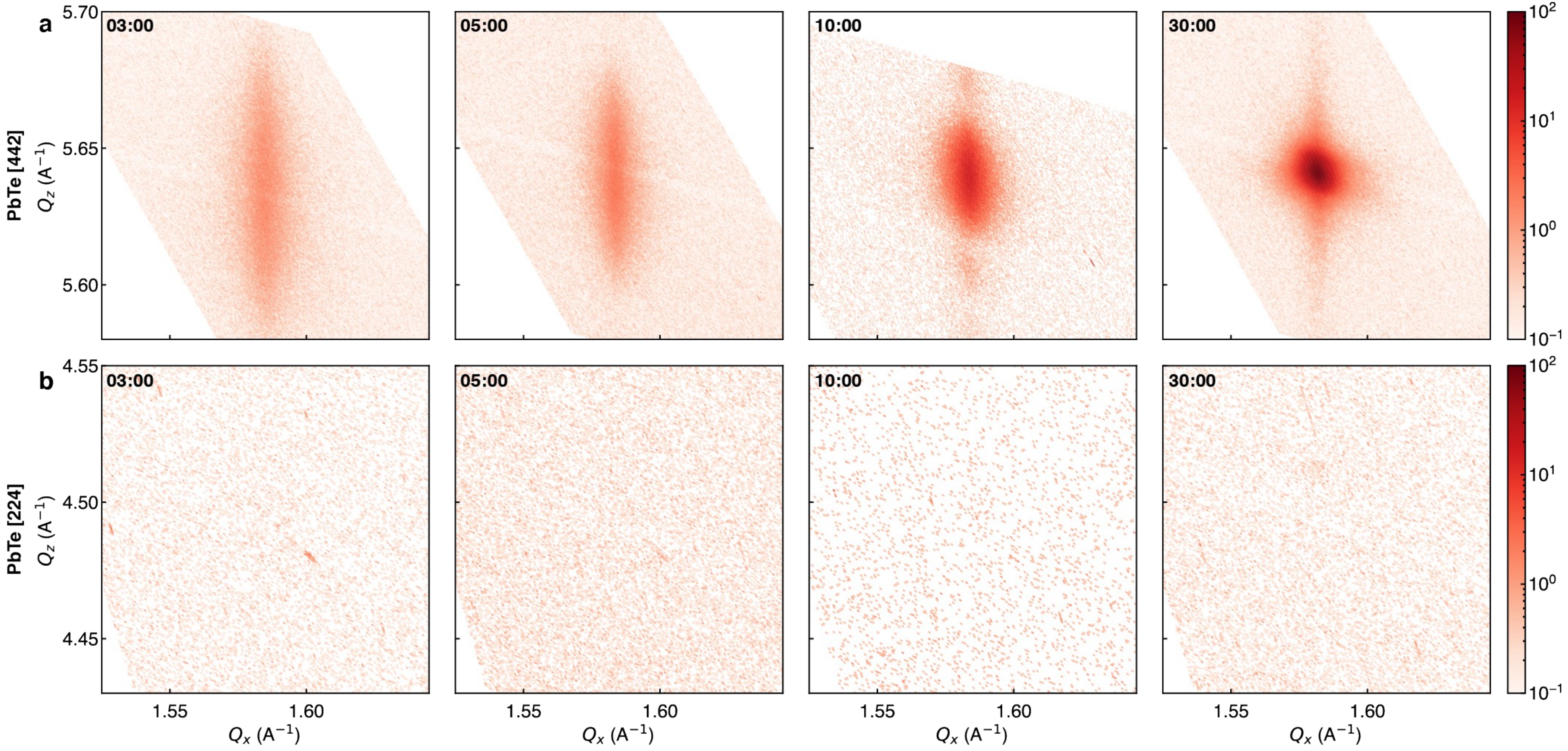
a
b
03:00
05:00
10:00
30:00
PbTe [442]
PbTe [224]
Q_z (A^{-1})
Q_x (A^{-1})
5.70
5.65
5.60
4.55
4.50
4.45
1.55
1.60
10^2
10^1
10^0
10^{-1}

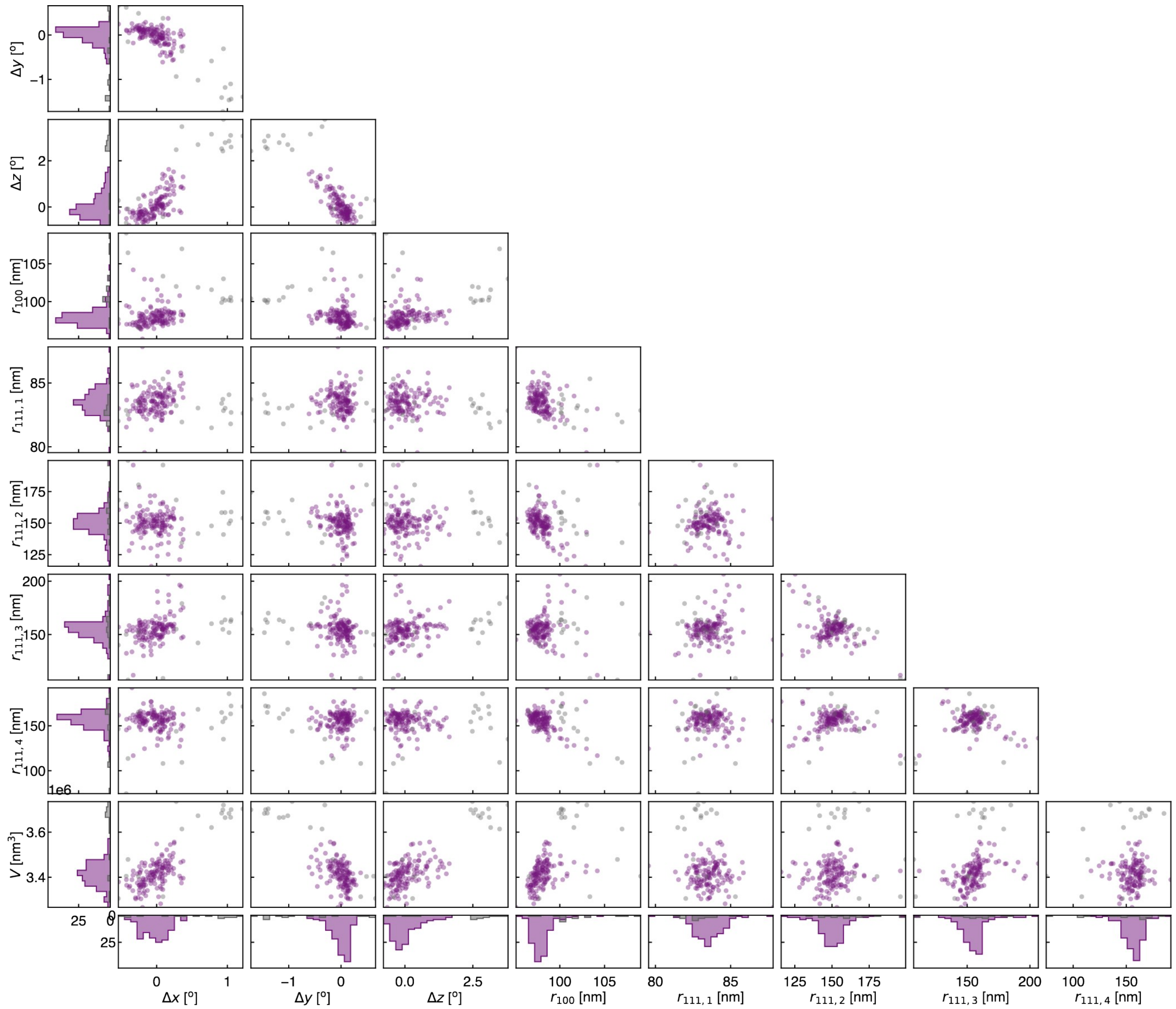

Δy [°]
Δz [°]
r_{100} [nm]
$r_{111,1}$ [nm]
$r_{111,2}$ [nm]
$r_{111,3}$ [nm]
$r_{111,4}$ [nm]
1e6
V [nm³]
Δx [°]
Δy [°]
Δz [°]
r_{100} [nm]
$r_{111,1}$ [nm]
$r_{111,2}$ [nm]
$r_{111,3}$ [nm]
$r_{111,4}$ [nm]

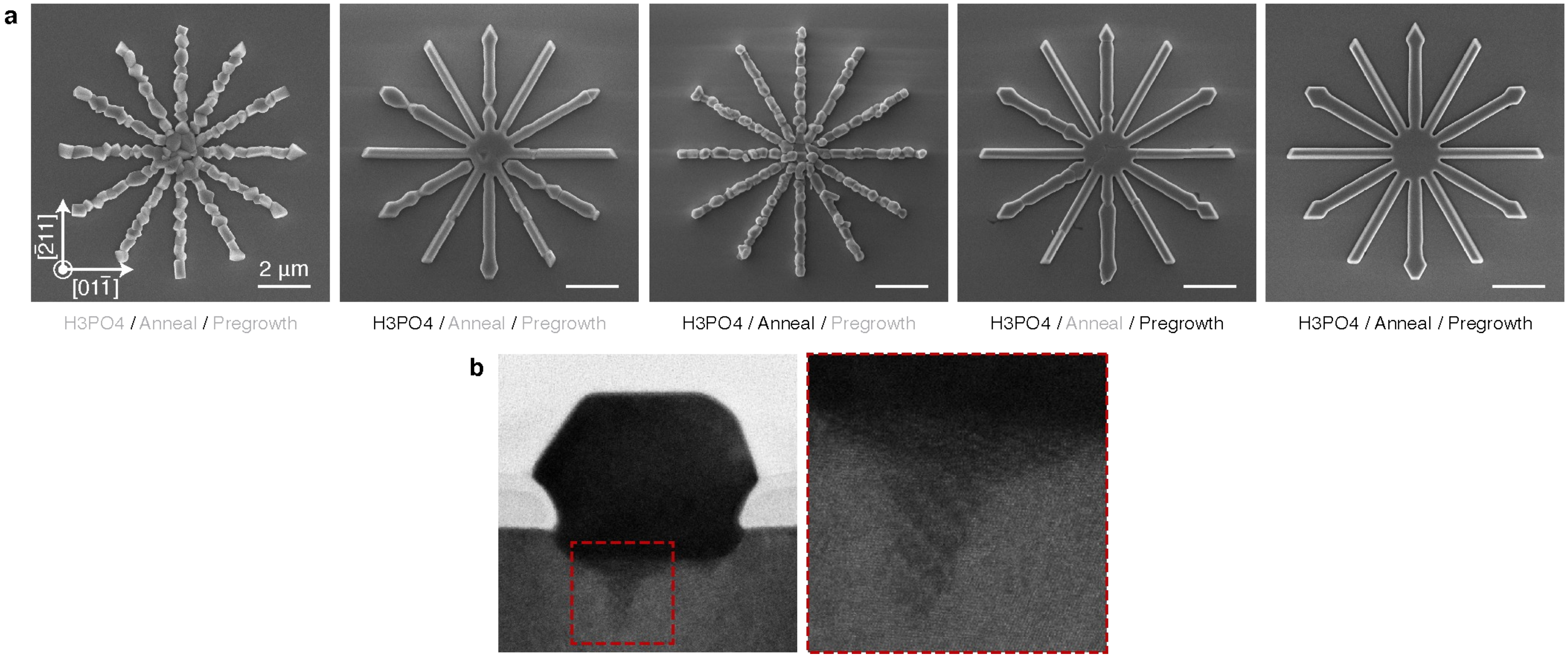
a
[$\bar{2}$11]
[01$\bar{1}$]
2 µm
H3PO4 / Anneal / Pregrowth
H3PO4 / Anneal / Pregrowth
H3PO4 / Anneal / Pregrowth
H3PO4 / Anneal / Pregrowth
H3PO4 / Anneal / Pregrowth
b

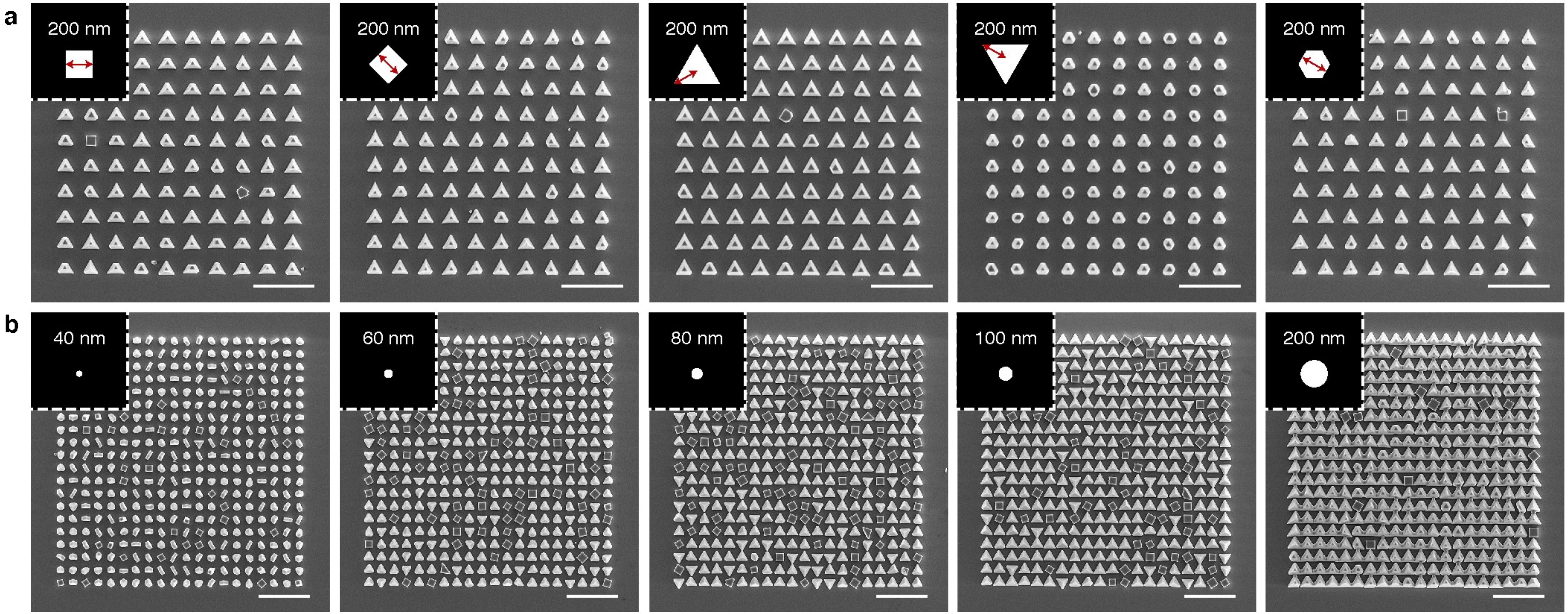
a
200 nm
200 nm
200 nm
200 nm
200 nm
b
40 nm
60 nm
80 nm
100 nm
200 nm

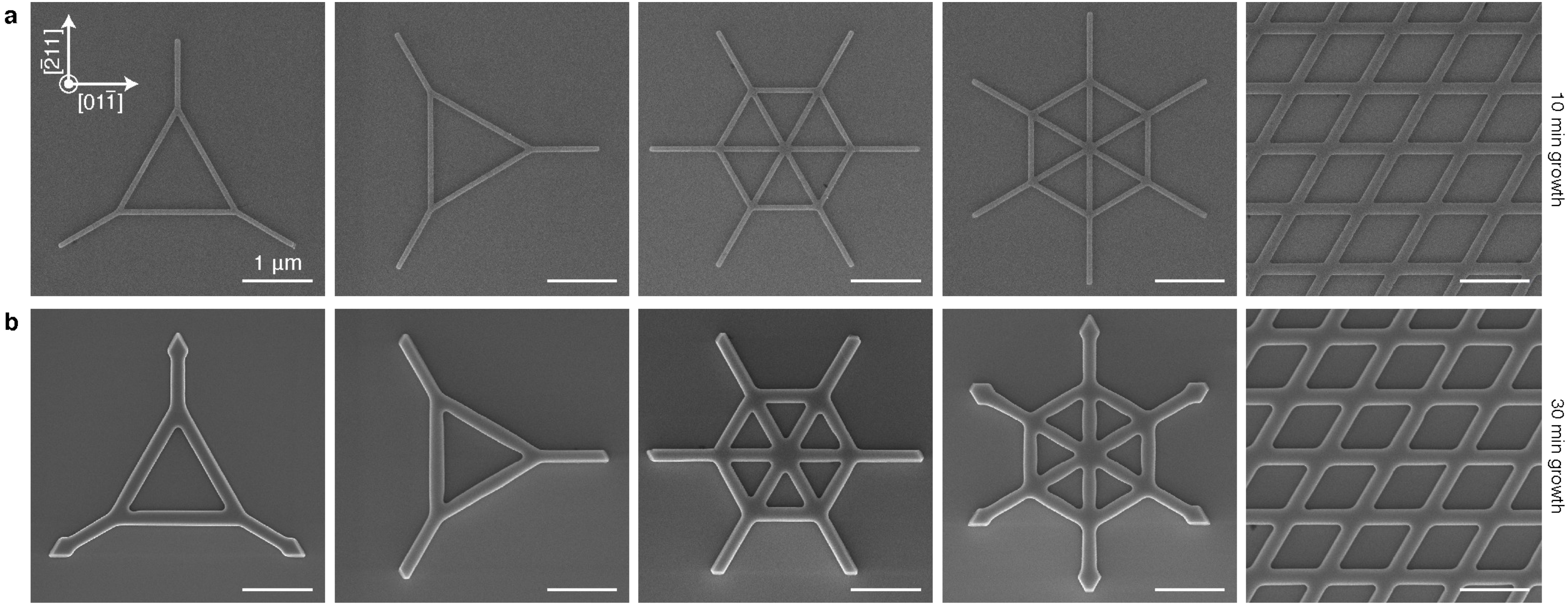
a
[$\bar{2}$11]
[01$\bar{1}$]
1 µm
10 min growth
b
30 min growth

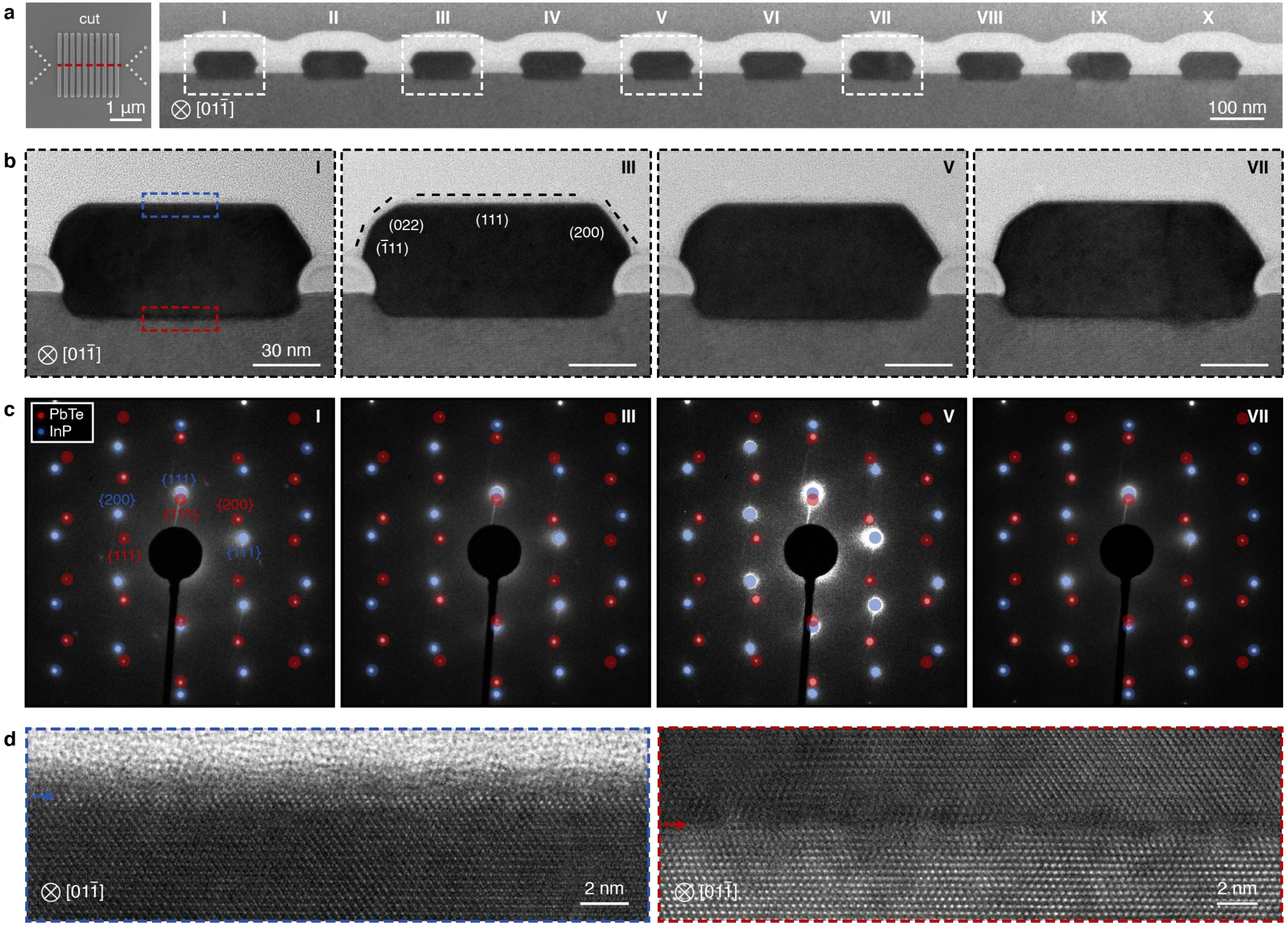
a
cut
1 μm
I
II
III
IV
V
VI
VII
VIII
IX
X
[01$\bar{1}$]
100 nm
b
I
III
V
VII
(022)
(111)
(200)
($\bar{1}$11)
[01$\bar{1}$]
30 nm
c
PbTe
InP
{111}
{200}
{200}
{111}
{111}
{111}
d
[01$\bar{1}$]
2 nm
[01$\bar{1}$]
2 nm

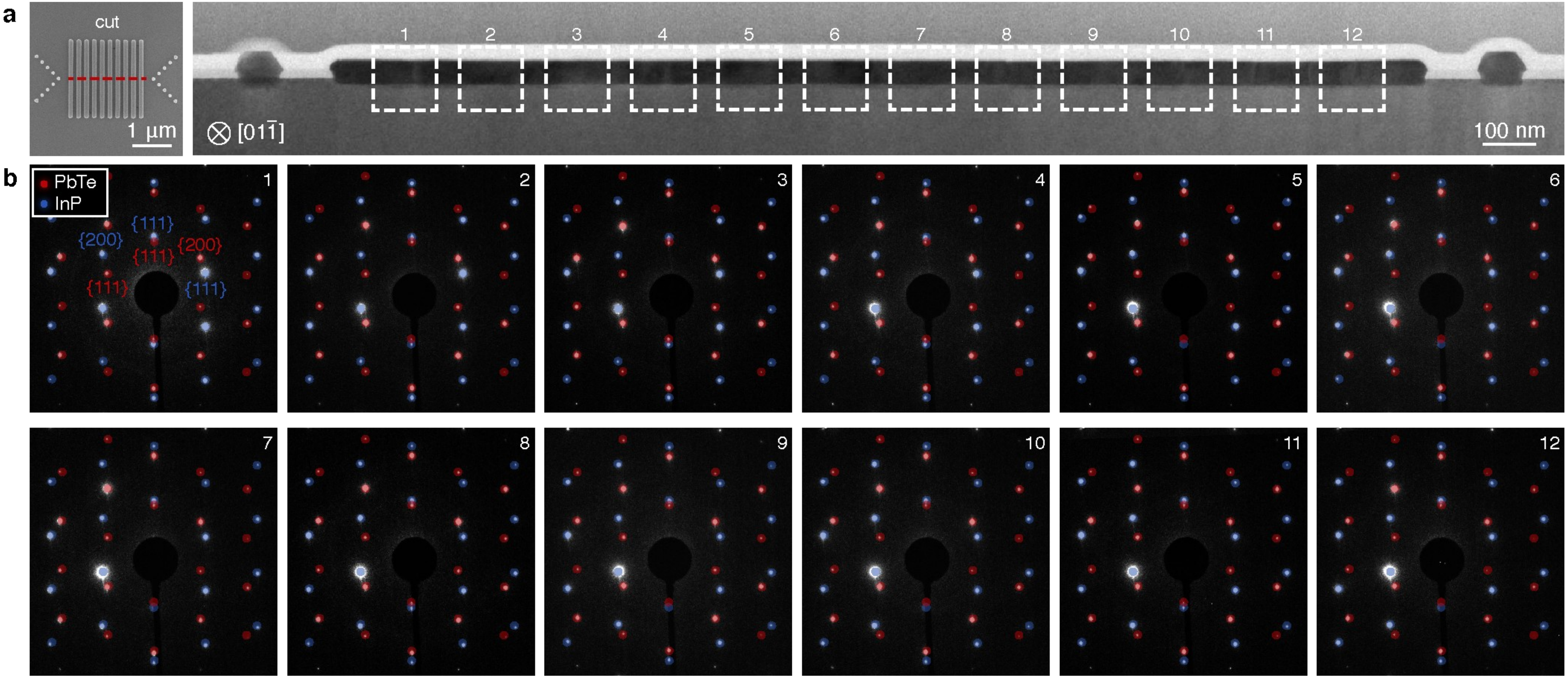
a
cut
1 µm
1
2
3
4
5
6
7
8
9
10
11
12
[01$\bar{1}$]
100 nm
b
PbTe
InP
{111}
{200}
{111}
{200}
{111}
{111}
1
2
3
4
5
6
7
8
9
10
11
12

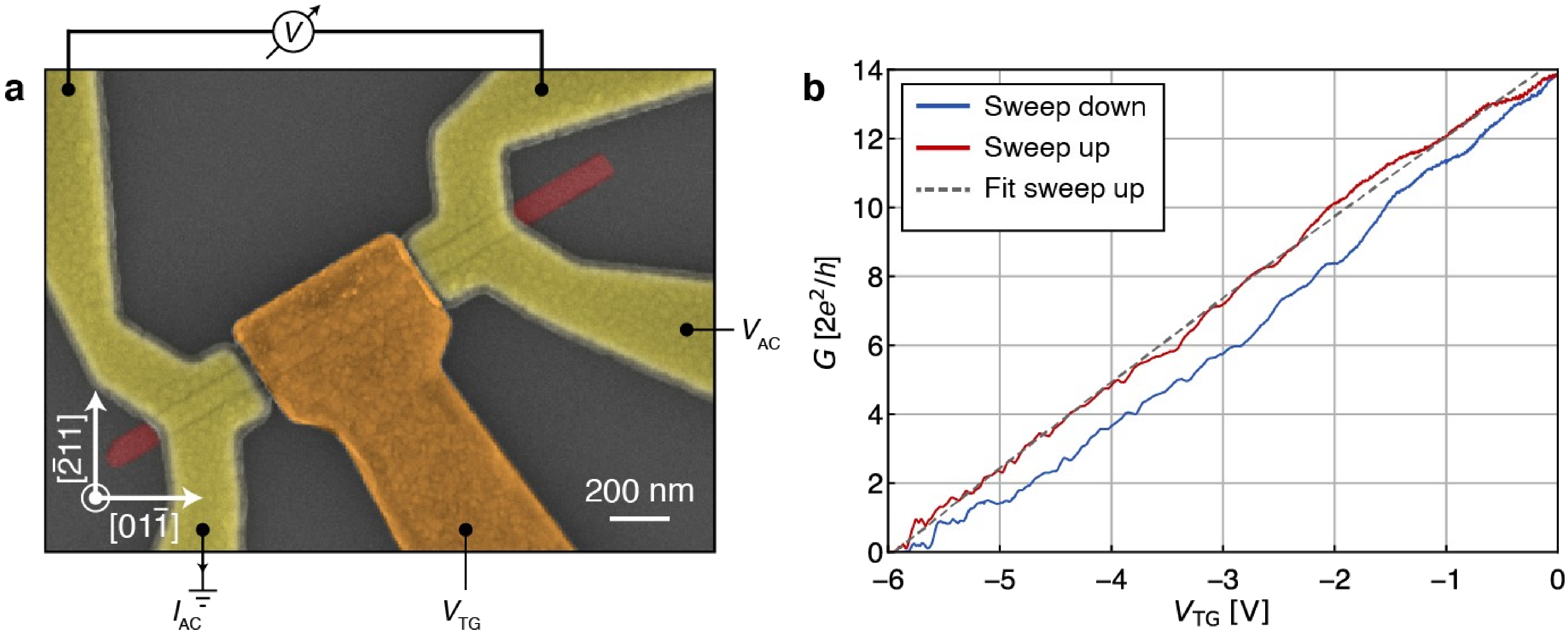
a
V
V_AC
I_AC
V_TG
[2̄11]
[011̄]
200 nm
b
Sweep down
Sweep up
Fit sweep up
G [2e²/h]
V_TG [V]
0
2
4
6
8
10
12
14
−6
−5
−4
−3
−2
−1
0

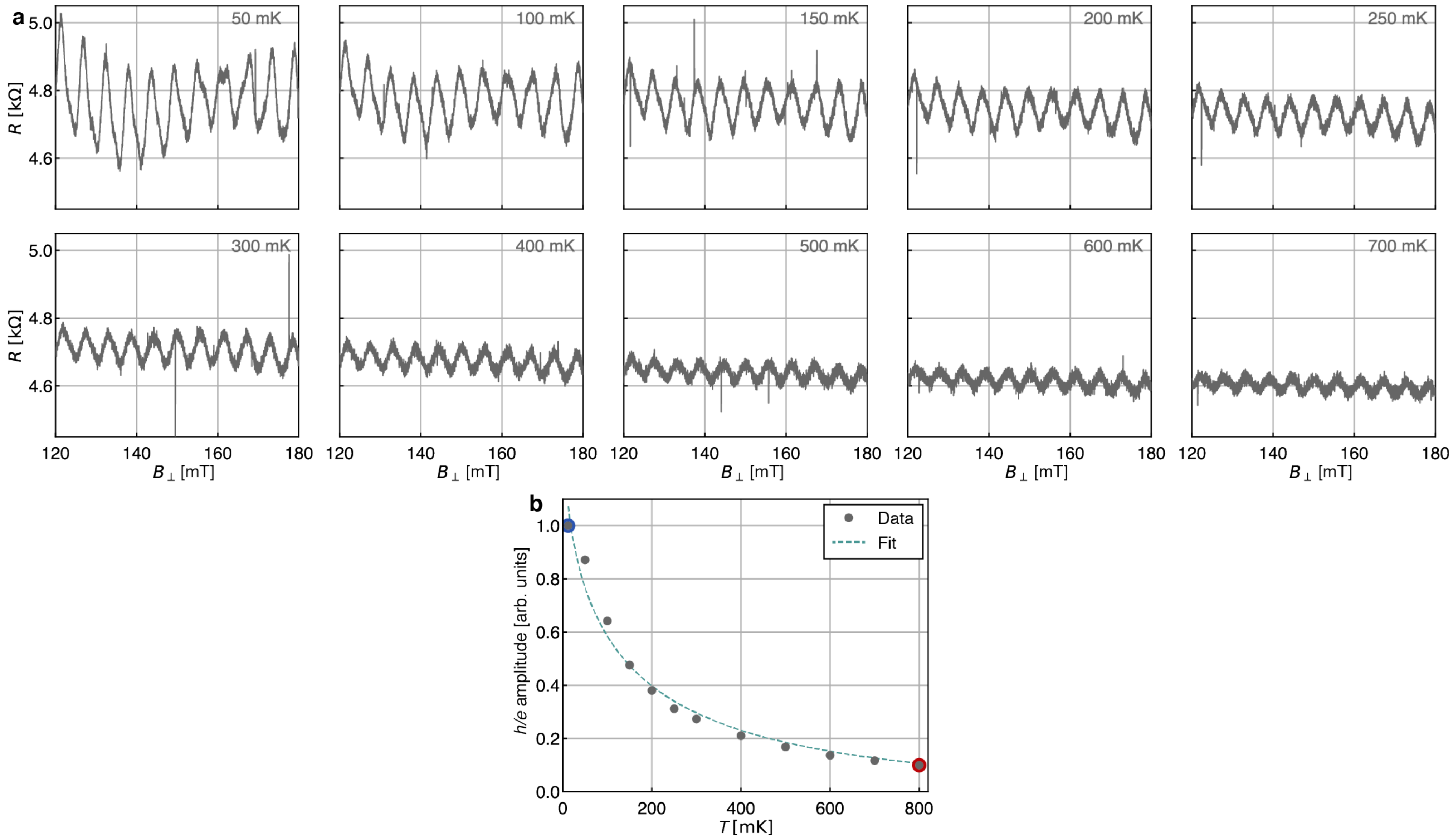
a
b
50 mK
100 mK
150 mK
200 mK
250 mK
300 mK
400 mK
500 mK
600 mK
700 mK
R [kΩ]
B ⊥ [mT]
Data
Fit
h/e amplitude [arb. units]
T [mK]

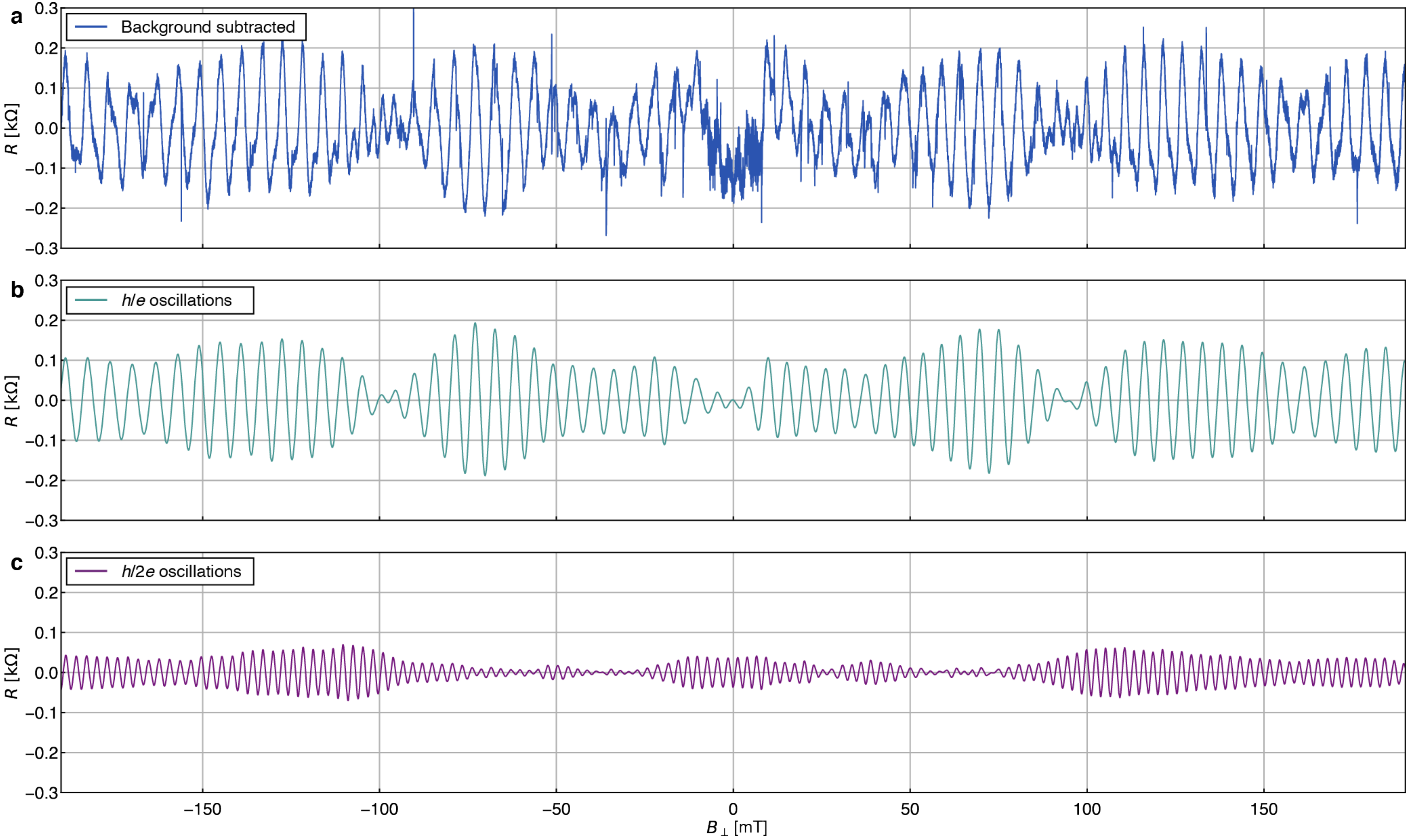
a
Background subtracted
b
h/e oscillations
c
h/2e oscillations
R [kΩ]
0.3
0.2
0.1
0.0
−0.1
−0.2
−0.3
−150
−100
−50
0
50
100
150
B⊥ [mT]

Outlook

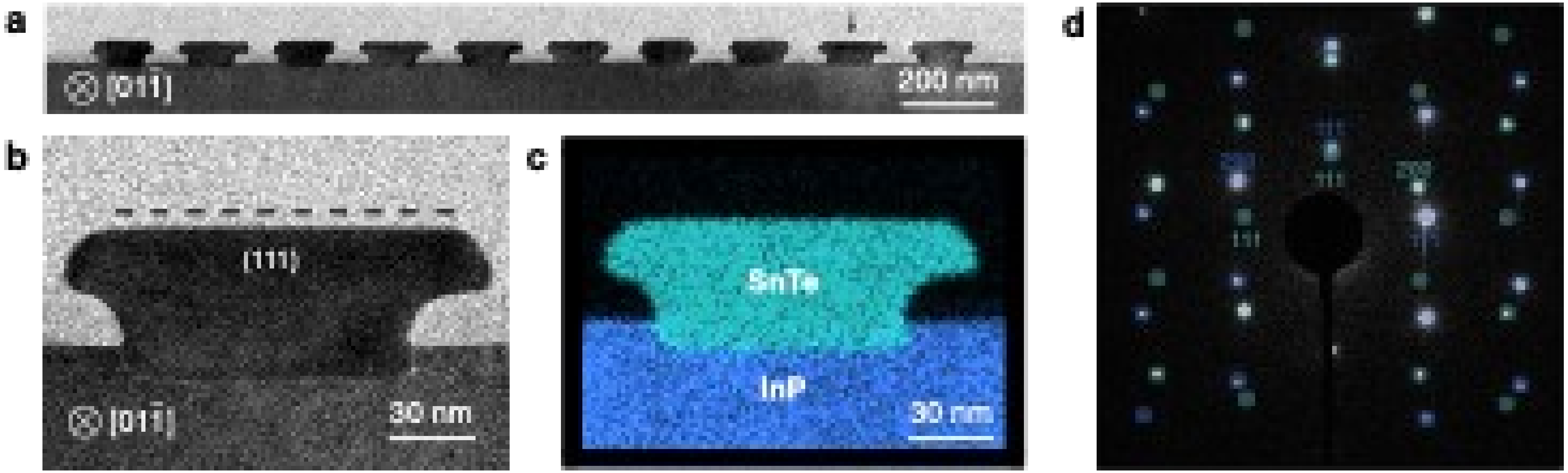

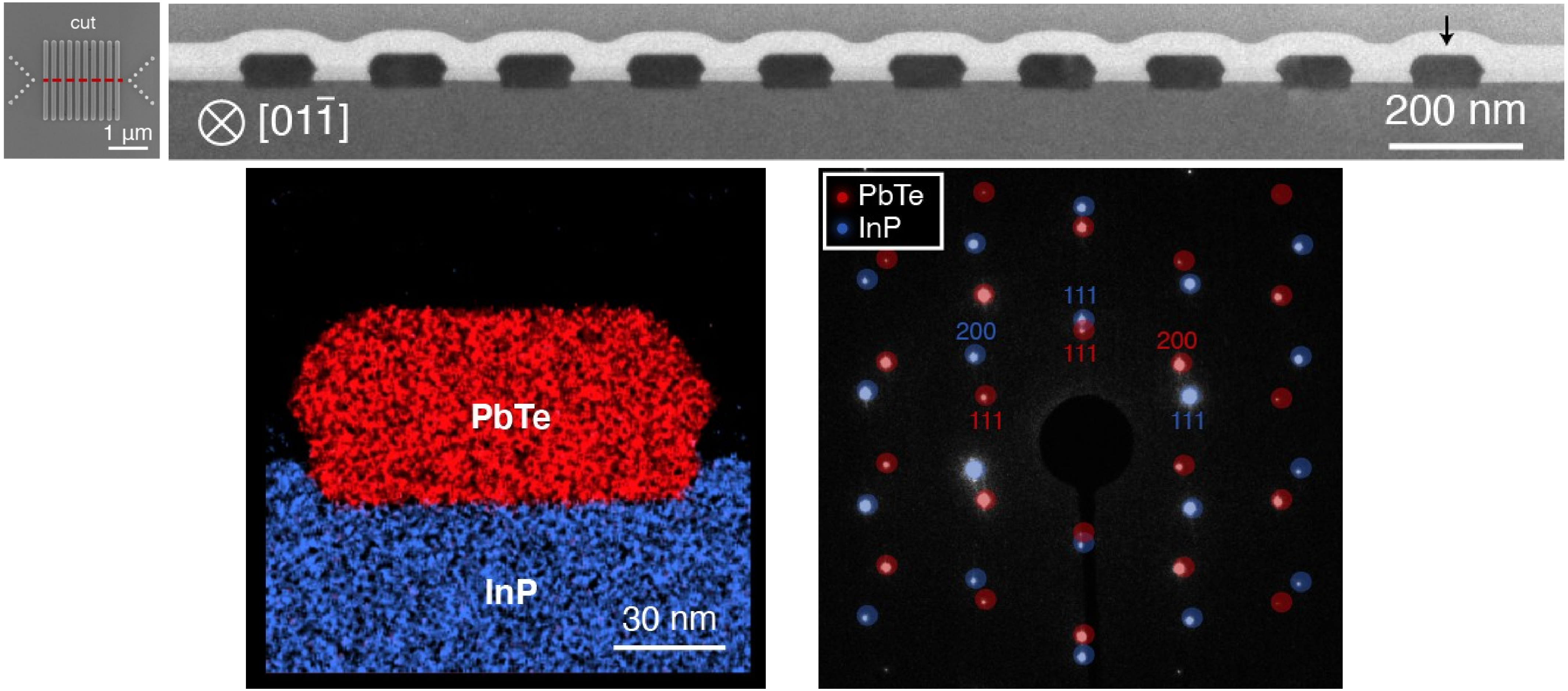
cut
1 µm
[01$\bar{1}$]
200 nm
PbTe
InP
30 nm
PbTe
InP
111
200
111
200
111
111

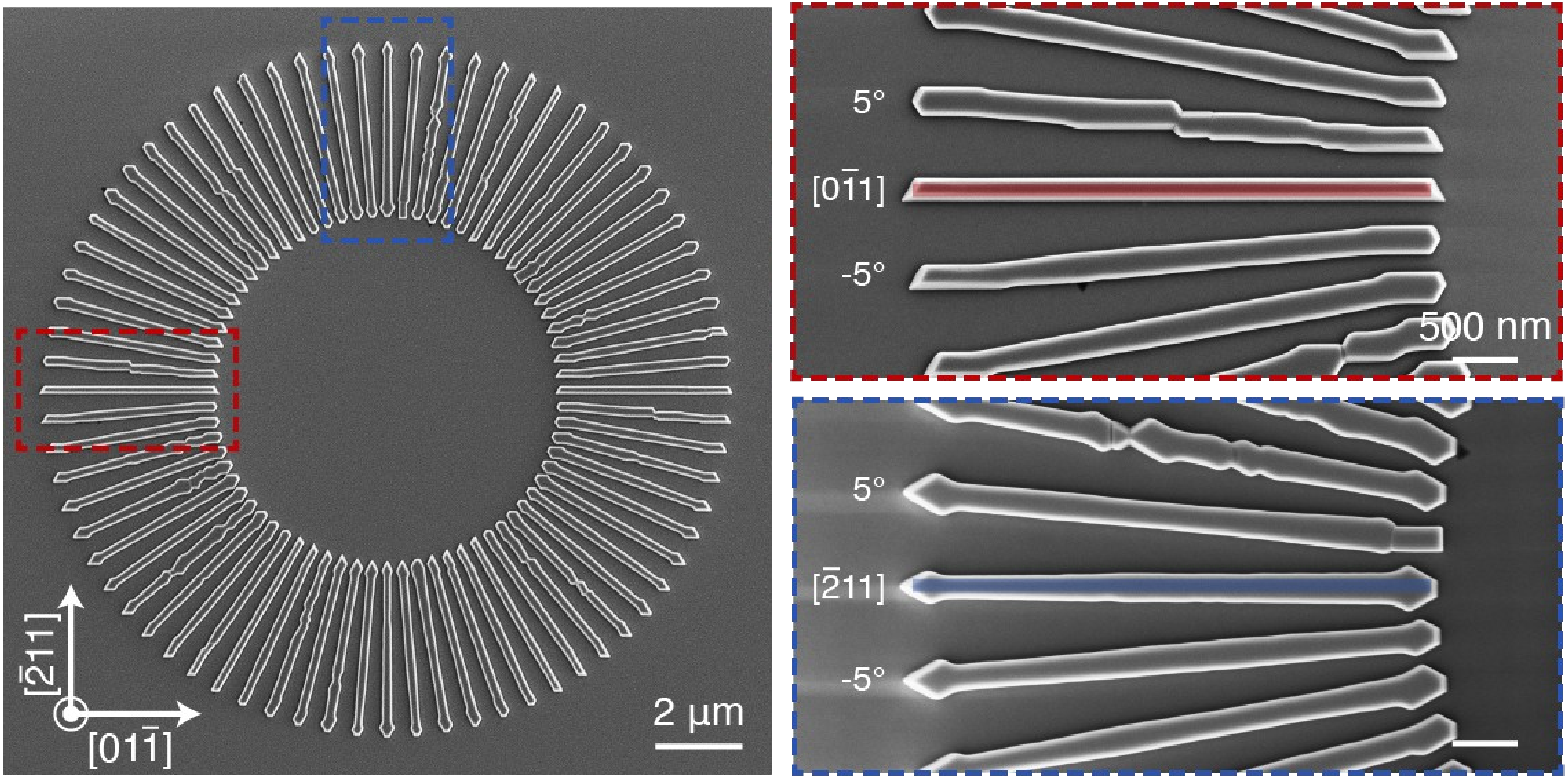
[2̄11]
[011̄]
2 µm
5°
[01̄1]
-5°
500 nm
5°
[2̄11]
-5°

university of groningen

Topological Superconductivity Based on Transition Metal Dichalcogenides

Justin Ye

Device Physics of Complex Materials

Zernike Institute for Advanced Materials, University of Groningen

Device Physics of Complex Materials

University of Groningen Zernike Institute for Advanced Materials

erc European Research Council

NWO

nano LabNL

FOM

QuMat Kickoff, 2022

3.2 Topological Superconductivity Based on Transition Metal Dichalcogenides

3.2: Topological superconductivity based on transition metal dichalcogenides	3 PhD* RUG, RU, UU

Aim: This research will develop two-dimensional topological superconductors based on transition metal dichalcogenides and their heterostructures. We will synthesize and characterize several transition metal dichalcogenides / van der Waal heterostructures, including FeSe on insulating $SrTiO_3$ (see also projects in Pillar 1). We will develop novel transport methods at ultra-low temperatures and high magnetic fields, to explore the various electronic and superconducting properties of these hybrid materials. In the clean regime with a mean free path longer than the coherence length, we will examine the topological aspects of the 2D superconducting states, including the yet unsolved topological phase in the Berezinskii-Kosterliz-Thouless transition.

T S D — *Intrinsic superconductivity in transition metal dichalcogenides* – PhD; Ye (RUG), Rösner (RU), Khajetoorians (RU).
We will fabricate TMD-based hybrid materials with a clean 2D superconducting state with very long mean free path in the normal state to facilitate the realization of a robust topological superconducting state. A 2H-type monolayer TMD can host a nodal topological superconductor where the nodal points appear when Ising spin-orbit interaction vanishes at certain points in the Brillouin zone. A strong Ising protection that disappears in one pocket gets reversely Ising-protected in the other pocket. For MoS_2 and WS_2, the Ising superconductivity is in the conduction band with protection residing at the zone edge. The competing pocket can be controllably introduced by adding a second layer, resulting in a Q pocket centered between the zone corner and zone center. We will use DFT calculations to predict the optimal location of the Fermi level. Simple devices will be fabricated to allow gate-controlled scanning probe spectroscopy, which we will use to study the superconductivity, and zero-energy states (see third sub-project).

S D C — *Probing unconventional order parameter symmetry* – PhD; Hussey (RU), Ye (RUG), McCollam (RU).
We will make a superconductor-insulator-superconductor (SIS) tunneling junction and use a tunneling experiment on TMDs under a high magnetic field (in collaboration with HFML in Nijmegen) to detect and differentiate the two possible phases of a nodal superconductor and nodal topological superconductor. We expect to observe a "V-shaped" spectrum for the nodal superconductor and a "V shape" spectrum *with low energy features* for the

C — *In-situ phase tuning of topological superconductors* – PhD (0.5 FTE)*; Swart (UU), Khajetoorians (RU).
A vacuum suitcase transfer infrastructure will be developed to transfer successful devices of projects 3.1 and 3.2 to advanced scanning tunneling spectroscopy set-ups. Phase-biased experiments will be developed and equipped with tunnel probe read-out. Corbino-disk type experiments will be performed where Majoranas are swapped at high frequency while probing the tunneling density of states. Furthermore, the zero-energy modes will be characterized by shot-noise measurements.

RUG/RU Projects

1. Intrinsic Topological Superconductivity
2. Probing Unconventional Order Parameter (HFML, Tunnelling measurement)

UU/RU Project

3. STM-based study (Majorana zero-energy mode)

Expertise involved

1. Nanofabrication/ SC devices (RUG).
2. DFT Theory (RU)
3. STM, UV growth characterization (RU/UU)

Topological Superconductors

Intrinsic topological superconductors

Sr_2RuO_4. *p* wave superconductor

$Cu_xBi_2Se_3$. T_c up to ~4 K was discovered in 2010

Engineered topological superconductors

S-wave SC + Semiconductor (large SOC) + B Field (Zeeman effect)

Semiconductor NW (large SOC) +S-wave SC

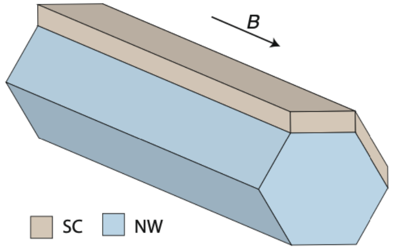

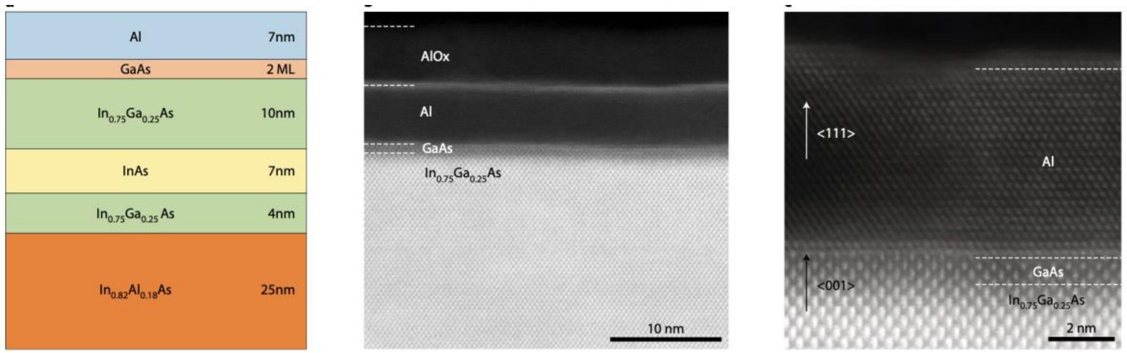

Review by Frolov, et al. Nature Physics

ARTICLE

Received 13 Jul 2013 | Accepted 4 Oct 2013 | Published 28 Oct 2013 DOI: 10.1038/ncomms3711

Topological Fulde–Ferrell–Larkin–Ovchinnikov states in spin–orbit-coupled Fermi gases

Wei Zhang[1] & Wei Yi[2]

Zhang, et al. Nature Comm. 2013

Topological metals and finite-momentum superconductors

Noah F. Q. Yuan[a,b,1,2] and Liang Fu[b,1,2]

[a]Shenzhen JL Computational Science and Applied Research Institute, Shenzhen 518109, China; and [b]Department of Physics, Massachusetts Institute of Technology, Cambridge, MA 02139

S-wave SC + large Rashba SOC + B Field (Zeeman effect)

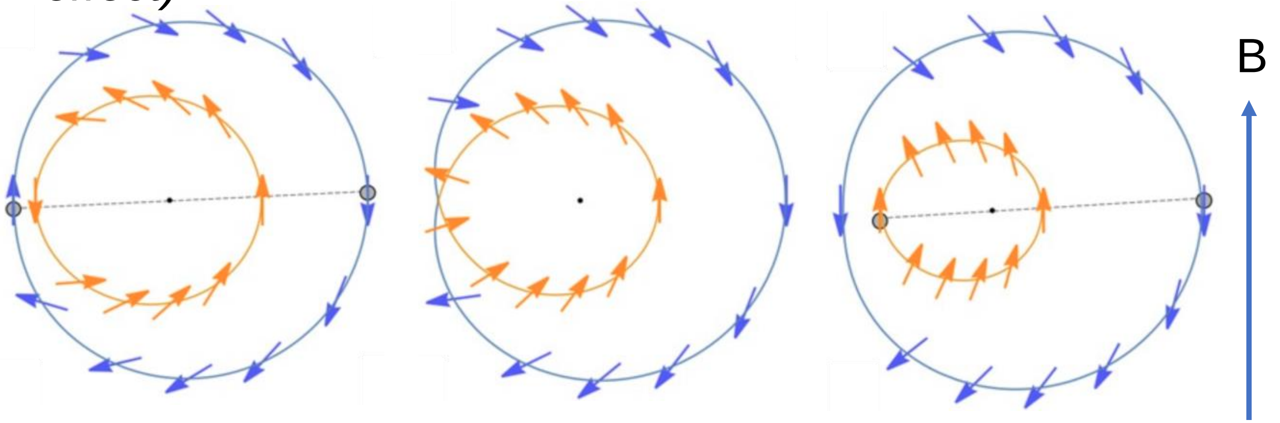

Noah F. Q. Yuan, and Liang Fu, PNAS 2021

Topic 1: Ion-Gated Transistors for Clean 2D Superconductivity

Channel Material
Si, GaAs
Au, Pt, Au, Co, etc.
TMDs and others:
MoS_2, WS_2

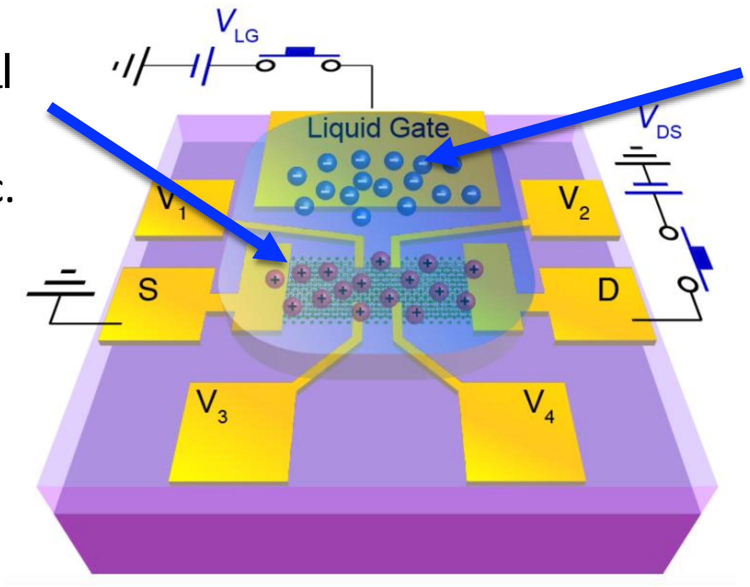

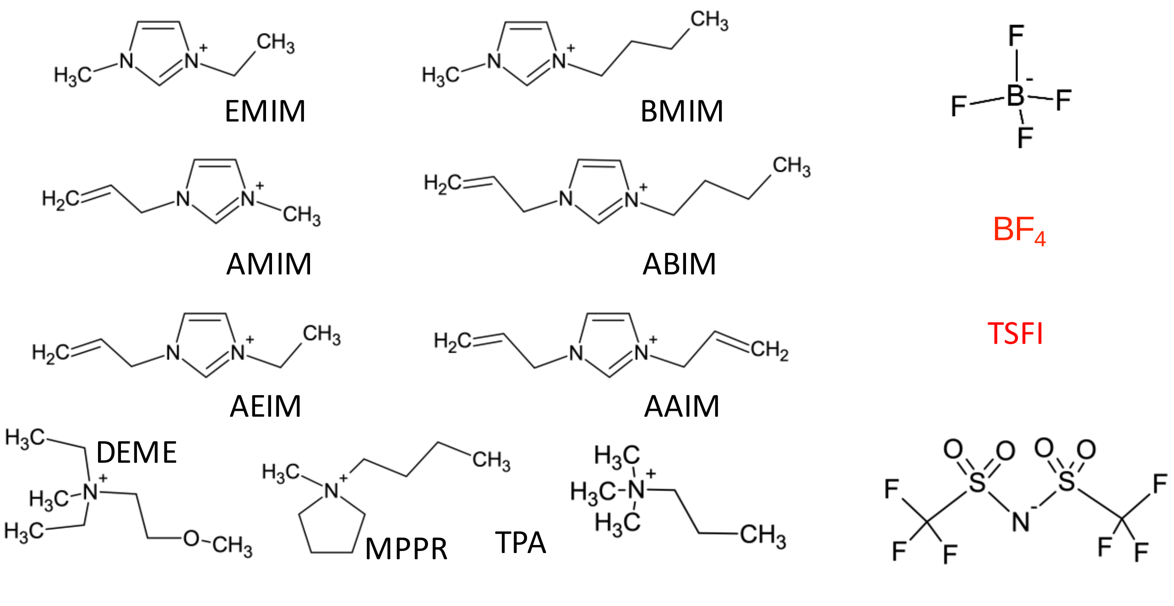

1. Start from a semiconducting TMDs, such as: MoS_2, WS_2
2. E field: 50 MV/cm, n_{2D}: ~10^{14} cm^{-2}
3. Electrostatically induced SC? Yes

Intrinsic Monolayer Superconductor

$1T'$ – WTe_2
$1T'$ – $MoTe_2$
$2H$ – TaS_2
$2H$ – $NbSe_2$
Monolayer BSCCO, etc.

Air Unstable
- Reduced T_c, compared with bulk.
- Reduced RRR, due to degradation.

Field-Induced Monolayer Superconductor

$2H$ – MoS_2
$2H$ – WS_2
$2H$ – $WS_2$2
ZrNCl, etc.

Air Stable
- T_c comparable or higher than bulk.
- Large RRR, Pristine crystal quality, no degradation.

Topic 1: Accessing Clean Superconductivity in 2D Single Crystals

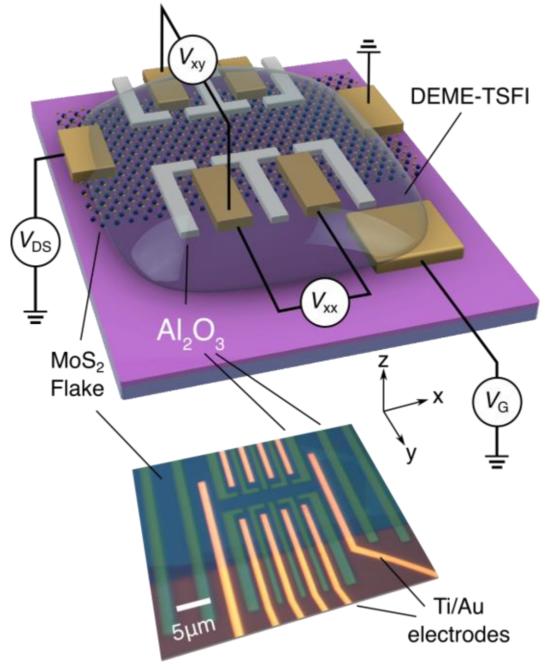

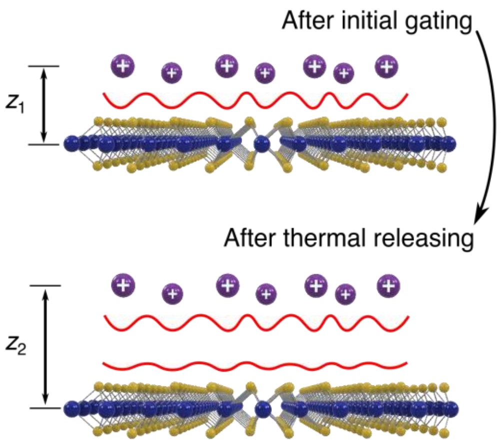

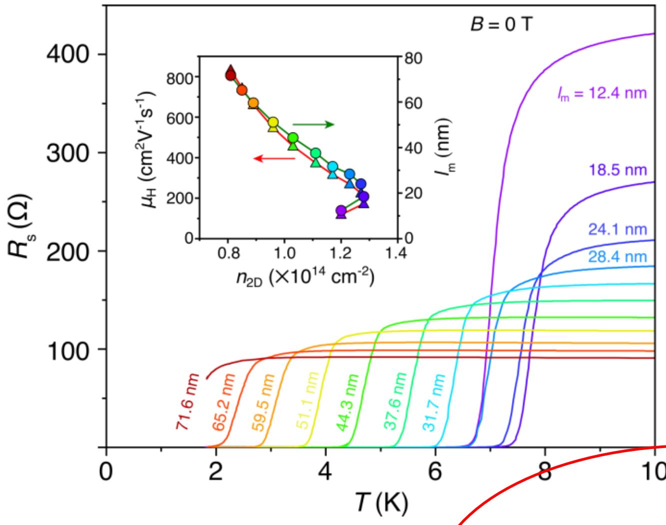

The clean superconducting regime:
Mean free path versus coherent length

$$\xi_0 \sim l_m$$

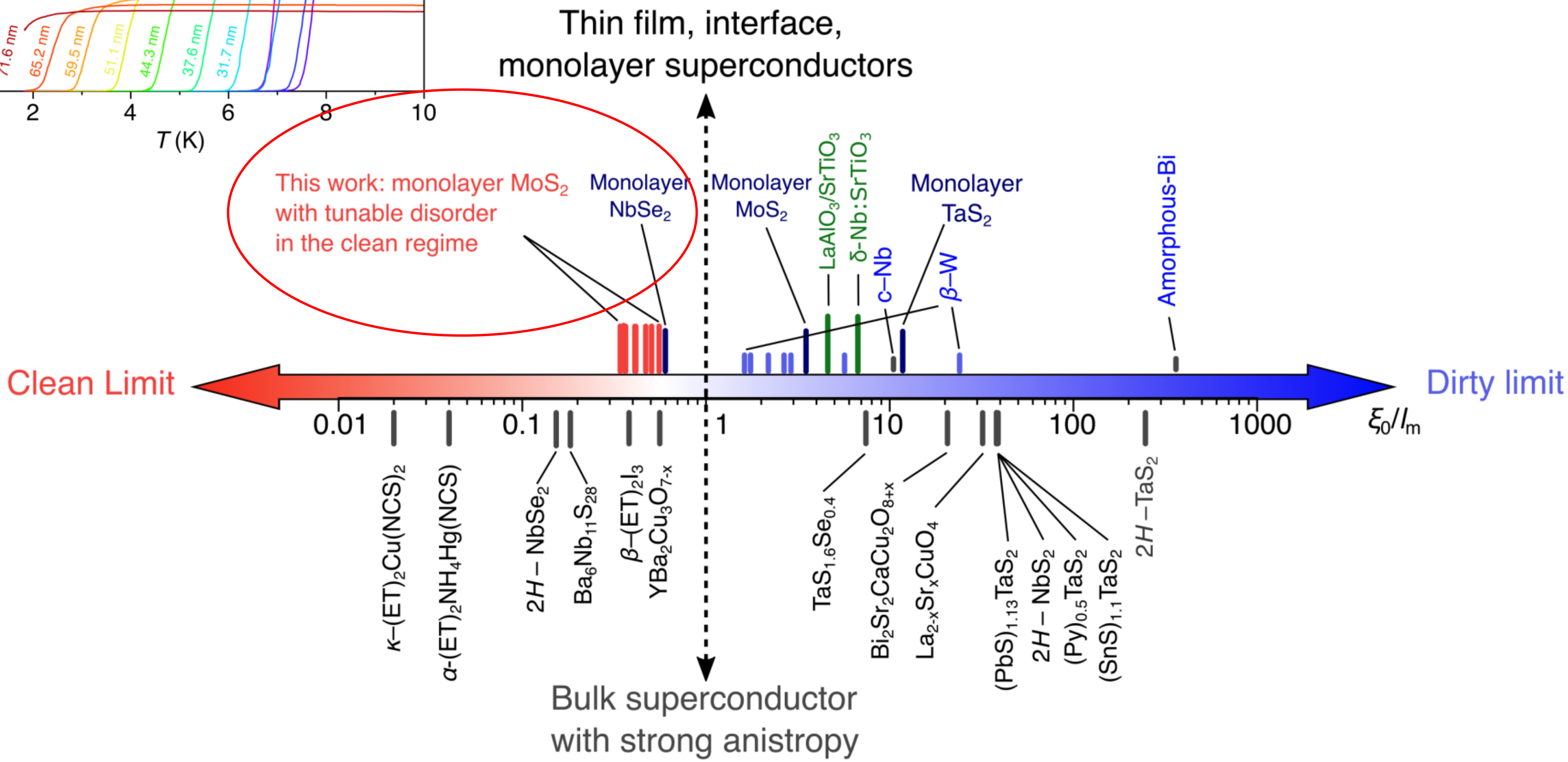

Ising superconductivity and Rashba SOC from Ionic Gating

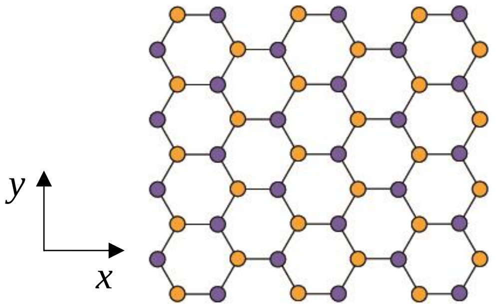

Inversion symmetry breaking

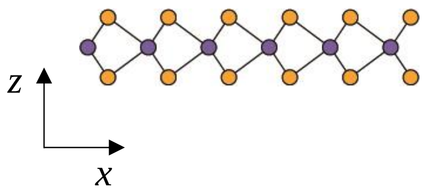

Ising SOC (β_{SOC})

Crystal structure of transition metal dichalcogenides (MoS_2, WS_2, $NbSe_2$…)

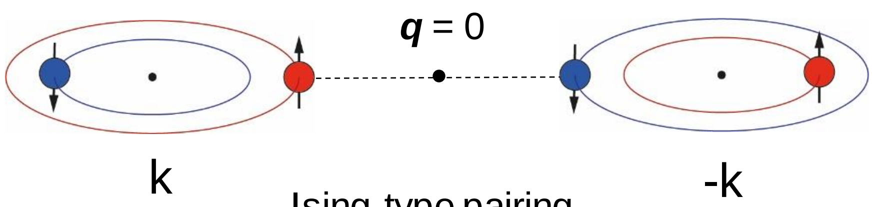

Ising-type pairing

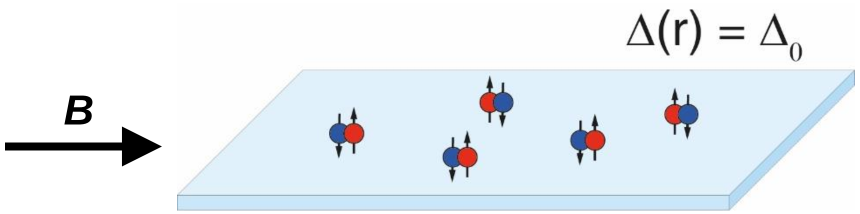

Uniform Ising superconductivity

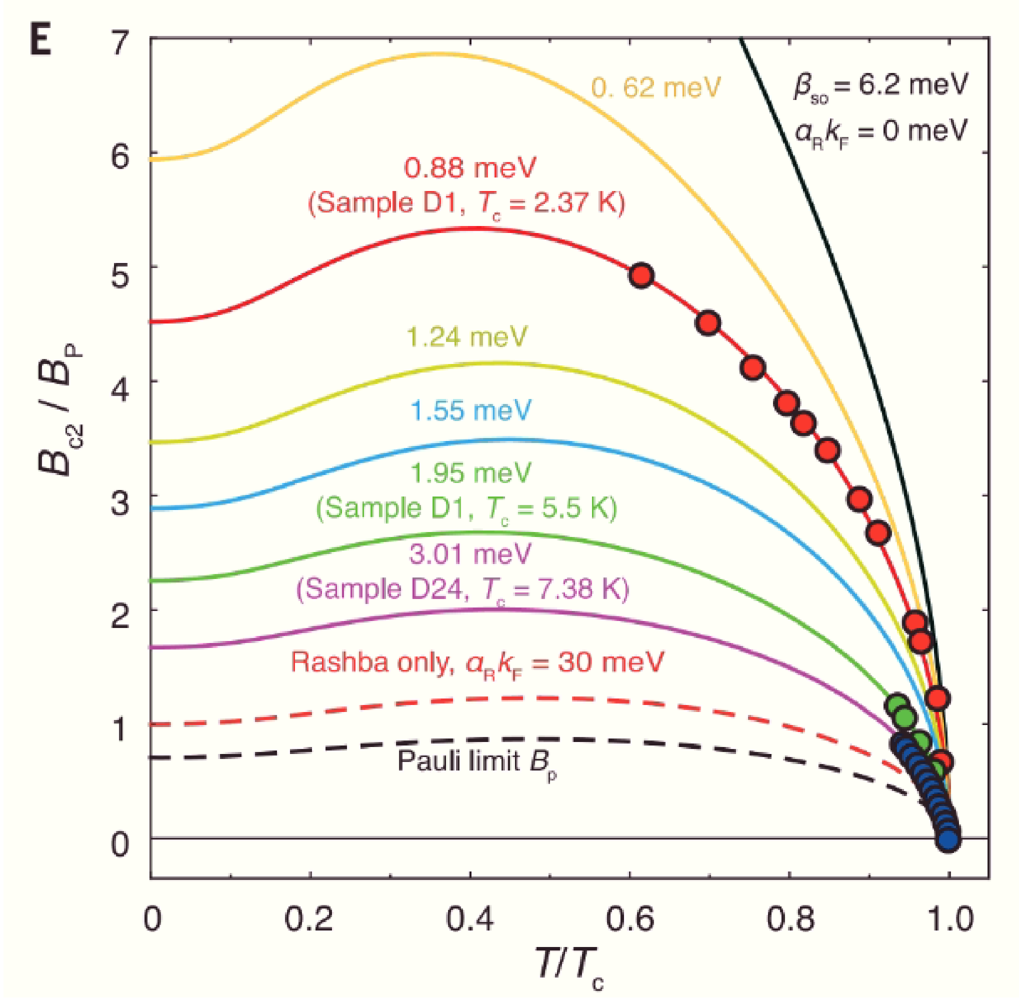

Upper critical field of Ising superconductivity in MoS_2

Lu, J. M., et al. "Evidence for two-dimensional Ising superconductivity in gated MoS2." *Science* 350.6266 (2015): 1353-1357.

Topic 2: Interlayer-Coupled Pairing by Stacking 2D Superconductors

Interlayer Interaction for New Quantum states

- Interlayer Hopping

Formation of flat band in twisted bilayer graphene (SC, Ferromagnetism)

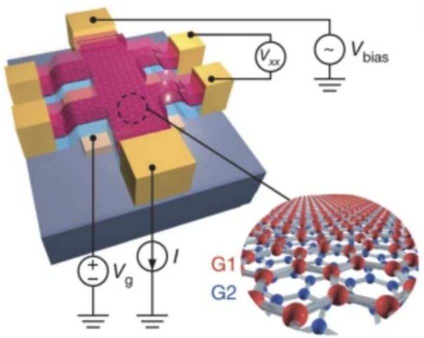

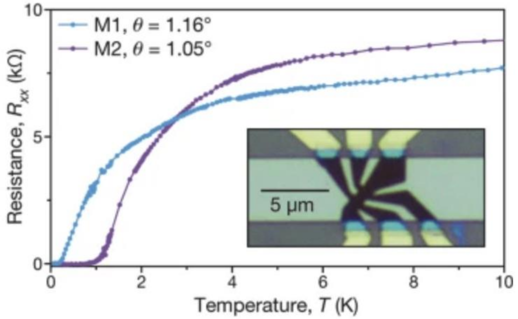

Yuan Cao, 556, 43 (2018)

- Interlayer Exchange interaction J

FM/AFM layer dependence in 2D Ferromagnets

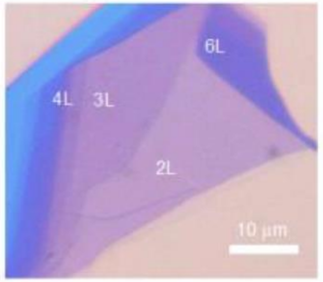

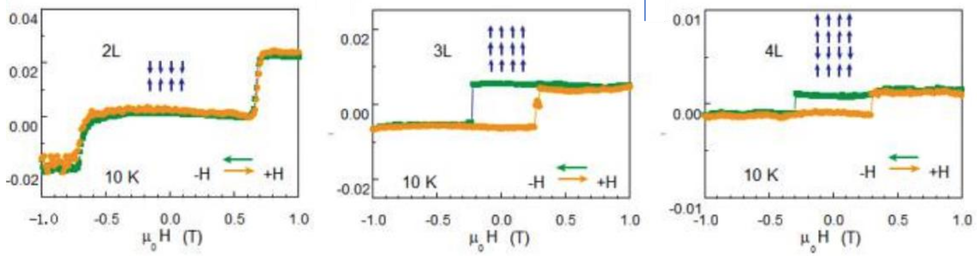

- Interlayer Josephson Interaction (tunneling) *t*

Formation of finite-momentum Cooper pairing

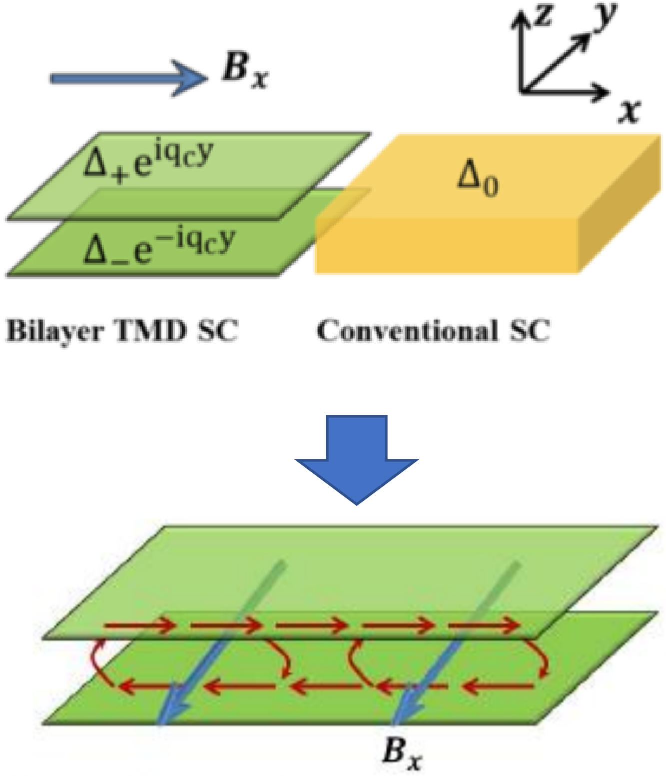

$$\hat{H}_0(\mathbf{p} = \epsilon\mathbf{K} + \mathbf{k}) = \xi_k + \epsilon\beta_{SOC}s_z\tau_z + t\tau_x$$

$$\hat{H}'_0 = \xi_k - \hbar v_Q k_y \tau_z + \epsilon\beta_{SOC}s_z\tau_z + t\tau_x$$

$$\Delta(\mathbf{r}) = \Delta_+(q_c)e^{iq_c y} + \Delta_-(-q_c)e^{-iq_c y}$$

Possibility of forming FFLO state

C. X. Liu, *PRL* **118**, 087001 (2017)

Finite momentum pairing in Ising superconductors (Orbital FFLO)

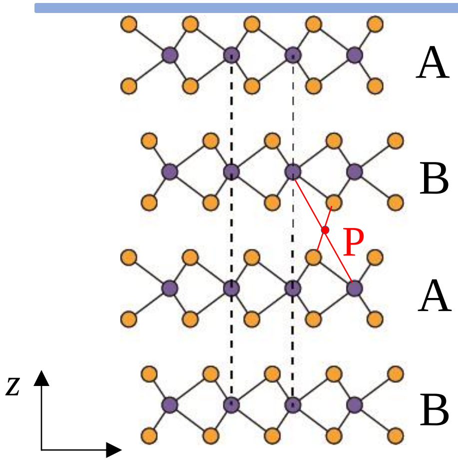

$2H$-NbSe$_2$

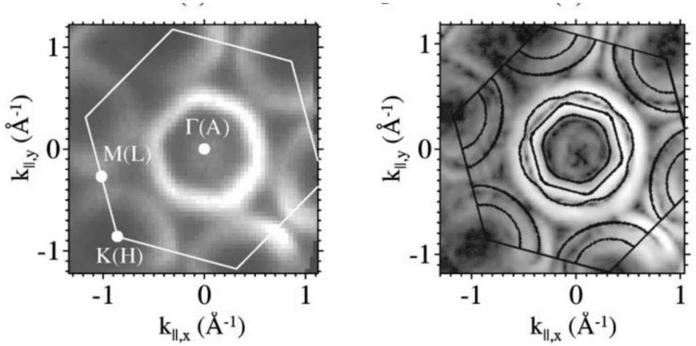

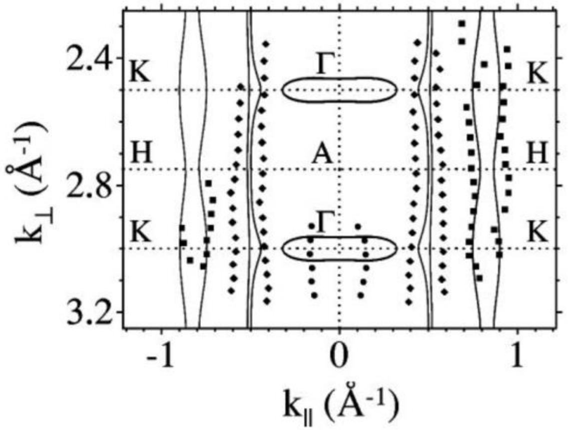

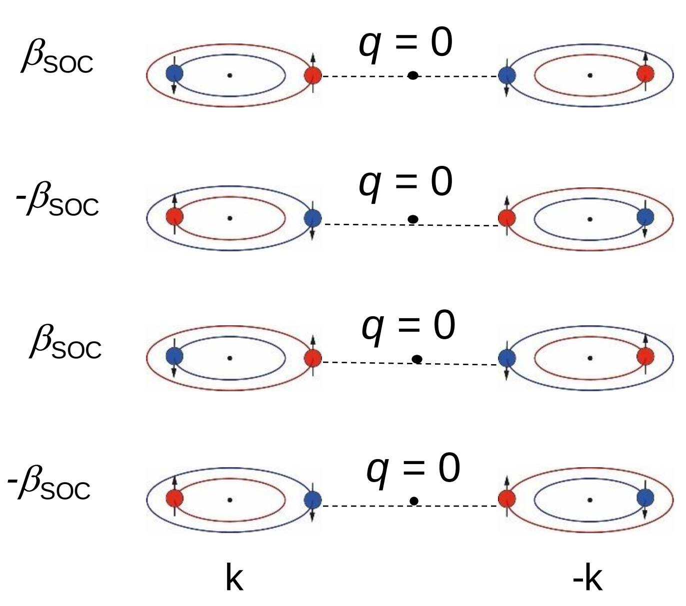

Ising pairing

Large $\boldsymbol{B}_\parallel$

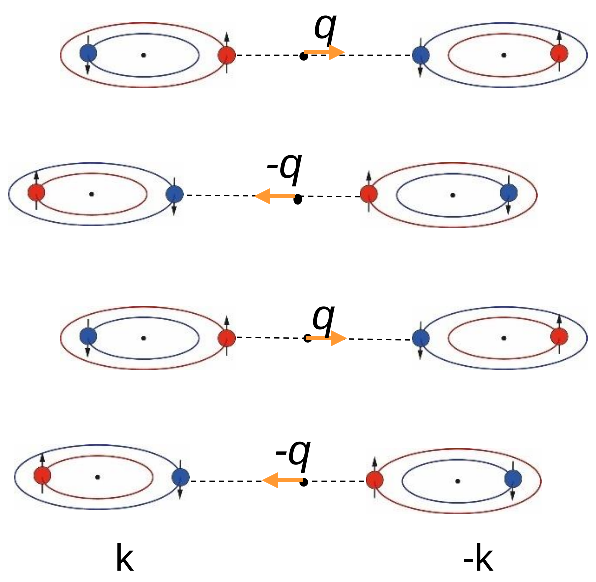

Finite momentum pairing

$\Delta(r) = \Delta_0$

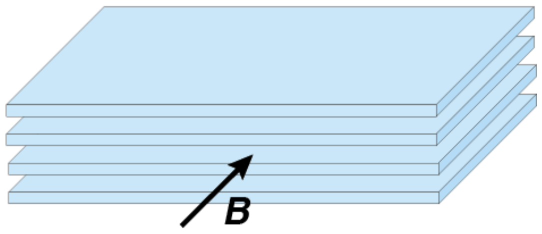

Uniform phase

$\Delta(r)$

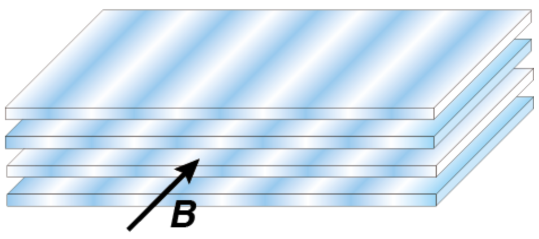

Non-uniform phase (orbital FFLO)

Liu *et. al*. PhysRevLett.118.087001

Majorana Bound States in Artificial Kitaev Chains

Srijit Goswami

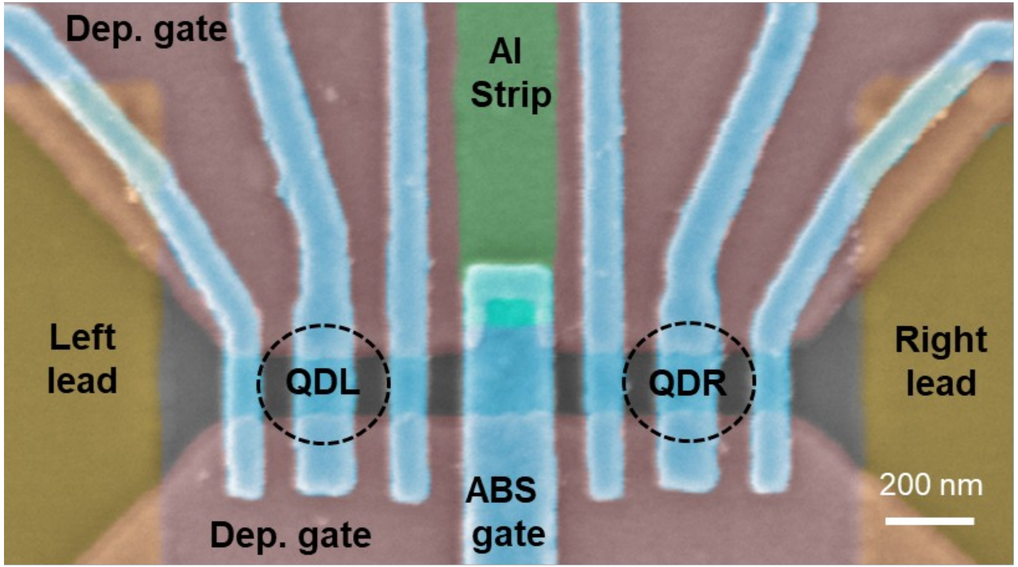

Delft

Qingzhen Wang
Bas ten Haaf
Ivan Kulesh
Christian Prosko
Christian Moehle
Ting Ke
Yining Zhang
Saurabh Karwal

Purdue

Di Xiao
Candice Thomas
Michael Manfra

QuTech TU Delft KAVLI INSTITUTE of Nanoscience Delft

Majorana Bound States in Artificial Kitaev Chains

Srijit Goswami

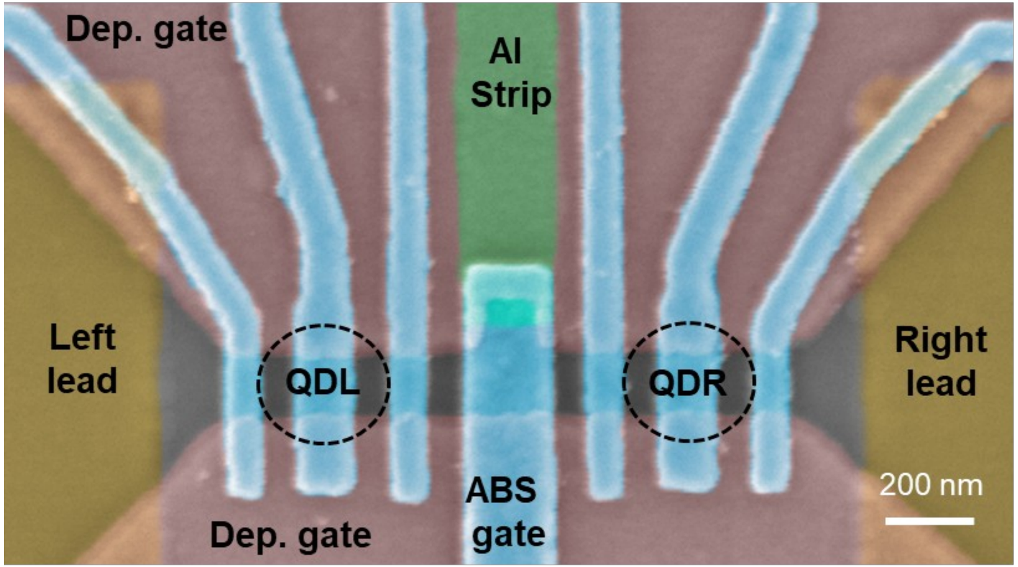

- Introduction to 2DEGs and Kitaev Chain
- Ongoing experiments in 2DEGs
- Goals within QuMat

QuTech TU Delft KAVLI INSTITUTE of Nanoscience Delft

1D hybrid systems for Majoranas

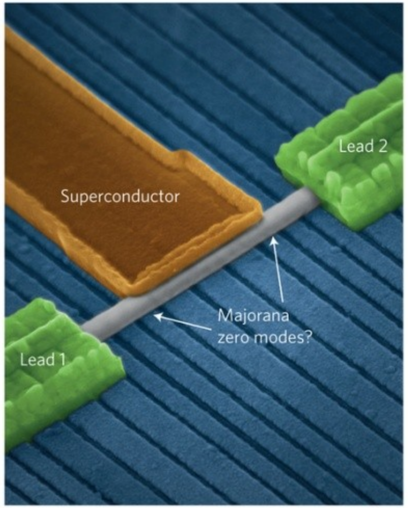

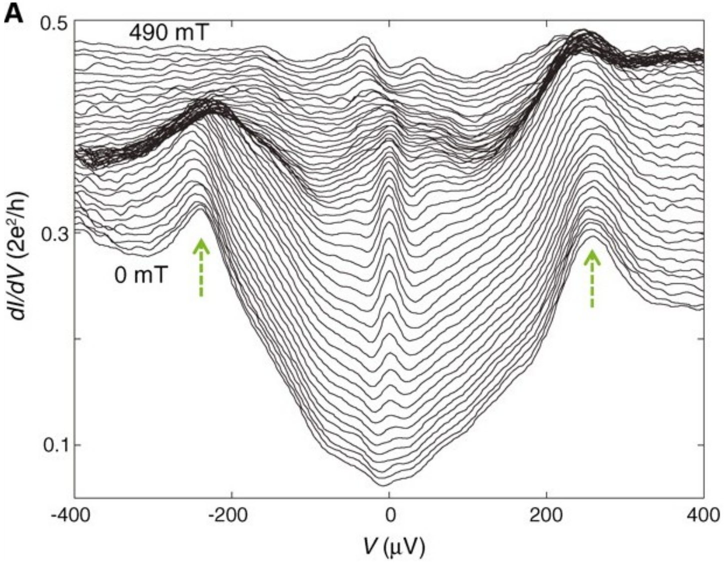

Lutchyn, *PRL* (2010)
Oreg, *PRL* (2010)

Mourik, *Science* (2012)

Current status

- Tremendous improvement in materials/hybrids
- Better fabrication protocols
- Many 'signatures' of Majoranas claimed
- Convincing demonstration of a global topological phase missing

QuTech

Why 2DEGs

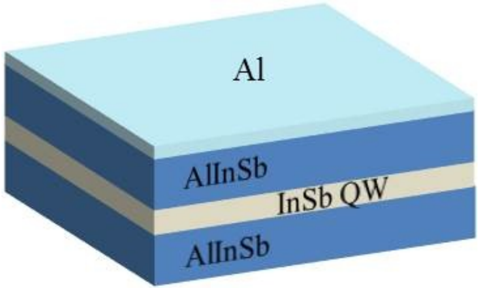

Top down nanofabrication

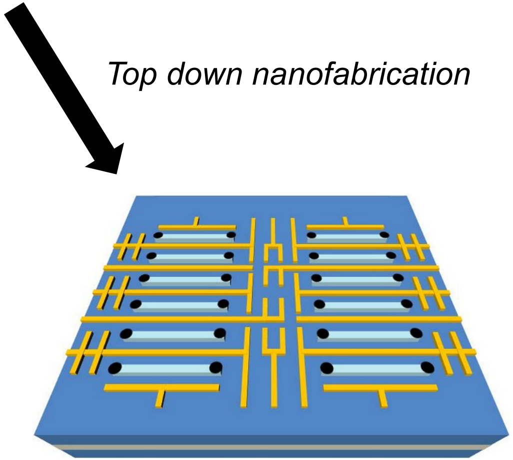

Exploit flexibility: understand microscopics

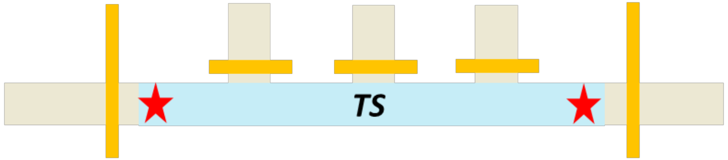

Are the MZMs really localized at the ends?
Are they correlated?
What's happening in the bulk?

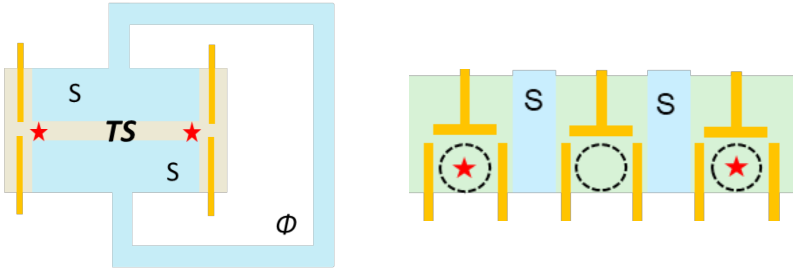

Better architectures beyond NWs?

Ternary 2DEGs

Wafer stack

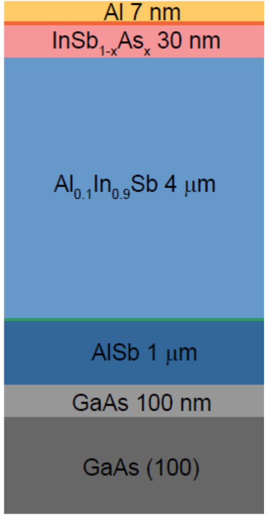

Moehle, *Nano Letters* (2021)

Strong spin-orbit interaction

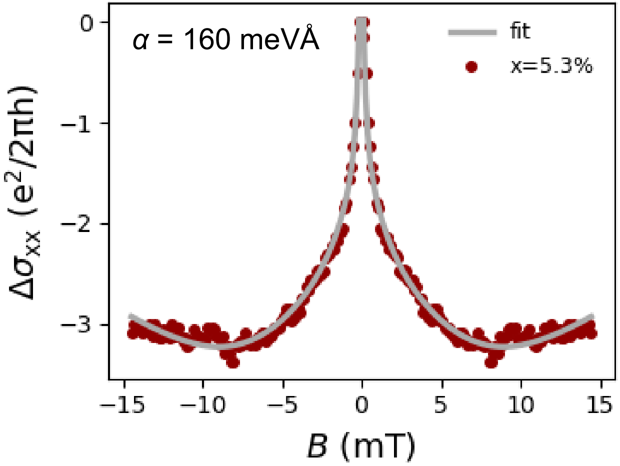

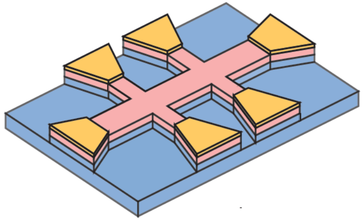

Strong induced superconductivity

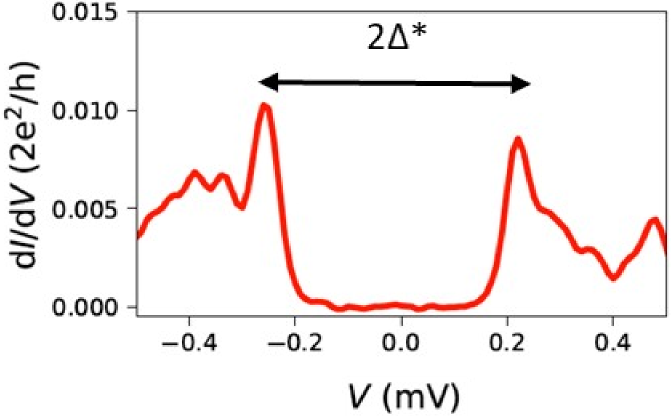

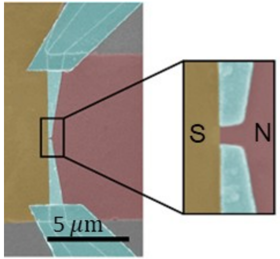

QuTech

Probing the bulk

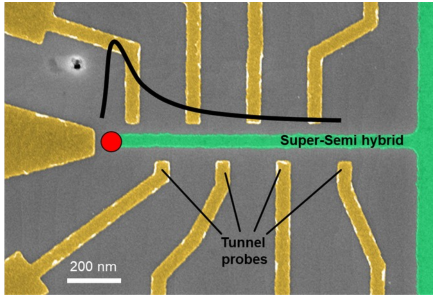

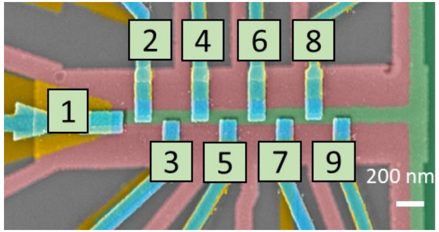

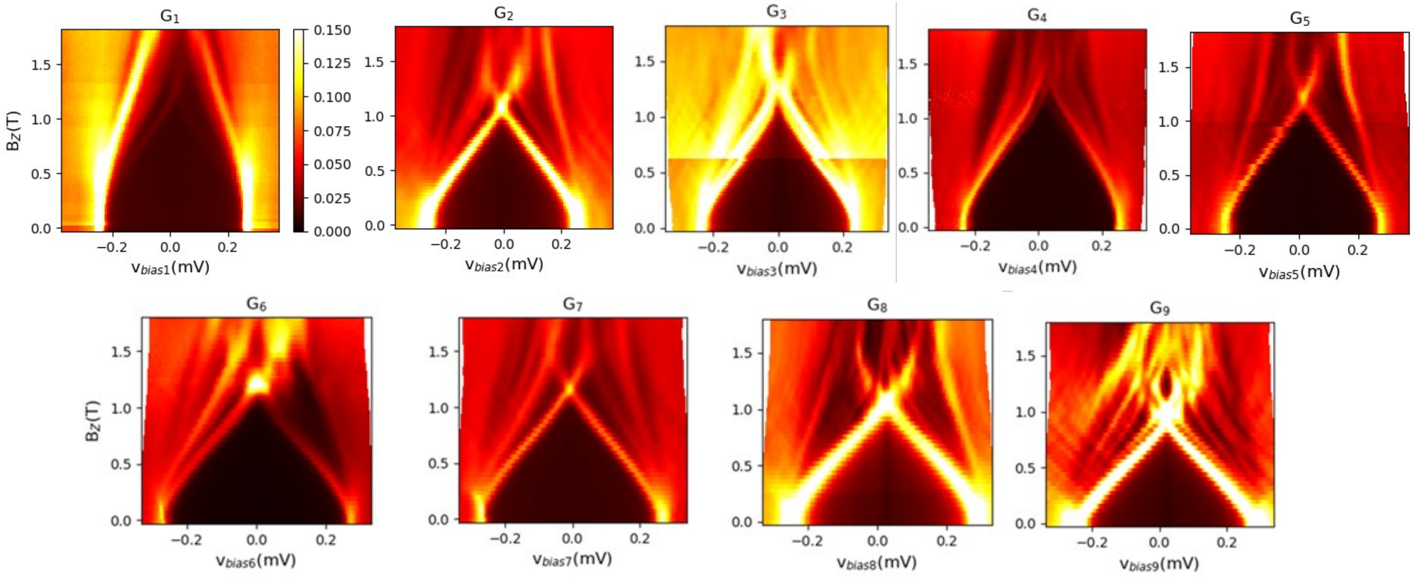

- No correlations; no extended state
- Strong local variations

→ Change in strategy

The Kitaev chain: Hamiltonian engineering

$$H=\sum_n -\mu_n c_n^\dagger c_n - t c_{n+1}^\dagger c_n + \Delta c_{n+1}^\dagger c_n^\dagger + h.c$$

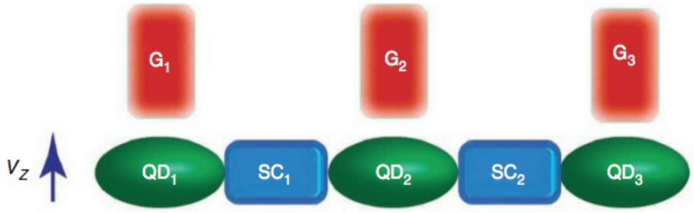

J. D. Sau and S. Das Sarma, Nat. Commun. (2012)

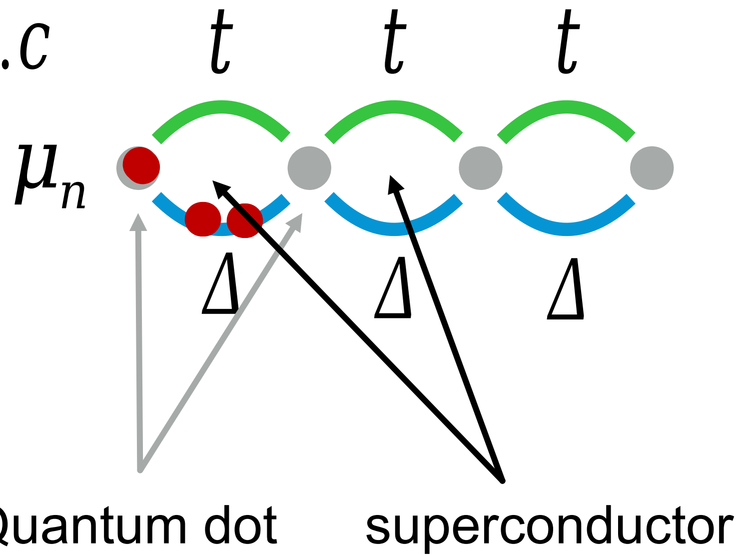

QuTech

QD-ABS-QD device

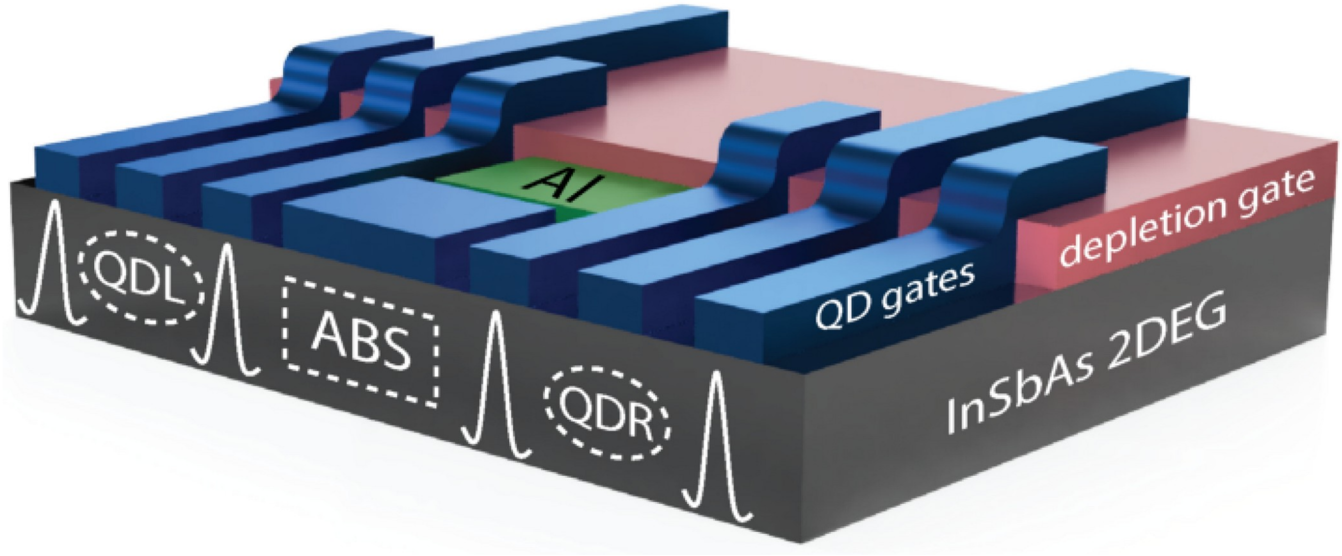

QD-ABS-QD device

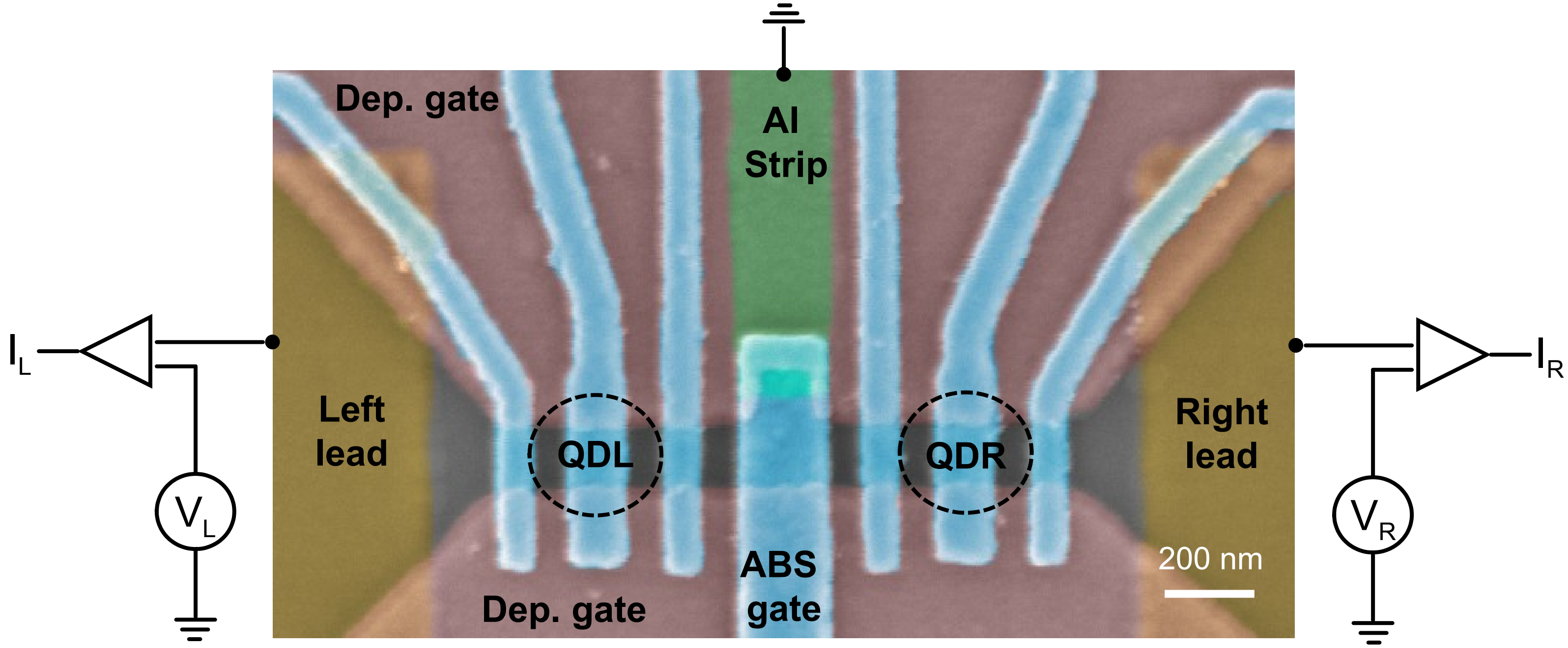

QuTech

Device elements

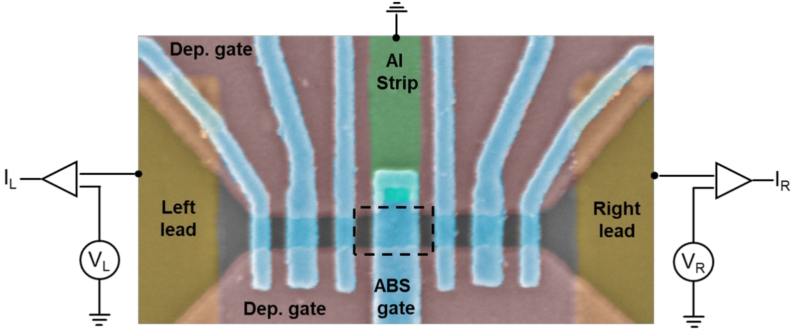

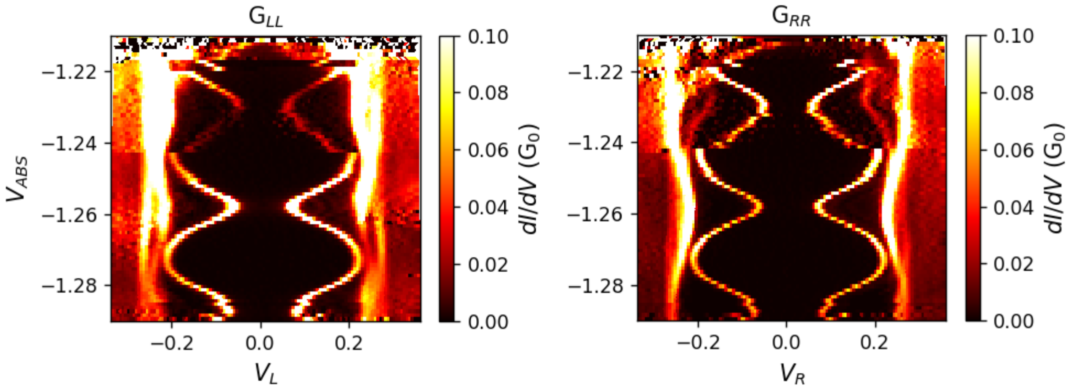

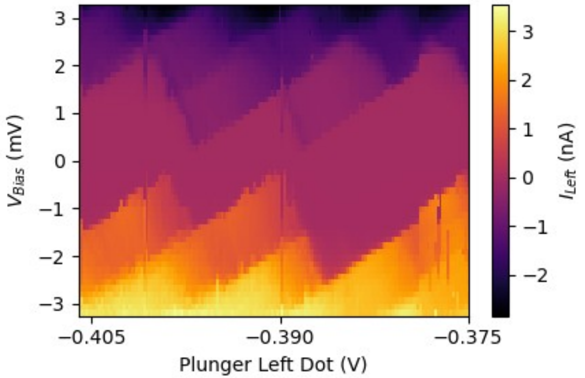

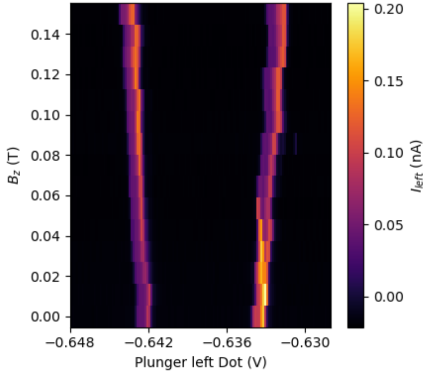

- Extended Andreev bound states
- Spin polarized QDs

QuTech

Elastic co-tunneling and Crossed Andreev reflection

ECT
(t)

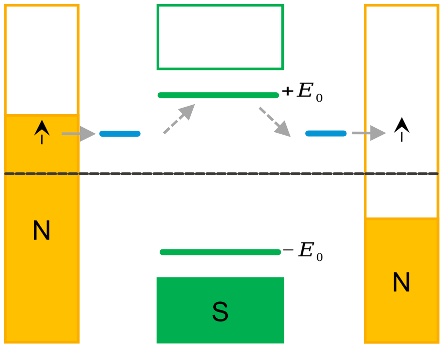

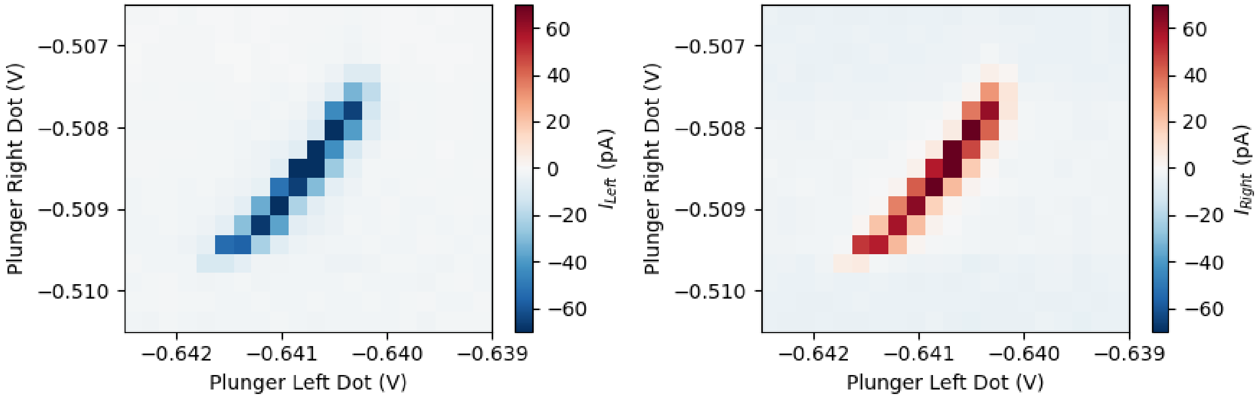

CAR
(Δ)

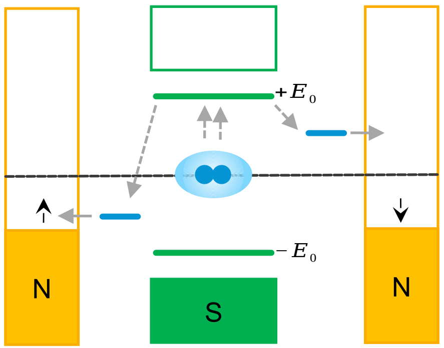

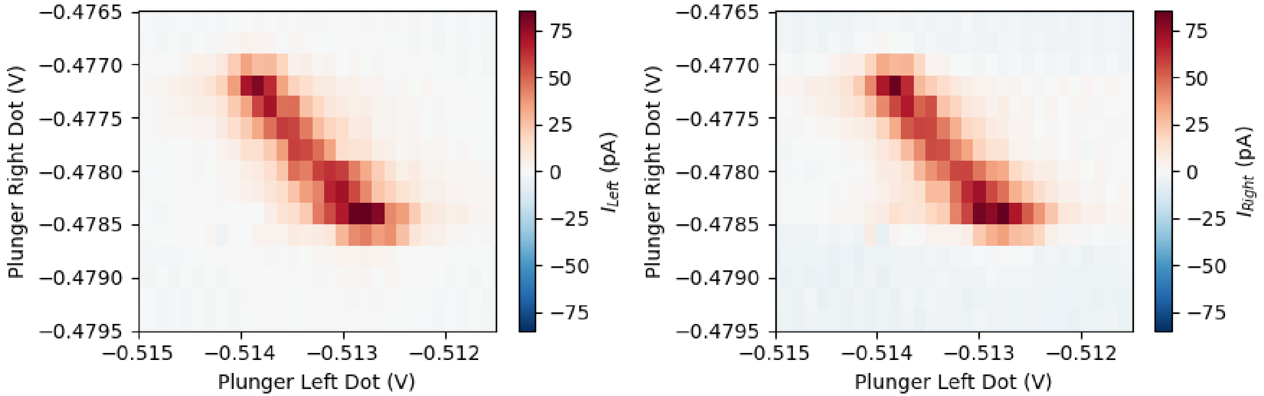

The ‘Poor Man’s Majorana’ proposal

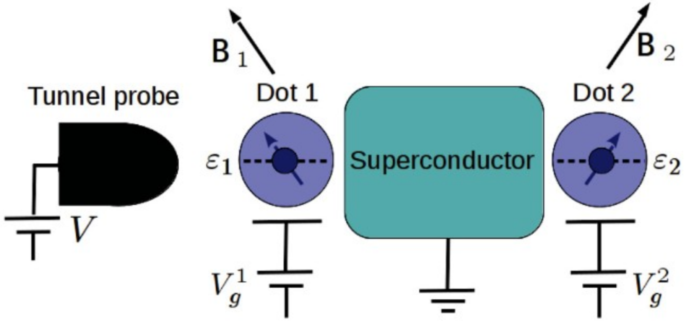

$$
\begin{array}{c|cccc}
 & |0,0\rangle & |1,1\rangle & |1,0\rangle & |0,1\rangle \\
\hline
\langle 0| & 0 & \Delta_{QD} & 0 & 0 \\
\langle 1,1| & \Delta_{QD} & \epsilon_1+\epsilon_2 & 0 & 0 \\
\langle 1,0| & 0 & 0 & \epsilon_1 & t \\
\langle 0,1| & 0 & 0 & t & \epsilon_2
\end{array}
$$

The ‘Majorana Sweet Spot’:

$$\epsilon_1 = \epsilon_2 = 0, t = \Delta_{QD}$$
$$\gamma_1 = d_1 + d_1^\dagger$$
$$\gamma_2 = i(d_2 - d_2^\dagger)$$

QuTech

Leijnse, M. & Flensberg, K. *Phys Rev B* **86**, 134528 (2012)

Within QuMat

Demonstrating topological protection

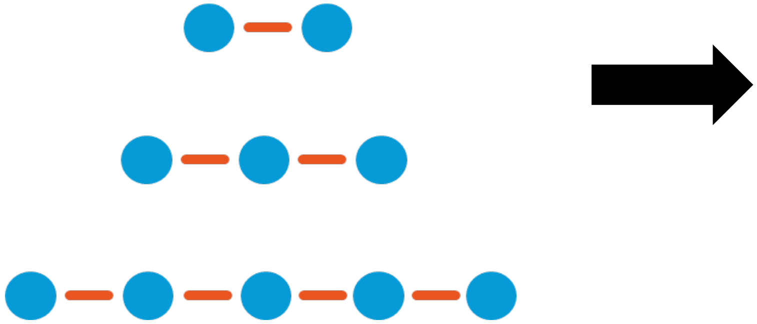

Parity Qubits with Kitaev chains

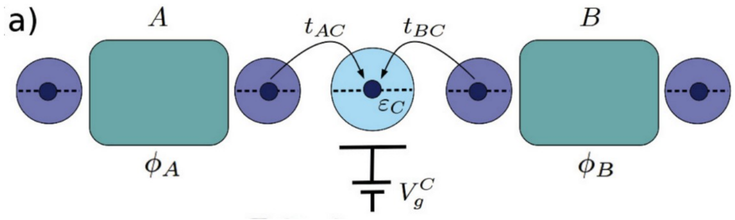

Leijnse & Flensberg, *PRB* (2012)

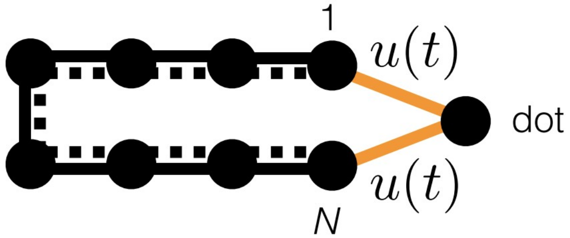

Széchenyi & Pályi, PRB (2017)